IMPACT OF DISTRIBUTED SYSTEM

by

JÜRGEN GRÄTER

A thesis submitted in partial fulfillment of the

requirements for the degree of

MASTER OF SCIENCE

(Mechanical Engineering)

at the

University of Wisconsin—Madison

1992

IMPACT OF DISTRIBUTED SYSTEM

Jürgen Gräter

Under the supervision of Professor W.A. Beckman and Professor J.W. Mitchell

at the University of Wisconsin—Madison

Many utilities within the US are faced with the decision to either reduce the peak demand of electricity or to build new generating capacity. One way to reduce the peak demand is to replace a large number of small energy systems with more efficient systems.

Water heating is the second largest user of energy in the residential sector, and replacement of conventional electric water heaters by solar domestic hot water systems (SDHW) with electric back–up has the potential to reduce both energy use and power demand. In this thesis, the impact on a utility of installing many SDHW systems in place of conventional electric systems is estimated by computer simulations.

Base case conventional and SDHW systems were chosen, and 4,000 simulations were performed that covered a wide range of system characteristics and load profiles. The system characteristics and the hot–water load were chosen for each individual simulation by random selection between specified limits. The simulations were performed for Madison in August using TRNSYS. The results of the 4,000 simulations were used to estimate the impact on energy and demand.

The results from simulating only the base case (average) system provide a good estimate for the total amount of electricity required during one month. However,

estimating the electrical demand reduction using the results of only the base case system yields misleading conclusions.

The transient behavior of a single system and its impact on demand is different from the average of many systems. The electric heater in both the SDHW system and the conventional system is either on or off. However, the heaters of many systems are not on and off at exactly the same time. The systems are not identical, and the hot water load is different in pattern and magnitude for each individual household. Therefore, the instantaneous electricity demand of many systems can not be estimated from the demand of one system.

Subgroups of the 4,000 cases were selected to see if a smaller group would predict the same impact as the 4,000 cases. It was found that it was possible to select as few as 500 cases to estimate the demand reduction. However, the confidence interval for the results is large for the smaller number of simulations.

The impact of SDHW systems on a utility may be significant. Replacing many conventional electric water heaters with SDHW systems supplying an average solar fraction of 60% yields a reduction of the peak hot water electricity load by 15% to 20% and a reduction of the hot water energy use by 60%. For an electric utility that has the peak load in August from 1:00 PM to 4:00 PM it yields a peak load reduction by 15% to 30% and energy use by 90% during their peak time. The highest peak for the utility usually occurs on the second of two consecutive very hot days with very high solar radiation. It was shown that the peak demand of the SDHW systems occurs on a day with very low solar radiation. Therefore, the peak demand of the SDHW system and the peak demand for the utility will not occur

coincidentally. The power demand of the SDHW systems during the utility peak time is over 70% less than the power demand by conventional electric systems.

A methodology for estimating the impact of many systems has been developed. It is possible to determine the impact from a smaller number than the total number of systems.

Acknowledgments

I applied for a scholarship to study in the U.S. in January 1991. However, I never really thought* about what it means to leave the place where I was born and where I lived for 25 years, to leave friends and family, to go to a foreign country and speak a foreign language. I got a scholarship from the German Academic Exchange Service and left Stuttgart, Germany, in August 1991. After only a few weeks in Madison, Wisconsin, I knew that the decision to leave Stuttgart and to study in Madison was the right one. Now, I have to say that I really enjoyed my stay in Madison. I met wonderful people here and I had a great time inside and outside of the University of Wisconsin—Madison.

I was lucky to live in the U.S. during the presidential elections†. Thanks to Mr. Perot, the texas billionaire, Mr. Bush, the "old" President of the U.S., and Mr. Clinton, the "new" President of the U.S. for making watching T.V. so much

*Sigmund Freud (1856–1939): "Itzig, wohin reit'st Du?" "Weiß ich, frag das Pferd." ("Itzig, where are you riding to?" "Don't ask me, ask the horse.") Letter to Wilhelm Fliess, 7 July 1898, in Aus den Anfängen der Psychoanalyse (Origins of Psychoanalysis, 1950)

†George Eliot (1819–1880): An election is coming. Universal peace is declared, and the foxes have a sincere interest in prolonging the lives of the poultry

fun during the presidential campaign. You guys really know how to make good TV commercials[‡]

The research I worked on in the Solar Energy Laboratory was really interesting. Thanks to my advisors John and Bill. The questions you asked me and the enthusiasm you showed helped me to continue and to finish this thesis[§] Thanks to Sandy who answered my "How does TRNSYS ..." questions and to Jack for founding the Lab more than 30 years ago. Thanks to the student members of the Lab, Al, Alex, Bernd, Bob, Bob and Bob, Colin, Dean, Dick, Dirk, Doug, Emily, Jim, Jörg, Kevin, Krista, Østein, Osama, Osman, Nate, Mark, Martin, Matthias, Mike, Paul, Sandy, Steve, Svein, Tammy, Tim, Todd, and to the staff members; Shirley who helped me in finding my way through the administrative things I had to do and to Jeff who explained TRNSYS to me and who tried really hard to be a good NETTREK opponent. You guys made this place a unique studying and working environment.

I want to thank my girl friend Heide who made our relationship not only survive but grow stronger with more than 5,000 miles between us.

[‡]Dorothy L. Sayers (1893–1957): Plain lies are dangerous: the only weapons left him the advertiser are the suggestio falsi and the suppressio veri, and his use even of these would be very much more circumscribed if one person in ten had ever been taught how to read....Those who prefer their English sloppy have only themselves to thank if the advertisement writer uses his mastery of vocabulary and syntax to mislead their weak minds. ...The moral of all this ...is that we have the kind of advertising we deserve. Spectator 19 Nov. 1937 "The Psychology of Advertising".

[§]Johann Wolfgang von Goethe (1749–1832): Es irrt der Mensch, so lang er strebt. Man is in error throughout his strife. Faust, pt.i (1808). Prolog im Himmel

Financial Support

Prof. Heisel from the Institut für Werkzeugmaschinen of the University of Stuttgart granted a scholarship funded by the German Academic Exchange Service which made it possible for me to study in Madison as a engineering special student in fall 1991 and spring 1992. During summer and fall 1992 I was funded by the Wisconsin Center for Demand Side Research via the Solar Energy Laboratory at the University of Wisconsin–Madison.

Contents

List of Tables

List of Figures

Nomenclature

Latin letters

A	area
A_c	collector area
b_0	incidence angle modifier coefficient
C	control function
c_p	specific heat
F	solar fraction
F_R	collector heat removal factor
H	height
H	daily irradiation on a horizontal surface
$\bar{H}$	monthly average daily irradiation
I	radiation
I_T	total radiation
I_b	beam radiation
I_d	diffuse radiation
L	load factor
m	mass
$\dot{m}$	mass flow rate
N_n	number of tank nodes
N_h	number of hours
N_S	number of simulations
P	power
Q	energy
$\dot{Q}$	rate of energy

(continued on next page)

Latin letters *(continued from previous page)*

R_b	ratio of beam radiation on a tilted plane to that on a horizontal plane
r	regression coefficient
S	absorbed solar radiation
T	temperature
T_{db}	dead band temperature
$T_{set,l}$	set point temperature for the water that is supplied to the load
$T_{set,t}$	set point temperature for the water in the tank
T_{load}	temperature of the water that is supplied to the load
T_{tank}	temperature of the water in the tank
t	time
U	overall heat loss coefficient
V	volume

Greek letters

α	absorptance
β	collector slope
η	efficiency
λ	load factor ratio
Θ	angle of incidence
ν	energy ratio
ρ	ground reflectance
τ	transmittance
$(\tau\alpha)$	transmittance absorptance product
Φ	latitude
ζ	maximum power demand ratio

Subscripts

a	ambient
b	beam
c	collector
c	cold
d	diffuse
e	electric
db	dead band
env	environment

(continued on next page)

Subscripts *(continued from previous page)*

h	hot
i	inlet
l	load
$load$	load
$loss$	losses
max	maximum
n	normal
set	set point
t	tank
w	warm
$SDHW$	solar domestic hot water system
HW	conventional electric water heating system

Miscellaneous

$\bar{x}$ mean of all x_i, $\bar{x} = \frac{1}{n_x} \sum_{i=1}^{n_x} x_i$

s_x^2 variance of x_i, $s_x = \frac{\sum_{i=1}^{n_x} (x_i - \bar{x})^2}{n_x - 1}$

s_x standard deviation of x_i, $s_x = \sqrt{s_x^s}$

Chapter 1

Introduction

Many utilities within the US are faced with the decision either to reliably reduce peak demand of electricity or to build new generation capacity. One possible way to reduce the peak demand is the installation of new and high efficient appliances within the buildings of their residential customers. Either the utility installs theses appliances themselves or they offer incentives for their customers to do so.

A difficulty is that the impact of many appliances on the utility load has to be estimated in order to evaluate if it is a good decision. The impact of one system is easy to estimate and can be done by either computer simulations or measurements. It is more difficult to determine impact of very many (several thousands or even hundred thousands) systems that are of the same type but all slightly different.

The example considered in this thesis is an electric water heater with a storage tank. All of the system parameters (e.g. storage volume, power of the auxiliary heater, insulation of the tank and others) are within a reasonable range, but have different impacts. They would have different impacts even if they had the same

parameters. For example; the environmental temperature for the storage tank is different from system to system; therefore, the heat losses from the tank to the environment would be different even if the systems were identical. Another very important parameter, the hot water load, varies from household to household.

In order to be able to promote a specific system, one has to estimate the impact of a large number of these systems on the utility electricity load profile. It is very important to determine for both the old and the new system: i) the peak electricity load, ii) when it occurs, and iii) the total electricity required during utility peak times.

Most utilities in the U.S. are summer peaking utilities, and the peak electricity load occurs usually in August in the early afternoon. It has been assumed that solar domestic hot water systems are a way to reliably reduce peak demand because they perform best during these utility peak hours.

This thesis will investigate the impact of many SDHW systems on a utility. Simulations of many systems will be used to perform this task. The results will be compared to the result of the simulation of a average system.

Chapter 2

Background

2.1 Electric Utility Load Profile

Electrical utilities generally categorize their system loads into a number of types based on the load factor at which they must be supplied. An example is given in Figure 2.1. For Figure 2.1 the peak, intermediate and base loads are defined as those which are greater than 80%, between 80% and 40%, and less than 40% of the maximum load [6]. Another possibility of defining peak, intermediate and base load is to use the hours of the day that the load has to be supplied. For example, one might define the peak load to be that load which has to be met for only one hour a day, the base load to be the load that must be met all the time, and the intermediate load to be all those between base and peak load.

Whatever definition for peak load is used, the energy supplied during these peak hours is the most expensive for several reasons: i) peak load plants have a very small load factor, therefore, the capital costs are very high, ii) to reduce

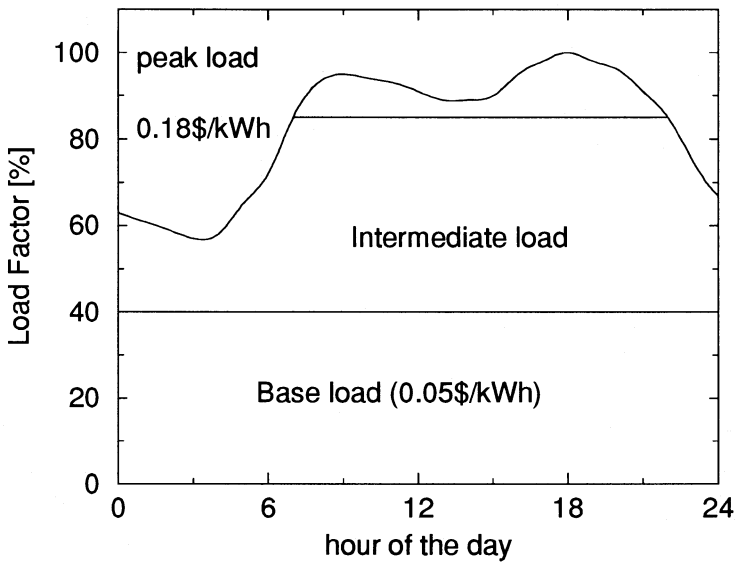

Figure 2.1: Typical utility daily load curve

the capital costs, one uses plants with lower capital costs like gas turbines, which results in extremely high fuel costs iii) the power lines and substations have to be designed to meet the peak load, which yields high capital cost. The power grid accounts for up to 50% of the cost for electricity delivered to residential customers. The costs resulting from the load of Figure 2.1 may vary from plant to plant or state to state but constitute a typical cost range.

The optimum load profile for the utilities would be a flat one; the load is constant over time. This would theoretically allow the utility to supply all the energy with relatively cheap base load power plants, e.g. very big coal or nuclear power plants.

Many utilities within the U.S. are approaching their generating capacity during their peak hours. As a consequence, they are faced with the decision either to build new (peak) capacity or to reduce peak demand. The construction of new generating

capacity is very expensive, therefore, the utilities are looking for a way to delay or maybe even avoid new construction.

One way to reduce peak demand is to install small energy generation systems at the building of their residential customers, e.g. solar domestic hot water systems, or to offer incentives to their customers to do it themselves. Most utilities are summer peaking utilities. Their highest yearly demand occurs in the early afternoon in mid August due to the high electricity demand for air conditioning. Solar systems perform very well during this time of the year and day. Well designed solar domestic hot water systems supply 65% to 85% of the energy load during August. It is commonly assumed that replacing electric water heaters by solar domestic hot water system has a potential to reduce peak demand [11, 6]; the question is how much?

2.2 Hot Water Load in Residential Buildings

Domestic water heating is second only to space heating as the largest user of energy in the residential sector [2]. The total amount of water used varies as well as the usage pattern for different consumer groups.

Many studies have been performed [1, 2, 9] to develop a hot water use data base. Becker [1] found the average hourly hot water use pattern for all families to be as shown in Figure 2.2.

However, the hot water load profile varies from household to household. An example is the variation between renters and seniors shown in Figure 2.3 which compares the water use pattern of senior citizens and renters [1]. An overall average

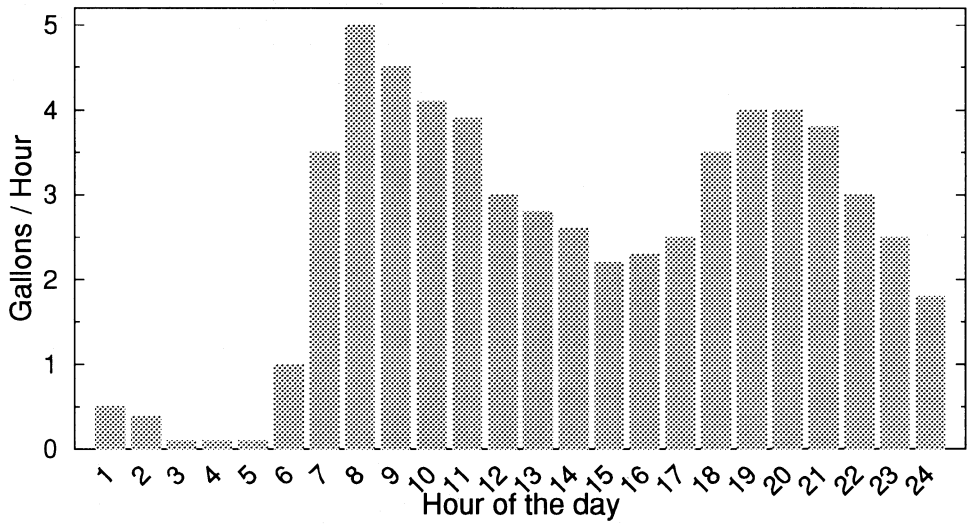

Figure 2.2: Average hourly hot water use — all families

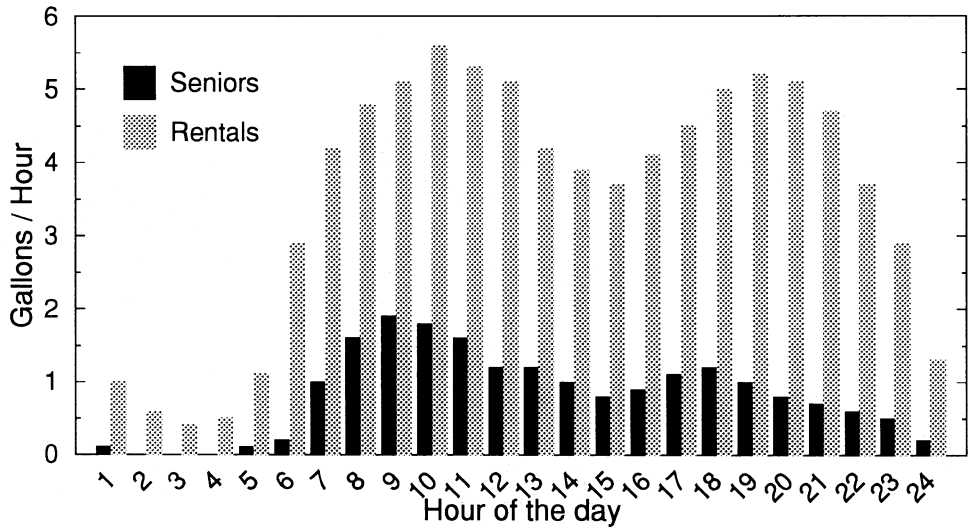

Figure 2.3: Average hourly hot water use — comparison of seniors to rentals

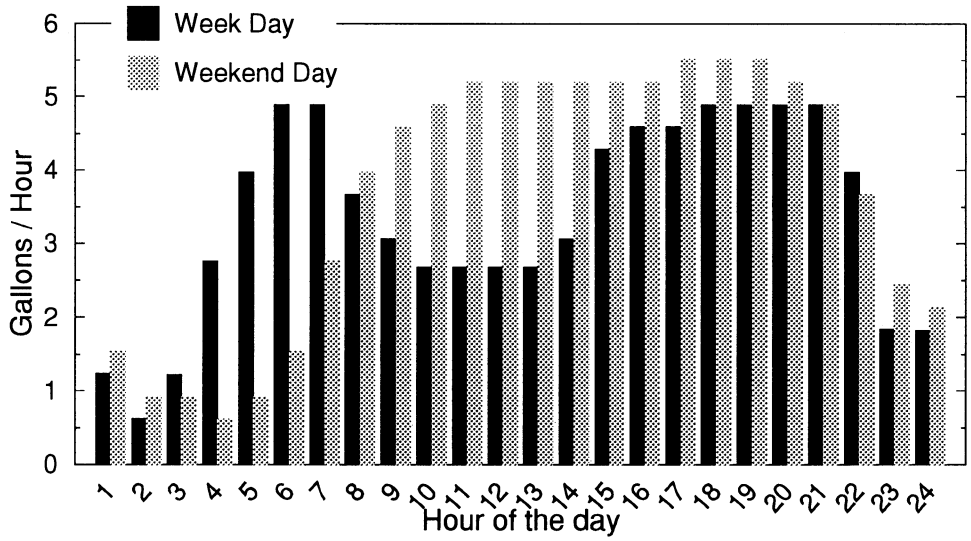

Figure 2.4: Average hourly hot water use — comparison of a week day to a weekend day

of hot water use per day for seniors is 24 gallons, while renters use 84 gallons per day. Hourly patterns for both groups also differ. The hourly use pattern for renters has the typical morning and evening peaks. The pattern for seniors indicates little usage between midnight and 7:00 AM, and it has a large variation from day to day.

The water usage pattern varies also from day to day for the same household. The average hot water use in Wisconsin for a week day and for a weekend day is given in Figure 2.4 and was adapted from a data base from the Wisconsin Center for Demand Side Research.

Many different hot water loads have been used for this research. Some are imaginary profiles, others are adapted from data from the Wisconsin Center for Demand Side Research as shown in Figure 2.4. The profiles are listed in detail in Appendix C.

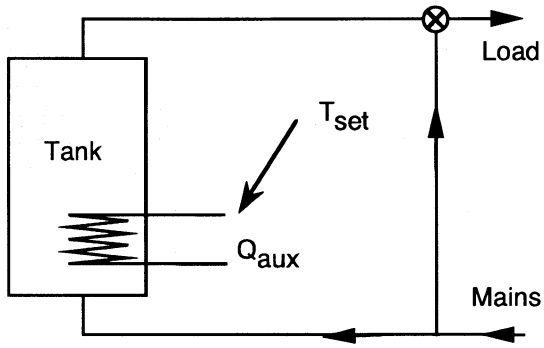

Figure 2.5: System diagram of a typical electric water heater

2.3 Water Heating Devices

2.3.1 Electric Water Heaters

A typical electric water heating system is shown in Figure 2.5. Water to supply the load is removed from the top of the tank. Cold water from mains to replace the load is put into the bottom of the tank. The water is heated by an electrical heating element located in the bottom of the tank†. This heating element has no variable power control; it is either on or off.

The user selects the set point temperature for the tank $T_{set,t}$. The desired temperature for the load $T_{set,l}$ is dependent on the use of the hot water. It is equal to the temperature of the tank for appliances like washing machines or dish washers, but it is lower for personal use.

†Some systems have two heating elements; one near the bottom and one located in the bottom of the top 2/3 of the tank. This additional heater provides quick recovery.

The temperature of the water in the tank T_{tank} is controlled by a thermostat setting. The heating element is turned on by the controller when the thermostat senses a temperature lower than the set point temperature $T_{set,t}$ minus a system specific dead band temperature T_{db}. It is turned off when the water reaches $T_{set,t}$. The dead band is required to avoid unstable system behavior.

If T_{tank} is greater than $T_{set,l}$ cold water from mains is mixed with the hot water to lower its temperature to the desired $T_{set,l}$. The mixing* is typically done by the water consuming appliance, e.g. one mixes cold and hot water in the shower.

Work has been done in this thesis involving an increase of the tank set point temperature $T_{set,t}$ to increase the storage capacity. For these simulations, the mixing valve was used in the TRNSYS simulation to lower the water temperature to the load set point temperature $T_{set,l}$.

2.3.2 Solar Domestic Hot Water Systems

A typical solar domestic hot water system is shown in Figure 2.6. Its main components include the solar collector, a storage tank and, typically, a heat exchanger.

Cold water is removed from an outlet located at the bottom of the tank, pumped through the solar collector, thereby heating the water up, and replaced into the tank through an inlet located at the top of the tank. The controller ensures that the fluid being circulated will be heated, not cooled, by its flow through the collector. An auxiliary heater is located in the top third of the tank to heat the water to the tank set point temperature $T_{set,t}$ if the collector is not capable of supplying the

*The mixing valve is sometimes installed directly after the tank outlet as a safety feature to prevent bodily injury to the user or damage to a appliance by over heated water.

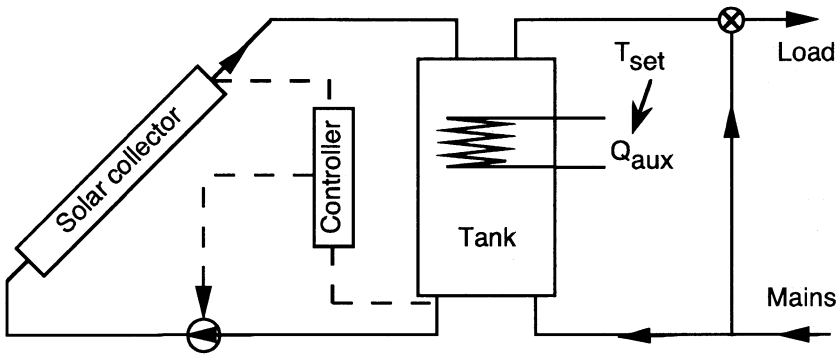

Figure 2.6: System diagram for the solar water heater

required energy. The hot water to the load is removed from the top of the tank and mixed with cold water from mains if its temperature is higher than the load set point temperature $T_{set,l}$. Cold replacement water from the mains is put into the tank through an inlet at the bottom of the tank.

The collector is exposed to ambient conditions. In most areas in the U.S. there needs to be freeze protection. This is typically done by using a freeze–proof coolant instead of water. For that reason, a heat exchanger is required between the collector loop and the tank. Heat exchanger were not included in the simulations performed in this study because the computing time per simulation would be increased by a factor of 2. Collector parameters were chosen so that system with a heat exchanger could be approximated as a system without a heat exchanger [3, Chapter 10.2].

2.4 TRNSYS

TRNSYS is a transient systems simulation program with a modular structure. It is well suited to detailed analyses of systems whose behavior is dependent on the passage of time.

A system is defined to be a set of components, interconnected in such a manner as to accomplish a specified task. For example, the components of the solar domestic water heating system analyzed in this research consist of a flat–plate solar collector, a hot water storage tank with internal electric backup heater, a mixing valve, temperature sensing controllers, pumps and piping. The system consists of these components and it is possible to simulate the performance of the system by collectively simulating the performance of the interconnected components.

2.4.1 Mathematical Description of Some Components

2.4.1.1 Storage Tank

The tank is modeled as a stratified fluid storage tank with internal electric heater. It is assumed that it consists of N fully mixed equal volume segments. The cold water from mains enters the tank at the bottom; the warm water from the solar collector enters below the auxiliary heater, cold water is removed from the bottom and sent to the collector and hot water to the load is removed from the top node.

An energy balance for the i'th tank segment gives [7]

$$\begin{aligned} m_i c_{p,t} \frac{\mathrm{d}T_i}{\mathrm{d}t} &= C_{\alpha,i}\dot{m}_h c_{p,t}\left(T_h - T_i\right) + C_{\beta,i}\dot{m}_{load} c_{p,t}\left(T_{mains} - T_i\right) \\ &\quad + UA_i\left(T_{env} - T_i\right) + C_{\gamma,i}\left(T_{i-C_{\gamma,i}} - T_i\right) c_{p,t} + \dot{Q}_i \end{aligned} \tag{2.1}$$

with

$$C_{\alpha,i} = \begin{cases} 1, \text{ if } i = \text{node of hot fluid inlet} \\ 0, \text{ otherwise} \end{cases} \tag{2.2}$$

$$C_{\beta,i} = \begin{cases} 1, \text{ if } i = \text{node of cold fluid inlet} \\ 0, \text{ otherwise} \end{cases} \tag{2.3}$$

$$C_{\gamma,i} = \dot{m}_h \sum_{j=1}^{i-1} C_{\alpha,j} - \dot{m}_L \sum_{j=i+1}^{N} C_{\beta,j} \tag{2.4}$$

Energy flows are calculated as follows:

$$\dot{Q}_{env} = \sum_{i=1}^{N} UA_i \left(T_i - T_{env}\right) \tag{2.5}$$

$$\dot{Q}_{load} = \dot{m}_L c_{p,t} \left(T_{load} - T_{mains}\right) \tag{2.6}$$

$$\dot{Q}_{in} = \dot{m}_h c_{p,t} \left(T_{collector} - T_N\right) \tag{2.7}$$

The electric auxiliary heater is off when it was off the previous time step and $T_{Thermostat} \geq T_{set,t} - T_{db}$. Otherwise, the rate of energy delivered to the tank from the heater is $P_{aux} = \min(P_{req}, P_{max})$. P_{req} is the energy required to heat the tank to the set point temperature divide by the length of the simulation timestep. P_{max} is the maximum power of the auxiliary heater. The model assumes that energy supplied to the tank from the heater is placed in the tank segment containing the heater, until the temperature of that segment is equal to the segment above. Energy is then added equally to both segments until they reach the temperature of the segment above, etc.

2.4.1.2 Solar Collector

A heat exchanger is usually used to separate the collector fluid from the tank fluid. In this thesis, it is assumed that F_R has been modified to account for the effect of the heat exchanger [3, Chapter 10.2].

The useful energy gain Q_u from a solar collector can be described by [3]

$$Q_u = A_c F_R\Big(S - U_L(T_i - T_a)\Big) \tag{2.8}$$

with A_c collector area

F_R collector heat removal factor including effect of heat exchanger

S absorbed solar radiation

U_L heat loss coefficient

T_i inlet fluid temperature

T_a ambient temperature

The absorbed solar radiation S is obtained by

$$S = I_b R_b \left(\tau\alpha\right)_b + I_d \left(\tau\alpha\right)_d \frac{1+\cos\beta}{2} + \rho_g (I_b + I_d) \left(\tau\alpha\right)_g \frac{1-\cos\beta}{2} \tag{2.9}$$

The three terms in this equation account for the beam, diffuse and ground reflected radiation.

The transmittance–absorptance product $(\tau\alpha)$ is a function of the angle of incidence. The ratio $\dfrac{(\tau\alpha)}{(\tau\alpha)_n}$ can be approximated from ASHRAE test result as

$$\frac{(\tau\alpha)}{(\tau\alpha)_n} = 1 - b_0\left(\frac{1}{\cos\Theta} - 1\right) \tag{2.10}$$

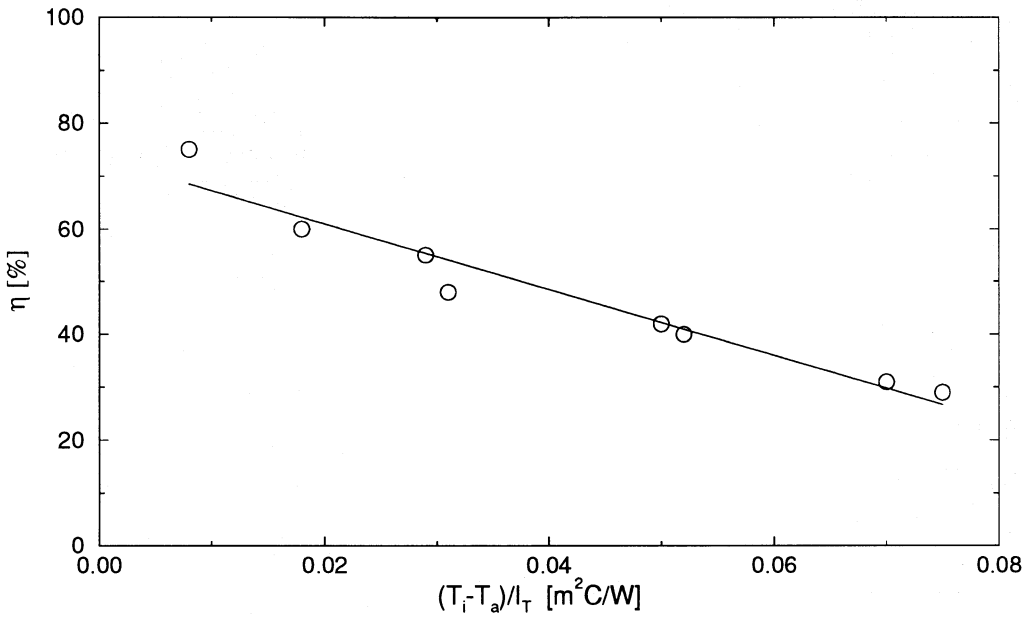

Figure 2.7: Experimental collector efficiency data

with b_0 incidence angle modifier coefficient

$(\tau\alpha)_n$ the transmittance absorptance product for incident radiation normal to the collector

$(\tau\alpha)$ the transmittance absorptance product for the angle of incidence Θ

Both b_0 and $(\tau\alpha)_n$ are found experimentally. The useful energy gain Q_u from the collector can be written as

$$Q_u = A_c I_T \left(F_R(\tau\alpha) - F_R U_L \frac{T_i - T_a}{I_T} \right) \tag{2.11}$$

$F_R(\tau\alpha)$ and $F_R U_L$ are obtained from collector test data and are modified for the effect of a heat exchanger. Collector test results are typically presented as plots of the collector efficiency $\eta = \dfrac{Q_u}{A_c I_T}$ versus $\dfrac{T_i - T_a}{I_T}$. To a good approximation for flat–plate collectors, the data can be represented as straight lines with the intercept $F_R(\tau\alpha)_n$ and the negative slope $F_R U_L$ (see Figure 2.7).

For the computer simulation, these equations are used to compute the useful collector energy gain [7]. A_c, b_0, β, $F_R(\tau\alpha)_n$ and $F_R U_L$ are constants supplied as parameters to the TRNSYS deck whereas I_b, I_d, Θ, ρ_g and T_a vary with time and are supplied to the collector by the radiation processor and T_i is supplied by the tank model.

2.4.1.3 Mixing Valve

The mixing valve is used to mix two incoming water streams with the flow rates $\dot{m}_c$ and $\dot{m}_h$ and the temperatures T_c and T_h to an outgoing of temperature $T_{set,l}$ and flow rate $\dot{m}_{load}$. Mixing is necessary if the temperature of the tank outlet T_t is higher than the set point temperature of the load $T_{set,l}$.

Inputs are the temperatures T_{set}, T_c and T_h, and the flow rate $\dot{m}_{load}$. The outputs $\dot{m}_h$ and $\dot{m}_c$ are calculated using mass balance

$$\dot{m}_{load} = \dot{m}_h + \dot{m}_c \tag{2.12}$$

and energy balance

$$T_{set,l}\dot{m}_{load} = T_h\dot{m}_h + T_c\dot{m}_c \tag{2.13}$$

to get

$$\dot{m}_h = \begin{cases} \dot{m}_{load}\dfrac{T_{set,l} - T_c}{T_h - T_c}, \text{ if } T_h \geq T_{set,l} \\ \dot{m}_{load}, \text{ otherwise} \end{cases} \tag{2.14}$$

$$\dot{m}_c = \dot{m}_{load} - \dot{m}_h \tag{2.15}$$

2.4.1.4 Piping, Pumps and Controllers

All components are assumed to be ideal. Heat losses from pipes and pumps are assumed to be negligible. The collector parameters can be modified to include duct and pipe loss factors [3, Chapter 10.3]. It is also assumed that the controller reads the temperatures and the set points exactly. The consumption of electrical energy for pumping and controls is not considered.

2.4.2 Information Flow and the TRNSYS Deck

The system is simulated by connecting the inputs and outputs of the individual components in the desired manner. The resulting set of algebraic equations are solved by using successive substitution and the differential equations are solved by the modified Euler method.

The system parameters and interconnections are specified in the TRNSYS deck. The TRNSYS decks used for this research are listed in Appendix D.

A useful way to present the program is an information flow diagram as presented in Figure 2.8†. All important subsystems for a SDHW system are displayed in this figure. Weather data, e.g. ambient temperature and radiation, are passed to the radiation processor which converts it to a form required by the solar collector. The solar collector and tank are connected to exchange flow rates and water temperatures. The controller on the collector side controls the operation of the collector; dependent on the temperature difference between the tank outlet to the collector and the collector outlet. The hot water demand and mixing valve

†This is not the usual TRNSYS information flow diagram. The usual TRNSYS information flow diagram shows the connections between the different subsystems in greater detail.

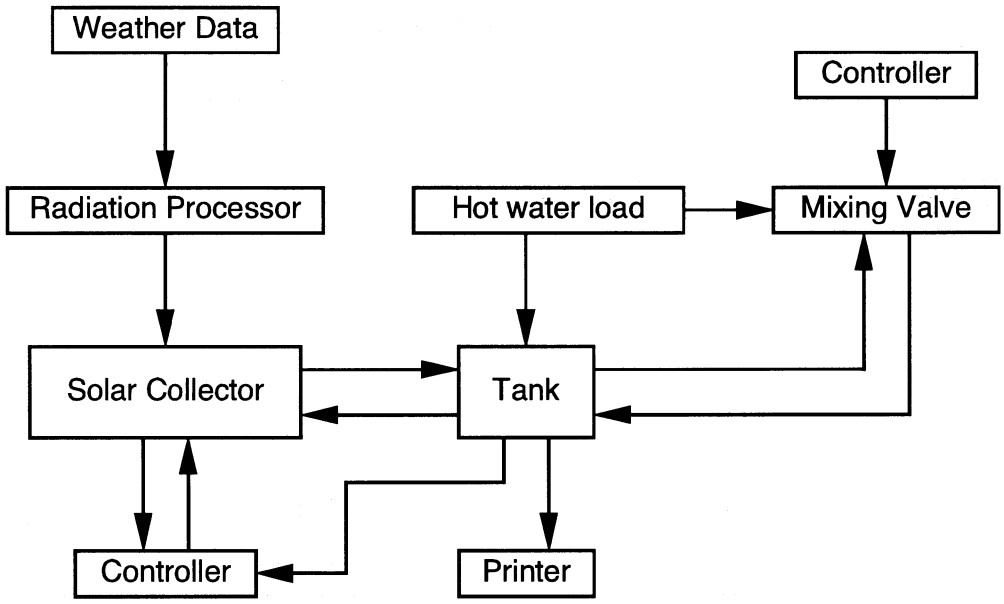

Figure 2.8: Information flow diagram for a TRNSYS simulation of the SDHW system

communicate with the tank in order to set the load–side flow rate. The controller at the mixing valve sets the desired temperature. The important information for this research is the energy delivered to the load and the electricity required. Both are available from the tank component and are sent to a disk file via a printer subroutine.

Figure 2.9 gives the information flow diagram for the conventional electric water heating system. It is the same as Figure 2.8 without the components required for the solar specific parts.

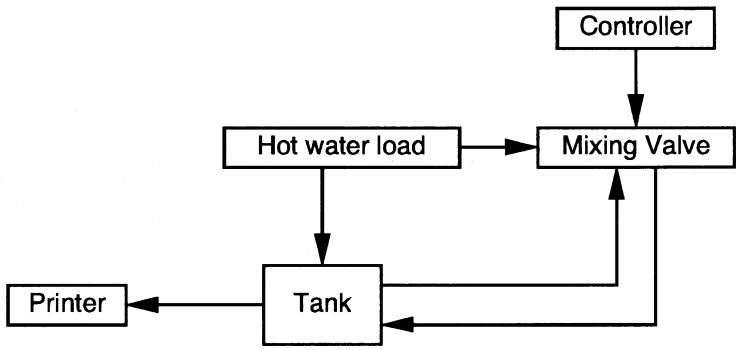

Figure 2.9: Information flow diagram for a TRNSYS simulation of the conventional electric water heating system

2.4.2.1 The TRNSYS Unit System

The TRNSYS unit system is based on the unit of mass kg, the unit of energy kJ, the unit of length m and the unit of time hr. All other units required are derived from these base units. For example, power is energy per time and has the unit kJ/hr. The units used in this thesis are conform with the TRNSYS system.

Chapter 3

Single System Simulation

The current "state of art" for estimating the impact of many systems is to simulate a single (average) system and extrapolate to the desired number of systems. This methodology is used in this chapter. It will be shown that this is a fast and accurate method to estimate the integrated performance data, e.g. monthly electricity consumption. On the other hand, this methodology yields misleading results for instantaneous performance (electrical demand) of the systems.

3.1 Electric Water Heater

A TRNSYS deck was set up (see Appendix D.1) to simulate the conventional electric water heating system shown in Figure 3.1. The important system parameters are given in Table 3.1. These parameters are the base case (average) values from the parameters used for the multiple TRNSYS runs in Section 4.4.1. The results of this simulation will be given in Section 3.3.

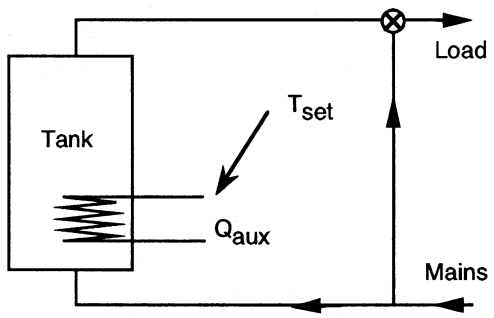

Figure 3.1: Electric water heating system

P_{max}	$10,800kJ/hr = 3kW$	$T_{a,t}$	$20°C$
T_{db}	$6°C$	$T_{set,t}$	$55°C$
U_t	$9.5kJ/m^2hrK$	V_t	$240l$

Table 3.1: Important system parameters for the conventional electric system

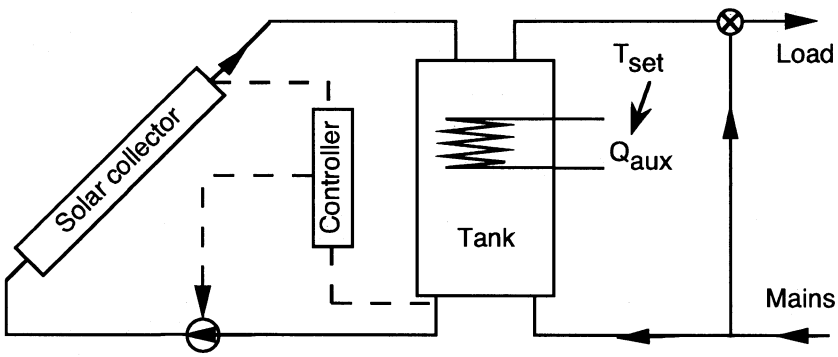

Figure 3.2: Solar domestic water heating system

3.2 Solar Domestic Hot Water System

A TRNSYS deck was set up (see Appendix D.1) to simulate the solar system shown in Figure 3.2. The system parameters are given in Table 3.2 These parameters are the base case (average) values from the parameters used for the multiple TRNSYS runs in Chapter 4.4.1. The results of this simulation will be given in Section 3.3.

A_c	$7m^2$	$F_R(\tau\alpha)$	0.65
F_RU_L	$12kJ/m^2hrK$	Location heater	1/3 from the top
P_{max}	$3kW = 10,800kJ/hr$	$T_{a,t}$	$20°C$
T_{db}	$6°C$	$T_{set,t}$	$55°C$
U_t	$9.5kJ/m^2hrK$	V_t	$800l$
β	45°		

Table 3.2: Important system parameters for the SDHW system

3.3 Comparison between the SDHW and the Conventional Electric System

The conventional electric system described in Section 3.1 is compared with the SDHW system described in Section 3.2.

3.3.1 Integrated Performance Data

Both the conventional electric and the SDHW system supply the same hot water load, Q_{load}

$$Q_{load} = \int_{t=0}^{t=N_h} \dot{m}_{load}(t)c_{p,load}(T_{set,t}(t) - T_{mains}(t))\mathrm{d}t = 1.77GJ \tag{3.1}$$

The conventional electric systems consumes $Q_{HW} = 1.86GJ$ to meet the load and the losses whereas the SDHW requires only $Q_{SDHW} = 0.64GJ$ to meet the same load and the losses. The solar fraction F is calculated using

$$F = \frac{Q_{HW} - Q_{SDHW}}{Q_{HW}} \tag{3.2}$$

to be $F = 65\%$.

3.3.2 Instantaneous Performance Data

Figure 3.3 displays instantaneous electrical power demand for both the electric and the SDHW system, for the first two days of August. The dotted line is the load P_{load} defined as

$$P_{load}(t) = \dot{m}_{load}(t) c_{p,load}(T_{set,l} - T_{mains}), \tag{3.3}$$

the full line is the electricity consumed by the SDHW system P_{SDHW}, and the dashed line is the electricity consumed by the conventional system P_{HW}.

The hot water draw is exactly the same for the conventional and the SDHW system and it is the average load computed in Chapter 4.4.1. It is low during night, gets higher in the morning and reaches a first peak at about 9:00 AM. Then, it lowers again during the day and reaches a second peak at 9:30 PM, and decreases to the low load during night.

The dashed line represents the electric power required by the conventional water heater P_{HW}. It shows the typical behavior of a system without variable power control. The heater turns on and stays on until the tank temperature reaches the set point temperature. Then, the heater turns off. The water temperature drops

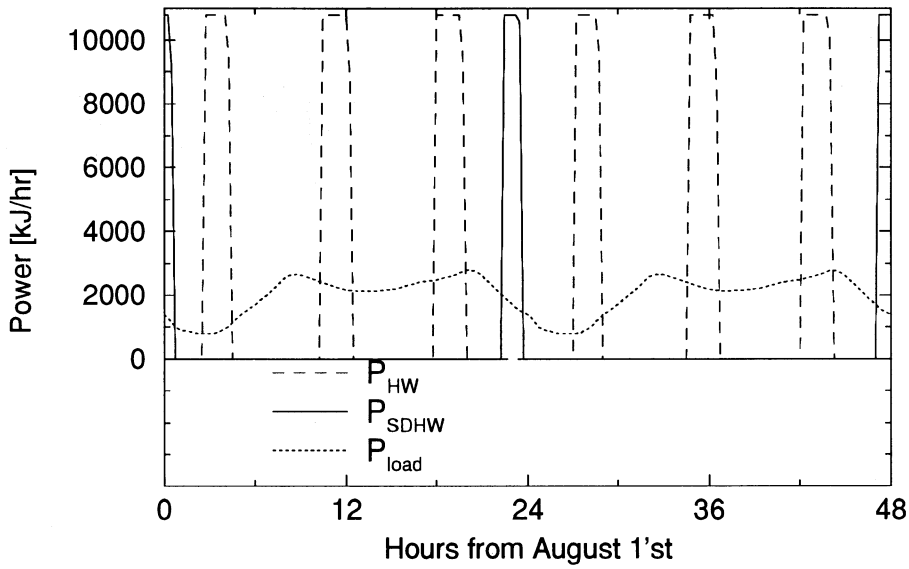

Figure 3.3: Electric power demand for the electric and the solar domestic water heating system. Plotted are the first two days of August.

due to the load and losses to the environment until it is below set point minus dead band temperature. At this point, the heater turns on again.

The full line shows the electric power required by the electric heater of the SDHW system P_{SDHW}. It shows a similar behavior to the heater for the conventional system and cycles on and off. The difference is that the heater for the SDHW systems stays off for a much longer period of time since there is energy supplied to the tank by the solar collector.

The electricity demand over a 15 minute period is also of interest. A way to present the demand is to use a cumulative frequency distribution as shown in Figure 3.4. A cumulative frequency distribution is obtained by taking all values for $P(t)$ and rearranging them so that $P(t) \geq P(t+1)$. The left most value is the maximum within the time period, the right most value is the minimum. The

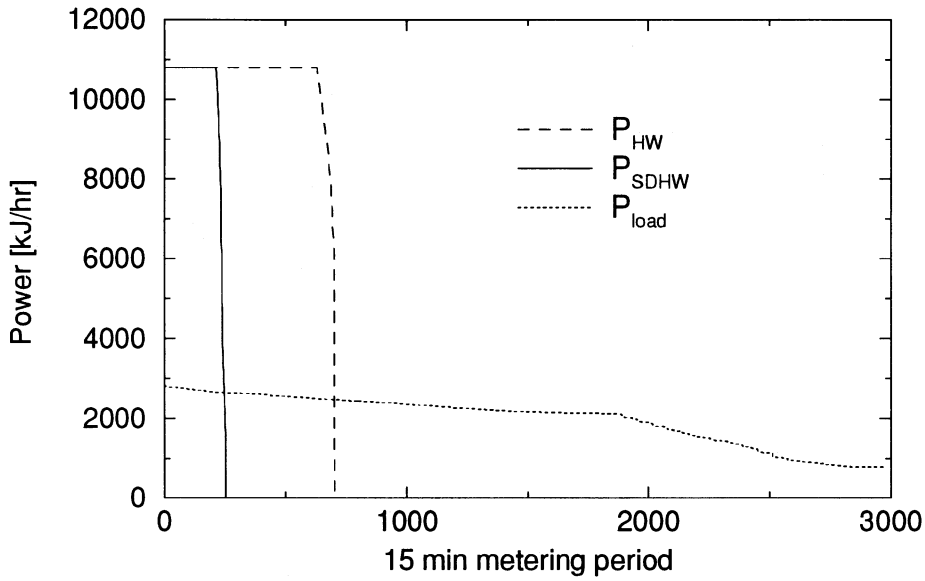

Figure 3.4: Cumulative frequency distribution for the electric and the solar domestic water heating system. Plotted are all 15 min periods for August.

area under the curve is the energy consumed during that time period. Cumulative frequency plots have to be interpreted carefully since the information about the order in which the different values occur is lost.

In Figure 3.4, the dashed, full and dotted line represent the power for the conventional system P_{HW}, the SDHW system P_{SDHW} and the load P_{load}. The peak electricity power for the single SDHW system $P_{SDHW,max}$ and the single conventional system $P_{HW,max}$ are identical and equal to the maximum power of the electric heater, P_{max}. For only one system, the electric power demand impact on the utility is the same for both conventional electric and SDHW systems.

Most utilities are summer peaking utilities with the peak load occurring in August in the early afternoon from 1:00 PM to 4:00 PM. For that reason, the performance of the systems within this time period is of interest. Figure 3.5 shows

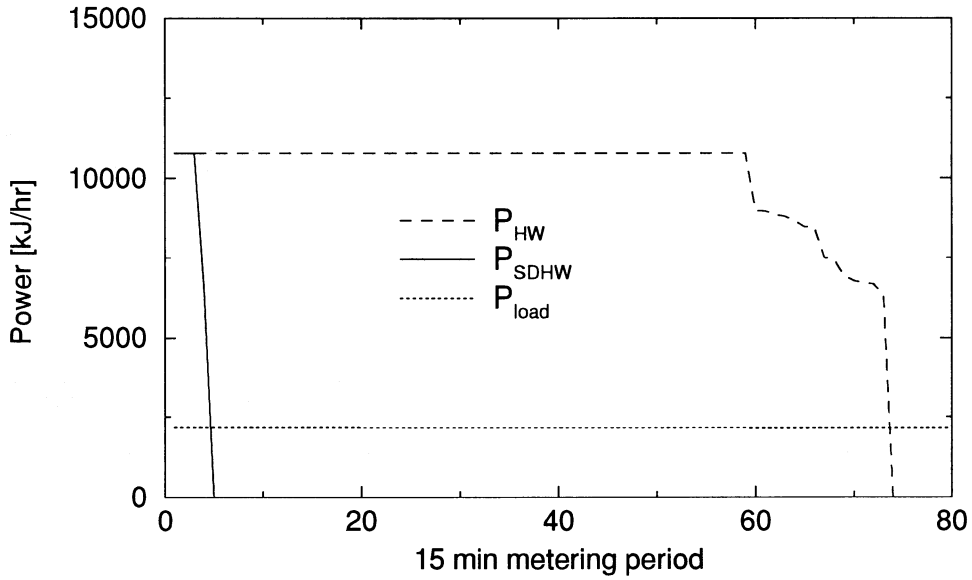

Figure 3.5: Cumulative frequency distribution for the electric water heating system. Plotted are the 80 15 minute periods between 1:00 PM and 4:00 PM for August with the highest power demand.

a cumulative frequency distribution for both systems for the hours between 1:00 PM and 4:00 PM. The graph shows the 80 left most 15 minute periods since the remaining 292 15 minute periods do not show any interesting information. P_{load} stays almost constant at its level and P_{HW} as well as P_{SDHW} stays at zero.

Figure 3.5 shows that the SDHW decreases the electricity consumption by about 90% during the peak demand. However, the peak demand is the same for both the SDHW and the conventional system. Note: The round corner for P_{HW} is caused by the simulation technique (see Section 2.4.1.1 on page 14) used for the tank model. In reality, the heater is either on or off.

3.4 Conclusions

This chapter shows the simulations and the results for of individual systems. The use of a SDHW system in place of a conventional electric water heating system yields a decrease of the energy consumption. However, the peak power demand is the same for both systems.

The question is, is it possible to draw conclusions for the impact of many system by extrapolating a simulation or measured data for a individual system? In both the SDHW and the conventional electric system, the heater is either on or off. However, for many systems, the heater is not on and off at exactly the same time. The systems are different and loads are different in pattern and magnitude for different households. Therefore, the results from the simulation of an individual system will be different from the average results of the simulation of many system.

Chapter 4

Multiple System Simulations

It was shown in Chapter 3 that employing the simulation of an individual system to estimate the impact of many systems on a utility might yield misleading results. Therefore, multiple system simulations were performed.

It is not feasible to simulate each individual system in detail. The system parameters for all systems are not know. The hot water load profile is different in magnitude and pattern for each installation.

A technique is required in order to simulate very many systems. The technique used here is based on the use of random numbers to modify base case system parameters and water loads modified within specified limits.

4.1 Methodology

The TRNSYS deck was split into four parts. Each part contains a logical block of the TRNSYS deck. This was done so that it is possible to easily create TRNSYS decks that simulate the same system with different hot water load profiles.

A range for the system parameters instead of a specific value is defined in the TRNSYS deck. For each single simulation the range for the parameter was replaced by a specific, randomly chosen value before TRNSYS was started.

The hot water load profile varies from household to household and even within a specific household from day to day (see Section 2.2 on page 8). To account for this fact, many different hot water load profiles were used in the simulations performed in this thesis. Some simulation series used different hot water load patterns consecutively without performing any randomization on the water load. Some simulation series selected a hot water load pattern randomly for a individual simulation out of a pool of different load patterns and modified the load pattern for each day of the simulation by randomly shifting it in time and scaling it in magnitude.

In order to be able to perform multiple TRNSYS simulations the process of creating a TRNSYS deck, changing parameters, creating a hot water load profile and including it into the TRNSYS deck, running TRNSYS, and processing the TRNSYS outputs has to be automized. Software has been developed to perform these tasks. The software and the methodology in detail is described in the following sections.

4.1.1 Generating TRNSYS Decks

Each individual simulation of a system requires an individual TRNSYS deck similar to the decks used for the simulations in Chapter 3. It is not practical to set up each deck manually and there is a large potential for errors when it is done manually. Therefore, it is necessary to make the construction of TRNSYS deck easier and

faster. For these reasons, the TRNSYS deck was split into four parts. Each part contains a logical block of information. The c–shell script file `gt` was written to generate TRNSYS decks automatically out of the four parts (it is listed in Appendix B.1 on page 96). It takes four arguments in the command line: `base`, `load`, `var` and `finvar`. These are the names of input files. Each input file is one block of the TRNSYS deck. They are explained below.

- `base` is a file containing the "base" TRNSYS deck, the statements between the `START` and `END` control cards. The variables uout1, uout2, uout3 and uout4 have to be used to refer to logical unit number of input or output files.
- `load` is a file containing a part of a TRNSYS deck which produces the output `[14,1]` that is used as the hot water load. The TRNSYS Units 13 and 14 are reserved for this part and may, therefore, not be used in another location of the TRNSYS deck.
- `var` is a file containing variable definitions for the TRNSYS deck. It defines only variables that are not likely to be changed.
- `finvar` is a c–shell script. It defines the variables `$prn` (filename extensions for the TRNSYS printer units), `$unom` (logical unit numbers used to refer to the names from `$prn`, have to be used in the `base` file), `$vars` (defines the names of special variables that are used for parametric studies) and `$vals` (containing the values for `$vars`).

The c–shell script file `gt` creates two files: a TRNSYS deck and a c–shell script called `runlastgt` in the current directory. `gt` is a c–shell script that executes the TRNSYS deck with a priority that can be specified by the user.

The name of the TRNSYS deck and all its output files is created from the names of the described input files. It is called `$base_$load_$var_$finvar`. The ending of the deck is `DCK`, of the TRNSYS output `.OUT`. The endings for the output producing components are specified in `$finvar`.

4.1.2 Randomizing the Parameters of the TRNSYS Deck

The system parameters are set to random values within specified limits. This task is completed by modifying a base TRNSYS deck which contains special commands used for randomization.

The FORTRAN77 program **randomdck** was written to modify an existing TRNSYS deck with random numbers. It searches through a input file for a occurrence of the the string `|r|-ll.ll+uu.uu` and replaces it by a random number between the lower limit `ll.ll` and the upper limit `uu.uu`. The program listing is in Appendix E.1.

The `|r|` expression is typically used in a TRNSYS equation statement and a TRNSYS variable is set to a random number, e.g. `TdbTnk=|r|+02.50+07.50` sets the variable `TdbTnk` to a value between inclusive 2.50 and 7.50.

The program **randomdck** reads three or more parameters from the standard input. The standard input is either input via the keyboard or a pipe from a control file. The first input is the full path name of a file containing random numbers between 0 and 1. The second parameter is the name of the input TRNSYS deck and the third is the name of the output TRNSYS deck. After the successful generation of the output file, **randomdck** attempts to read the next parameter from standard input. If it reads the "end of file marker" it exits, otherwise it dumps

the last parameter and reads the name of the next input file and name of the next output file. A typical control file would be:

```
random.data
old-1.dck
new-1.dck
more
old-2.dck
new-2.dck
```

This control file tells randomdck to read the random numbers from the disk file `random.data`, generate `new-1.dck` from `old-1.dck` and, after reading the separator `more`, generate `new-2.dck` from `old-2.dck` and exit.

4.1.3 Generating Random Numbers

The FORTRAN77 program `randomdck` does not generate random numbers itself. An algorithm for generating random numbers [8] in FORTRAN77 was tested and it was found that this algorithm does not produce good random numbers. The period of the random numbers is less than 100,000. It produces the same numbers every time it is called with the same seed. Therefore, Xlisp–Stat was used to generate the random numbers. Xlisp–Stat has a built in generator (see Appendix A.2).

4.1.4 Randomizing the Hot Water Load

A variety of different hot water load profiles were used in this thesis. They are displayed in Appendix C. In order to randomize the hot water load for the TRNSYS simulations the following steps were performed.

1. A basic daily load pattern was randomly selected out of a pool of different daily load patterns

2. The basic daily pattern was shifted by a random number between plus or minus one hour for every day of the simulation

3. The basic daily load was scaled with a random number between 0.75 and 1.25 for every day of the simulation

The water load was randomized using the Xlisp-Stat program `randomize-load` (see Appendix A.1 on page 92). The program performs the steps listed above given the file names of the daily load patterns, the maximum and minimum shift and the maximum and minimum scale. The output of the program, a randomized monthly hot water load pattern, is written to a disk file.

4.1.5 System Simulation

Typically a series of commands has to be executed for one simulation. For the multiple TRNSYS runs, these commands have to be repeated a specified number of times. A c–shell script file was used to execute the required commands and is displayed in Appendix B.2 on page 99.

The c–shell script file is set up for 4,000 runs. It saves the results of the TRNSYS simulation to a disk file every 100 runs. The inner loop of the script file runs Xlisp–Stat to generate random numbers and to randomize the hot water load profile. Then, the TRNSYS deck is built by `gt` using the new, randomized deck and load. TRNSYS is run, the monthly output is added to the sum of the preceding simulations, and the loop is closed.

4.2 Conventional Electric Hot Water System

The first test for the multiple TRNSYS runs is to determine if the characteristic on/off pattern which was seen for the individual TRNSYS runs still occurs. A multiple TRNSYS run deck was set up to simulate a conventional electrical hot water system displayed in Figure 3.1 on page 23.

4.2.1 Simulation Series A

The hot water loads for these simulations were not randomized. The loads A–T and WA–WI (see Appendix C on page 100) were used in sequence. The system parameters and their limits for the randomization used for the simulations are shown in Table 4.1.

U_t	$9.5kJ/m^2hrK \pm 40\%$	P_{max}	$3kW = 10,800kJ/hr$
$T_{set,t}$	$55°C$	T_{db}	$5°C \pm 40\%$
V_t	$240l \pm 40\%$	H_t	$0.6m \pm 20\%$

Table 4.1: System parameters for multiple TRNSYS runs series A

The runs were performed in groups of 29 simulations since 29 different hot water load patterns were used. Since simulations for 36 groups were performed, the total number of TRNSYS runs N_S is $N_S = 29 \times 36 = 1,044$ runs. Figure 4.1 shows the power demand and the load for the 1,044 systems normalized to one system P_{HW} and P_{load}.

$$P_{HW}(t) = \frac{P_{HW,total}(t)}{N_S} = \frac{\sum_{i=1}^{N_S} P_{HW,i}(t)}{N_S} \tag{4.1}$$

and

$$P_{load}(t) = \frac{P_{load,total}(t)}{N_S} = \frac{\sum_{i=1}^{N_S} P_{load,i}(t)}{N_S} \tag{4.2}$$

with $P_{HW,total}$ electric power demand for the sum of all systems

$P_{HW,i}$ power demand for system i

P_{HW} normalized electric power demand

$P_{load,total}$ hot water load for the sum of all systems

$P_{load,i}$ hot water load for system i

P_{load} normalized hot water load

N_S Number of systems/simulations

4.2.1.1 Instantaneous Performance

The peak electricity demand is expected to be considerably lower than the maximum total power of all heaters, since it is very unlikely that the heater of all 1,044 systems are operating at the same time. Figure 4.1 the plot of the power demand during the first two days of August shows that the maximum of P_{HW} in the first two days of August is $3,300kJ/hr$. The cumulative frequency distribution of the power demand during all 15 minute periods in August (Figure 4.2) shows that the maximum in the month is $3,570kJ/hr$ which is 1/3 of the maximum power of the heating element $P_{max} = 10,800kJ/hr$.

The average tank size is $240l$. Ignoring the losses, a fully heated tank is capable of meeting the load of $300l$ per day for 19 hours. Therefore, one would expect that a time delay between hot water load and electricity demand would be seen. Surprisingly, this time delay does not show up in the plot in Figure 4.1.

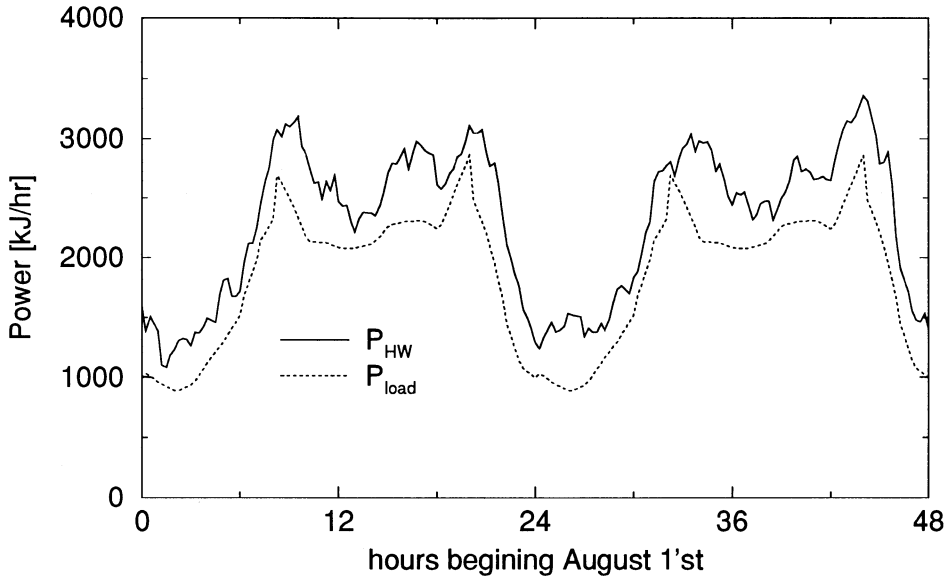

Figure 4.1: Electrical power demand of 1,044 conventional electric systems P_{HW} and the corresponding hot water load P_{load} normalized to one system in multiple TRNSYS runs series A

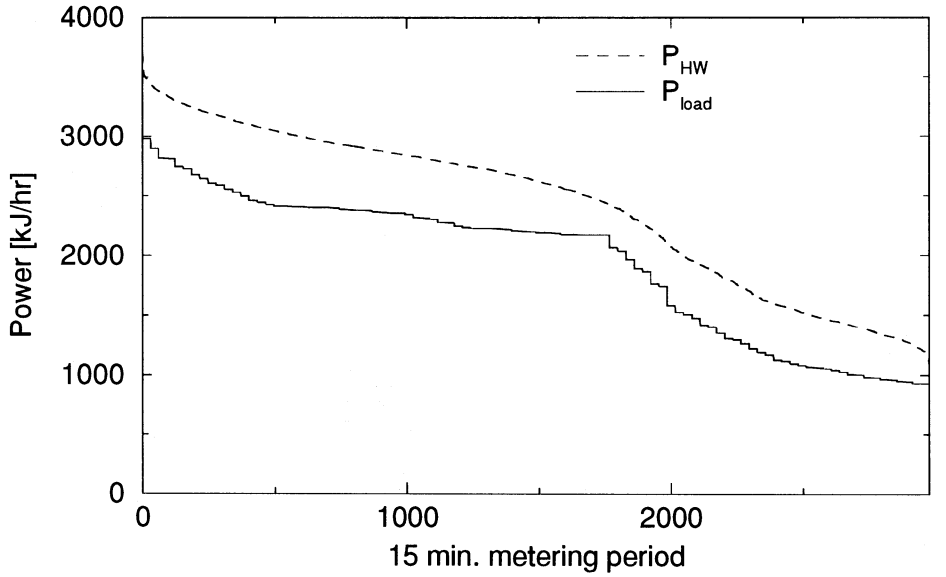

Figure 4.2: Cumulative frequency distribution of the power demand normalized to one system for 1,044 conventional electric systems in multiple TRNSYS runs series A. Plotted are all 15 minute periods of the month August.

4.2.1.2 Estimating the Power Demand

From Figure 4.1, it is concluded that the electrical demand P_{HW} can be approximated by the sum of the hot water load P_{load} and losses P_{loss} at any time. The losses from the tank are

$$P_{loss}(t) = \sum_{i}^{N_n} \Big((T_{t,i}(t) - T_a(t)) U_{L,i} \Big) \tag{4.3}$$

with N_n number of nodes

$T_{t,i}$ temperature of node i

T_a ambient temperature for the tank

$U_{L,i}$ loss coefficient for node i

The temperatures of the tank nodes change only within the dead band of the controller which is $5°C \pm 40\%$. The ambient temperature for the tank is constant, since the tank is located within a building, generally in the basement. Therefore, the losses can be assumed to be constant and can be calculated by

$$P_{loss} = \frac{\int_{t=0}^{N_h} \Big(P_{HW}(t) - P_{load}(t) \Big) \mathrm{d}t}{N_h} \tag{4.4}$$

with N_h being the number of hours within the simulated time periods (744 for August). For the TRNSYS runs in Section 4.2.1, Equation 4.4 yields $P_{loss} = 471 kJ/hr$.

A way to estimate $P_{HW}(t)$ without running a great number of simulations would be useful. This can be done by performing a single TRNSYS simulation with the

base case (average) system parameters and the average hot water load. P_{loss} can be estimated using

$$P_{loss} = \frac{\int_{t=0}^{N_h} P_{HW,avg}(t)\mathrm{d}t - \int_{t=0}^{N_h} P_{load,avg}(t)\mathrm{d}t}{N_h} \tag{4.5}$$

Equation 4.5 yields $P_{loss} = 485kJ/hr$ which is only 3% greater than the result from Equation 4.4.

Another way to estimate P_{loss} is the use of Equation 4.3 which is rewritten to

$$P_{loss} = U_t A_t \Delta T \tag{4.6}$$

A cylindrical tank with the volume $V_t = 0.24m^3$ and the height $H_t = 0.6m$ has a surface area $A_t = 2.2m^2$. $U_t = 9.5kJ/m^2Khr$ is given in Table 4.1. ΔT is the temperature difference between the water in the tank and the ambient temperature of the tank. The ambient temperature is assumed to be $20°C$. The temperature of the water varies with time and tank node. The temperature of the top node never goes below $T_{set,t} - T_{db} = 50°C$. The temperature of the bottom node probably goes down to $T_{mains} = 17°C$. The average water temperature is estimated to be $40°C$. With these data, Equation 4.5 yield $P_{loss} = 423kJ/hr$. Table 4.2 compares the estimates of the losses obtained by different methods. It shows that the estimate obtained by a single TRNSYS run of the average system supplying the average load yield a result that differs less than 3% from the estimate obtained by performing multiple TRNSYS runs. Estimating the tank losses by the use of the tank loss coefficient and an estimate of the overall average tank temperature yield a loss that is 10% too small.

methodology	P_{loss}
running multiple TRNSYS simulations and use Equation 4.4	$471kJ/hr$
running a single TRNSYS simulation of the base (average) system that meets the average hot water load and use Equation 4.5	$485kJ/hr$
computing the tank surface area, estimating the average tank temperature and use Equation 4.6 with the tank loss coefficient U_t for the base case system	$423kJ/hr$

Table 4.2: Comparing P_{loss} estimates acquired by different methods

The electricity can now be estimated knowing the constant losses and the hot water load

$$P_{est}(t) = P_{load,avg}(t) + P_{loss} \tag{4.7}$$

Equation 4.7, with $P_{loss} = 471kJ/hr$, was used to generated Figure 4.3, which is a plot of the estimated power demand versus the TRNSYS computed power demand. A linear regression yields the equation $y = 0.88 \times x + 307$ and the regression coefficient $r = 0.96$. A good agreement between estimation and "real" data can be seen. The estimate tends to be to be too high for a small power demand and too low for a high power demand (see Table 4.3).

P_{TRNSYS}		$P_{estimated}$	error
1,000	$\times 0.88 + 307 =$	1,187	+19%
4,000	$\times 0.88 + 307 =$	3,827	−4%

Table 4.3: Comparing estimated with TRNSYS power demand for series A using Equation 4.7 with $P_{loss} = 471kJ/hr$.

In order to investigate the impact of the constant losses P_{loss} on the estimate for the power demand, Equation 4.7 is used with $P_{loss} = 423kJ/hr$ to compute

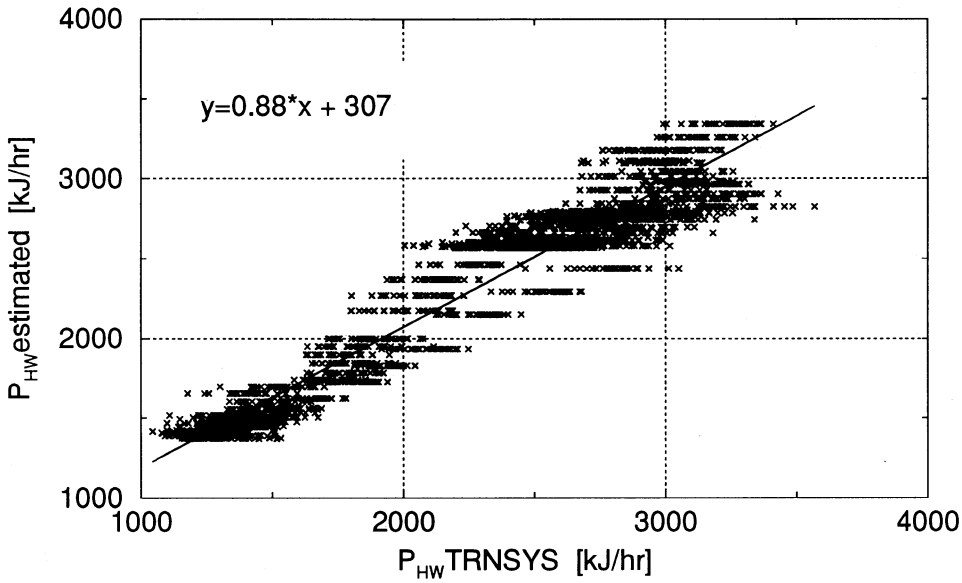

Figure 4.3: Estimated versus simulated power demand for series A using $P_{loss} = 471kJ/hr$.

Figure 4.4. A linear regression gives the correlation coefficient $r = 0.96$ and the linear equation $y = 0.88 \times x + 245$. Table 4.4 gives the estimates for $P_{TRNSYS} = 1,000$ and $P_{TRNSYS} = 4,000$. It shows that low power demand is over estimated and high demand is under estimated. Comparing Table 4.3 with Table 4.4 and Figure 4.3 with Figure 4.4 shows that a decrease of P_{loss} by 10% improves the estimate for low power demands but makes the estimate for high power demand worse.

P_{TRNSYS}		$P_{estimated}$	error
1,000	$\times$ 0.88 + 245 =	1,125	+13%
4,000	$\times$ 0.88 + 245 =	3.765	−6%

Table 4.4: Comparing estimated with TRNSYS power demand for series A using Equation 4.7 with $P_{loss} = 423kJ/hr$.

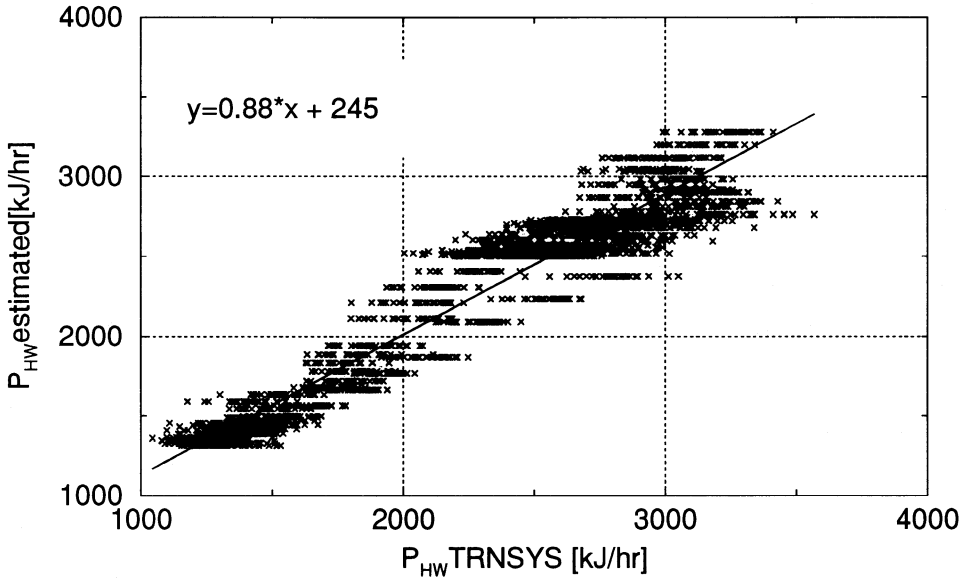

Figure 4.4: Estimated versus simulated power demand for series A using $P_{loss} = 423kJ/hr$

It is important to realize that the trnsys output is the result of 1,044 system simulations using 29 different hot water load patterns and 1,044 randomly generated conventional hot water systems. The simulations require many hours of computing time. Whereas the estimated performance is obtained by estimating the tank losses and the average hot water load profile, which can be easily done with considerably less computational effort.

4.2.2 Simulations Series B

The preceding section shows that there is a good agreement between simulated power demand and estimated power demand. In order to investigate if this agreement is dependent on the load profile, simulation series B was performed. In series B a conventional electric water heating system was simulated with the same

system parameters like the system in the simulation series A (see Section 4.2.1). The system parameters are listed in Table 4.5. however, different hot water loads were used. The daily water use load patterns were A–J, M–U, and WA–WI from Appendix C on page 100.

U_t	$9.5kJ/m^2hrK \pm 40\%$	P_{max}	$3kW$
$T_{set,t}$	$55°C$	T_{db}	$5°C \pm 40\%$
V_t	$240l \pm 40\%$	h_t	$0.6m \pm 20\%$

Table 4.5: System parameters for multiple TRNSYS runs series B

4.2.2.1 Instantaneous Performance

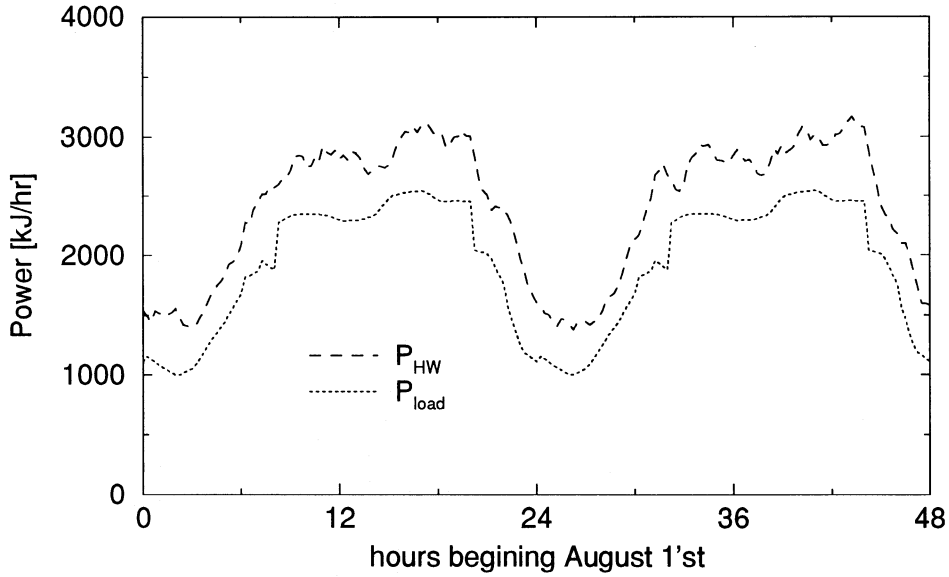

Figure 4.5: Electrical power demand of 4,144 conventional electric system P_{HW} and the corresponding hot water load P_{load} in multiple TRNSYS runs series B normalized to one system. Plotted for the first two days of August.

Figure 4.5 shows the electrical demand P_{HW} and the hot water load P_{load} for the first two days of August of the multiple TRNSYS simulations series B. Since this is a conventional electric system all days are very similar to each other. One can see that the electricity demand P_{HW} follows the hot water load P_{load}.

4.2.2.2 Estimating Power Demand

The tank losses were estimated using Equation 4.4 which yields $P_{loss} = 488kJ/hr$ and differs from the losses for series A by 3%. Using Equation 4.7 to calculate P_{est} and plotting P_{est} versus the TRNSYS output yields Figure 4.6. A linear regression gives the correlation coefficient $r = 0.98$ and the linear equation $y = 0.92 \times x + 185$. The linear regression is used for Table 4.6.

P_{TRNSYS}		$P_{estimated}$	error
1,000	$\times$ 0.92 + 185 =	1,105	11%
4,000	$\times$ 0.92 + 185 =	3.865	3%

Table 4.6: Comparing estimated with TRNSYS power demand for series B using Equation 4.7 with $P_{loss} = 488kJ/hr$.

The agreement between the estimation and the simulation is better for the series B than for series A (compare to Figure 4.3 and Figure 4.4). The high demand is less under–estimated and the low demand is less over–estimated. One possible reason for the improvement, the larger number of runs, will be discussed later.

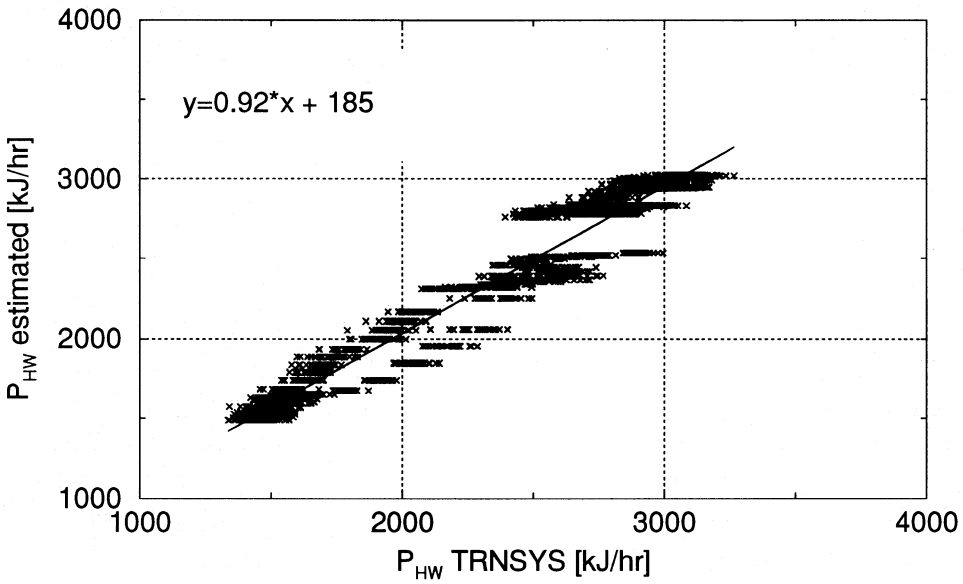

Figure 4.6: Estimated versus simulated electrical power demand for series B

4.2.3 Conclusions

The energy and power demand of a conventional electric water heating system was analyzed in Section 4.2. The analyses was done using multiple TRNSYS simulations of systems with system parameters chosen randomly within specified limits. 29 different hot water load patterns were used for simulation series A and 28 for simulation series B.

It was shown that the electrical power demand can be estimated from the average hot water load profile $P_{load,avg}$ and constant loss term P_{loss} using

$$P_{est}(t) = P_{load,avg} + P_{loss} \tag{4.8}$$

The losses P_{loss} can be estimated from the tank specifications. However, it is suggested that a single TRNSYS simulation be run for the base case (average) system with the average hot water load in order to estimate the losses.

4.3 SDHW System

In the multiple TRNSYS runs series A (Section 4.2.1) and series B (Section 4.2.2) for a conventional electric hot water system it was shown that the on/off pattern that was shown in the simulation of an individual system (Section 3.1) disappears when many simulation are run. It was shown as well that the maximum power demand is significantly reduced in the multiple TRNSYS simulations compared to the single TRNSYS simulation.

Multiple TRNSYS runs were performed for the SDHW system shown in Figure 3.2 on page 23 to determine the maximum electric power demand of an ensemble of SDHW systems and to investigate if the on/off pattern (shown in Figure 3.3) disappears in the same way as for the conventional electric water heating system.

4.3.1 Simulations Series D

As in series A, the hot water loads A–T and WA–WI from Appendix C were used in sequence. Since there were 29 different hot water load profiles, the runs were performed in groups of 29. The total number of runs N_s performed was $N_s = 70 \times 29 = 2,030$ simulations. Important system parameters are displayed in Table 4.7

U_t	$9.5kJ/m^2hrK 50\%$	P_{max}	$3kW = 10,800kJ/hr$
$T_{set,t}$	$55°C$	$T_{db,t}$	$5°C \pm 80\%$
A_c	$7m^2 \pm 30\%$	$T_{db,c}$	$6°C \pm 20\%$
β	$45 \pm 30\%$	$F_R(\tau\alpha)$	$0.65 \pm 20\%$
F_RU_L	$12kJ/m^2hrK \pm 20\%$	b_0	$0.1 \pm 20\%$

Table 4.7: System parameters for multiple TRNSYS runs series D

The electrical power demand of the auxiliary heater for the sum of all 2,030 systems normalized to one system is displayed in Figure 4.7 and Figure 4.8. The dotted line is the water load P_{load} and the full line is the electrical demand off the auxiliary heater P_{SDHW}.

$$P_{SDHW}(t) = \frac{P_{SDHW,total}(t)}{N_S} = \frac{\sum_{i=1}^{N_S} P_{SDHW,i}(t)}{N_S} \tag{4.9}$$

and

$$P_{load}(t) = \frac{P_{load,total}(t)}{N_S} = \frac{\sum_{i=1}^{N_S} P_{load,i}(t)}{N_S} \tag{4.10}$$

with $P_{HW,total}$ electric power demand for the sum of all SDHW systems

$P_{HW,i}$ power demand for system i

$P_{load,total}$ hot water load for the sum of all SDHW systems

$P_{load,i}$ hot water load for system i

N_S Number of systems/simulations

Figure 4.7 shows the performance of the systems during two consecutive good weather days. The electrical demand follows the hot water load until 8:30 AM. At this time, the electrical demand goes down while the hot water load increases. P_{SDHW} decreases until noon and stays at a very low level of about $150kJ/hr$ until 6:00 PM. After that, P_{SDHW} increases to P_{load} and, afterwards, follows the decreasing P_{load} to the low load during the night. Figure 4.8 shows another good weather day followed by a bad weather day. The electric energy demand P_{SDHW} follows the hot water load P_{load} during the entire bad weather day and does not decrease during the sunshine hours as it does for the good weather days.

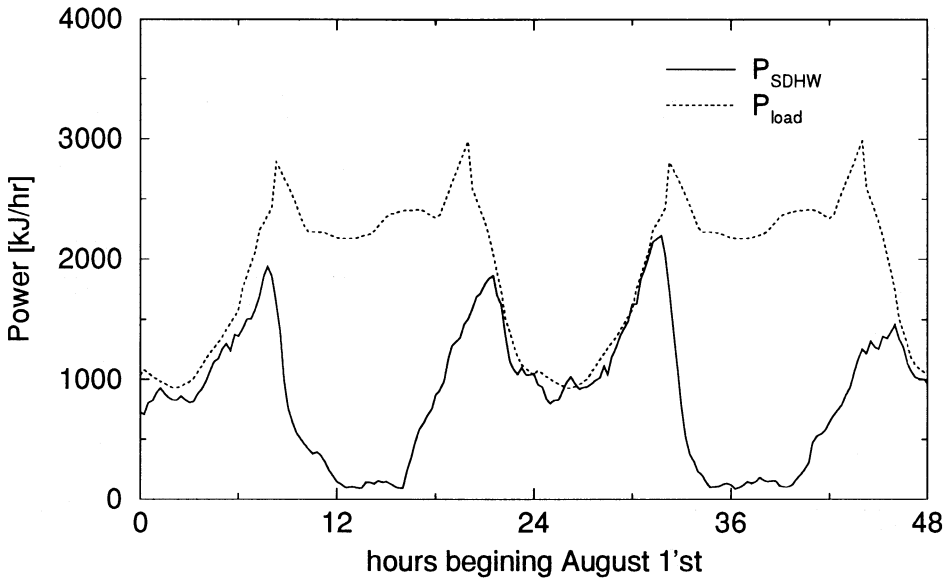

Figure 4.7: Electrical power demand for 2,030 SDHW systems P_{SDHW} in multiple TRNSYS runs series D normalized to one system. Plotted for the first two days of August.

The cumulative frequency distribution of the power demand during all 15 minute periods in August is given in Figure 4.9. The peak electricity demand is $P_{SDHW,max} = 2,980kJ/hr$ which is 1/4 of the maximum power $P_{max} = 10,800$ of the auxiliary heater. The on/off behavior of the heater does not occur for the average of the 2,030 system simulated here.

4.4 Comparison of the SDHW System with the Conventional Electric System

In order to compare the two systems, one has to be sure that both the conventional electric and the SDHW system supply exactly the same hot water load and that

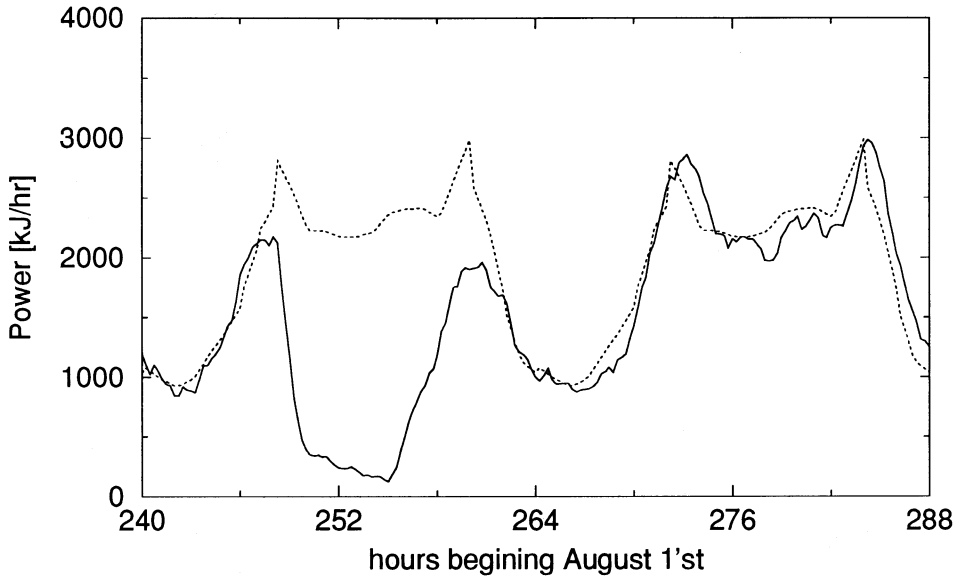

Figure 4.8: Electrical power demand for 2,030 SDHW systems P_{SDHW} in multiple TRNSYS runs series D normalized to one system. Plotted for August 11 and August 12.

the tanks have the same parameters, e.g., loss coefficient and power of the electric heating element. This requirement was achieved by simulating both the SDHW and the conventional electric system with one single TRNSYS deck.

A TRNSYS deck was written containing the system parameters and the required information for the randomization. Its information flow is described in Figure 4.10. The TRNSYS deck contains two tanks; one is connected to the solar collector and one is not. Both tanks are connected to the same hot water load profile generator. The electricity demand of the heater in the solar system and the electricity demand of the conventional electric system are logged to a disk file.

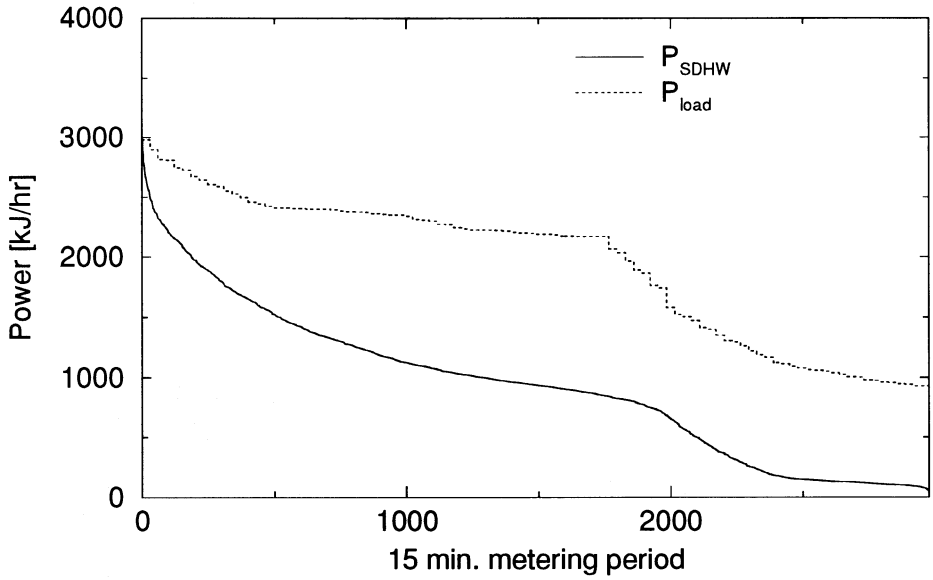

Figure 4.9: Cumulative frequency distribution of the power demand normalized to one system for 2,030 SDHW systems in multiple TRNSYS runs series D. Plotted are all 15 minute periods of the month August.

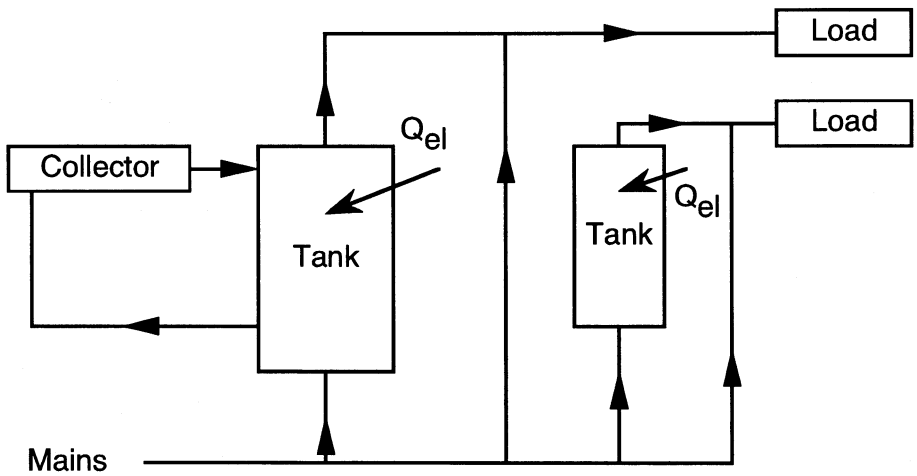

Figure 4.10: Information flow diagram for the TRNSYS deck to compare a conventional electric with a SDHW system

All power demands P and energy usages Q computed or plotted in this section are the results of many simulations normalized to one system using

$$P_{SDHW}(t) = \frac{P_{SDHW,total}(t)}{N_S} = \frac{\sum_{i=1}^{N_S} P_{SDHW,i}(t)}{N_S} \tag{4.11}$$

$$P_{HW}(t) = \frac{P_{HW,total}(t)}{N_S} = \frac{\sum_{i=1}^{N_S} P_{HW,i}(t)}{N_S} \tag{4.12}$$

$$P_{load}(t) = \frac{P_{load,total}(t)}{N_S} = \frac{\sum_{i=1}^{N_S} P_{load,i}(t)}{N_S} \tag{4.13}$$

with

$P_{SDHW,total}$	electric power demand for the sum of all SDHW systems
$P_{SDHW,i}$	power demand for SDHW system i
P_{SDHW}	normalized electric power demand of the SDHW systems
$P_{HW,total}$	electric power demand for the sum of all conventional electric systems
$P_{HW,i}$	power demand for the conventional electric system i
P_{HW}	normalized electric power demand
$P_{load,total}$	hot water load for the sum of all SDHW or all conventional electric systems
$P_{load,i}$	hot water load for the SDHW system i or the conventional electric system i

(continued on next page)

(continued from previous page)

P_{load} normalized hot water load

N_S Number of systems/simulations

4.4.1 Simulations Series F

Simulation series F was performed to compare the maximum electric demand and the electrical energy consumption of a SDHW with a conventional electric system. The impact of the number of simulation in a series on the results was analyzed using the simulation series F. 10,000 individual simulations were performed in series F and the results were combined into 100 groups of 100 simulations.

The hot water load for both the conventional electric and SDHW system was randomized. For each individual run, a basic daily hot water load profile was chosen by random selection out of the loads K, L, M, P, Q–T, and WA–WI (see Appendix C). This basic daily load pattern was modified for each day of the simulation by shifting randomly in time between minus one and plus one hour and by scaling it by a random number between 0.75 and 1.25. The base system parameters and the ranges are listed in Table 4.8.

$V_{t,SDHW}$	$800l \pm 40\%$	$V_{t,HW}$	$240l \pm 40\%$
U_t	$9.5kJ/m^2hrK \pm 50\%$	P_{max}	$3kW = 10,800kJ/hr$
$T_{set,t}$	$55°C$	$T_{db,t}$	$6°C \pm 50\%$
A_c	$7m^2 \pm 30\%$	β	$45 \pm 30\%$
$F_R(\tau\alpha)$	$0.65 \pm 20\%$	F_RU_L	$12kJ/m^2hrK \pm 20\%$
b_0	$0.1 \pm 20\%$	$T_{udb,c}$	$6°C \pm 20\%$

Table 4.8: System parameters for multiple TRNSYS runs series F

4.4.1.1 Monthly Performance

The monthly energy consumption of 10,000 systems normalized to one system in August for both the SDHW and the conventional electric system is given in Table 4.9. The total load normalized to one system for both the SDHW and the conventional electric system is $Q_{load} = 1.78GJ$. The electrical energy required to meet the load is $Q_{HW} = 1.85GJ$ for the conventional electric system and $Q_{SDHW} = 0.70GJ$ for the SDHW system. The average solar fraction is

$$F = \frac{Q_{HW} - Q_{SDHW}}{Q_{HW}} = 62\% \tag{4.14}$$

System	Q_{load}	$Q_{electric}$	Solar fraction
conventional electric	$1.78GJ$	$1.85GJ$	—
SDHW	$1.78GJ$	$0.70GJ$	62%

Table 4.9: Monthly electric energy consumption of the conventional electric and SDHW system normalized to on system for multiple TRNSYS runs series F

4.4.1.2 Instantaneous Electrical Demand

The instantaneous electrical power demand of 4,000 randomly selected systems normalized to one system is given in Figure 4.11 and Figure 4.12. It can be seen that the electricity demand of the conventional system P_{HW} approximately follows the hot water load P_{load} plus some nearly constant losses P_{loss} in both Figures (compare to Section 4.2). The electricity demand of the SDHW system P_{SDHW} has a different pattern in Figure 4.11 and Figure 4.12. Figure 4.11 represents the first two days of August, which had two good weather days. P_{SDHW} and P_{HW}

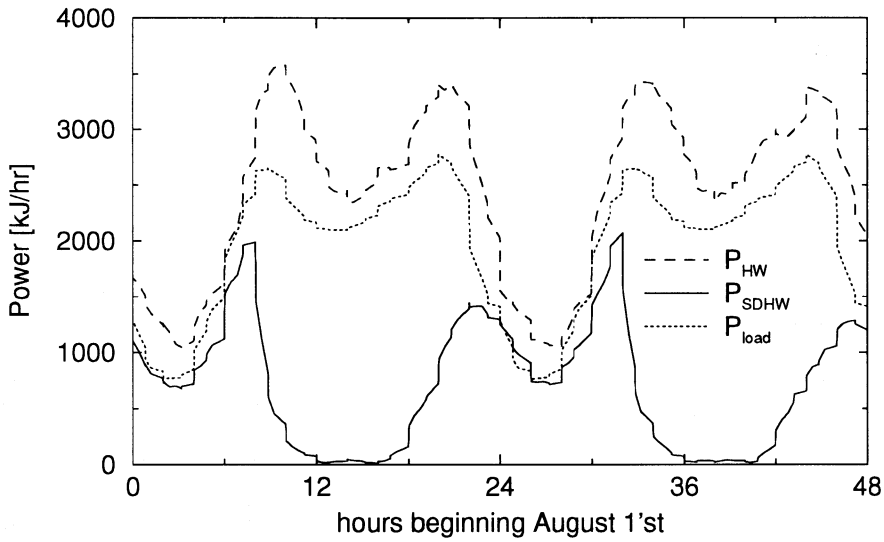

Figure 4.11: Electric power demand comparison between 4,000 conventional electric and SDHW systems in multiple TRNSYS runs series F normalized to one system. Plotted for the first two days of August.

are almost the same in the night and in the early morning hours. In the morning hours, from about 6:30 AM the solar collector performs very well. The hot water load is met by the solar collector and no electric backup is required. Figure 4.12 is the plot for two bad weather days and shows that the solar collector performs poor. Even so, the electricity required by the SDHW system is less than the electricity required by the conventional electric system.

The objective of this thesis is to compare the SDHW with the conventional electric water heating system. For this study the hot water load pattern is not affected by the replacement of the electric system by a SDHW system. Therefore, the impact of the SDHW system can be determined by computing the reductions

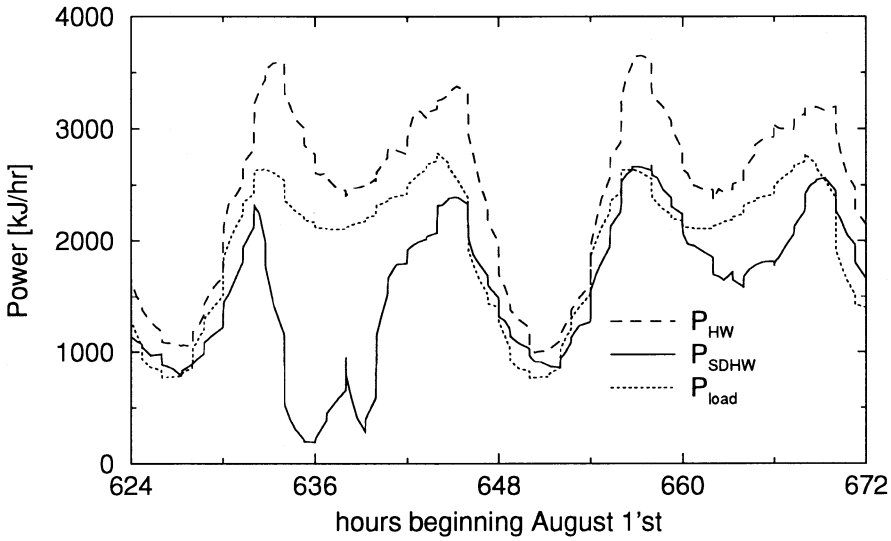

Figure 4.12: Electrical power demand comparison between 4,000 conventional electric and SDHW systems in multiple TRNSYS runs series F normalized to one system. Plotted for August 26 and August 27.

in power and energy demand by the SDHW system. We define ζ the ratio of the maximum electric power demand of the SDHW to the conventional electric system

$$\zeta = \frac{P_{max,SDHW}}{P_{max,HW}} \tag{4.15}$$

with $P_{max,SDHW}$ the maximum electrical power demand of the SDHW system; $\max[P_{SDHW}(t)]$

$P_{max,HW}$ the maximum electrical power demand of the conventional electric system; $\max[P_{HW}(t)]$

The ratio of the electric energy is ν (which is one minus the solar fraction)

$$\nu = \frac{Q_{SDHW}}{Q_{HW}} \tag{4.16}$$

The load factor L of all systems is also of interest. The load factor is the ratio of the energy consumed during a time period, e.g. a month, divided by the product

of the maximum power demand during the time period and the length of the time period.

$$L = \frac{\int_{t=t_{start}}^{t_{end}} P(t)\mathrm{d}t}{P_{max,consumed}(t_{end} - t_{start})} \tag{4.17}$$

The ratio of the load factors λ is defined by

$$\lambda = \frac{L_{SDHW}}{L_{HW}} \tag{4.18}$$

Figure 4.13 shows the cumulative frequency distribution of the power demand of the SDHW system P_{SDHW}, of the conventional electric system P_{HW}, and the corresponding load P_{load}. P_{SDHW} has its maximum at $2,890kJ/hr$ falls very fast to under $2,000kJ/hr$ after 200 time periods and is below $500kJ/hr$ at 2,050 periods. The power demand of the conventional electric system P_{HW} starts with its peak of $3,680kJ/hr$ stays above $2,500kJ/hr$ up to 1,800 periods and falls to its minimum of $940kJ/hr$.

The cumulative frequency distribution of the power demand during the peak period from 1:00 PM to 4:00 PM of the SDHW system and the conventional electric system is given in Figure 4.14. P_{HW} is almost flat; the maximum is $2,740kJ/hr$ and the minimum is $2,320kJ/hr$. The power demand of the SDHW system shows a totally different behavior. It falls very fast from the maximum of $1,910kJ/hr$ to $130kJ/hr$ at 70 time periods and descends very slowly to its minimum of $10kJ/hr$.

The power, energy, and load factor ratios can be obtained from the cumulative frequency distributions, e.g. Figure 4.13 or Figure 4.14. The maximum power ratio ζ is the ratio of the two left most points for P_{HW} and P_{SDHW}. The energy ratio ν is the ratio of areas under the P_{SDHW} curve and the P_{HW} curve. From Figure 4.13

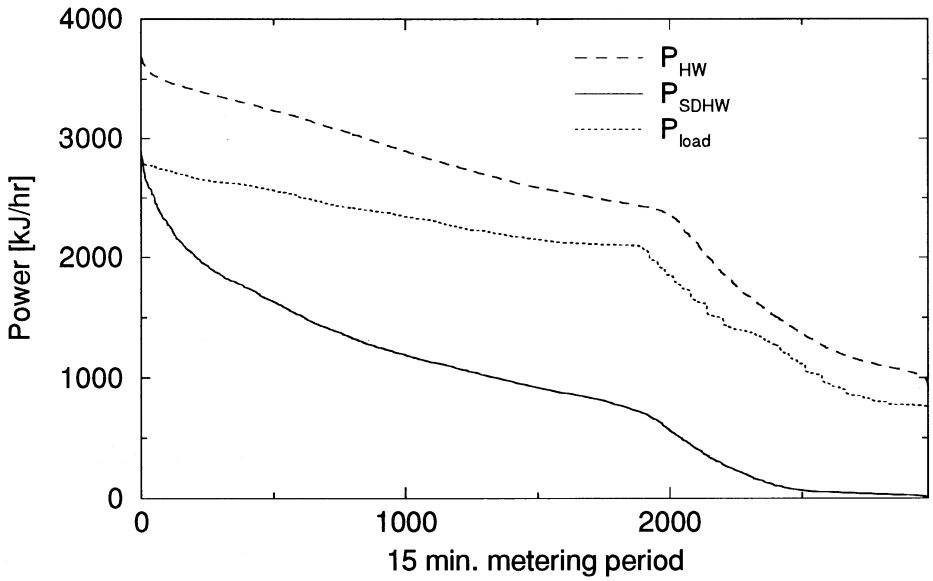

Figure 4.13: Cumulative frequency distribution of the power demand normalized to one system for 4,000 conventional electric and SDHW systems in multiple TRNSYS runs series F. Plotted are all 15 minute periods of the month August.

$\zeta = 0.79$, $\nu = 0.38$ and $\lambda = 0.48$. These values show that the peak electric demand is reduced by 21%, the energy consumption in August by 62% and the load factor by 52%. Figure 4.14, the cumulative frequency distribution for the 15 minute periods between 1:00 PM and 4:00 PM of August yield $\zeta = 0.70$, $\nu = 0.09$ and $\lambda = 0.13$, the peak electric demand is reduced by 30%, the energy consumption by 91% and the load factor by 87%. These values show that the SDHW system does reduce both power demand and energy consumption.

Figure 4.14 shows that the electrical demand for the SDHW system P_{SDHW} is greater than $500kJ/hr$ for 13% of the 15 minute periods from 1:00 PM to 4:00 PM and greater than $1,000kJ/hr$ for 9%. Since the information about the order in which the demand occurs is lost in the cumulative frequency distribution, it is not

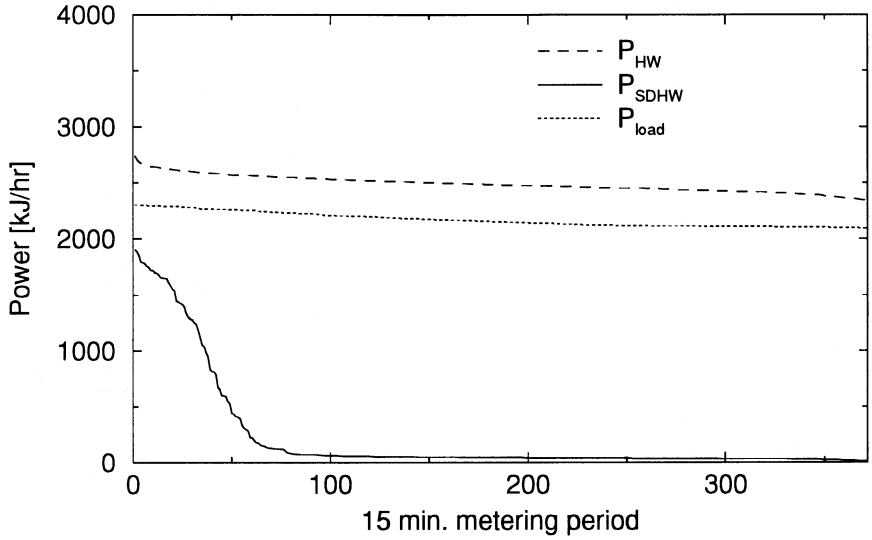

Figure 4.14: Cumulative frequency distribution of the power demand normalized to one system for 4,000 conventional electric and SDHW systems in multiple TRNSYS runs series F. Plotted are 15 minute periods of the month August between 1:00 PM and 4:00 PM.

possible to directly determine how many days the electrical demand goes above a specified limit. Table 4.10 gives the number of days† with a power demand above a specified limit for both the SDHW and the conventional electric system.

Table 4.10 shows there are three days with the electric demand of the SDHW system P_{SDHW} over $1,000kJ/hr$ and six days with P_{SDHW} over $500kJ/hr$ from 1:00 PM to 4:00 PM, whereas the demand of the conventional electric system P_{HW} exceeds $2,500kJ/hr$ in all but one day during August.

The daily irradiation H was found to be $7,536MJ/m^2$, $6,278MJ/m^2$ and $3,141MJ/m^2$ for the days in which the power demand of the SDHW systems was over $1,000kJ/hr$ between 1:00 PM and 4:00 PM. The daily irradiation values

†a day is counted if there is a least one 15 minute period within the specified time limits in which the electric demand exceeds the specified limit.

		number of days					
limit $[kJ/hr]$		500	1,000	1,500	2,000	2,500	3,000
1:00 PM–4:00 PM	HW	31	31	31	31	30	0
	SDHW	6	3	3	0	0	0
all hours	HW	31	31	31	31	31	30
	SDHW	31	31	30	19	5	0

Table 4.10: Number of days with a power demand above a specified limit for one or more 15 minute periods

were $11,451 MJ/m^2$, $13,736 MJ/m^2$ and $9,987 MJ/m^2$ for the three days in which the maximum power demand of the SDHW systems was between $500 kJ/hr$ and $1,000 kJ/hr$. It can be seen that these irradiation values for the SDHW peak power demand days are considerably lower than the monthly average daily irradiation for Madison in August which is $\bar{H} = 19.39 MJ/m^2$

The highest peak for the utilities is caused by high air–conditioning loads during hot days. Therefore, the two peaks (total utility load and electrical demand of the SDHW systems) may not occur coincidentally. That being the case, the benefits of the SDHW system compared to the conventional electric system are higher than the estimates for the maximum demand fractions ζ. The power demand for water heating is reduced from more than $2,500 kJ/hr$ to less than $500 kJ/hr$. The values of ζ and ν can be looked at as a "worst case" analysis.

4.4.2 Impact of Group Size on the Result of Multiple Simulations

It was shown that many simulations are required in order to estimate the performance of many systems. A single simulation of the base case (average) systems yields misleading result for the instantaneous performance. How many simulations are required to yield reliable instantaneous electrical power demand estimates?

Figure 4.15 shows the electric power demand for both the conventional electric and the SDHW system for 10,000 TRNSYS runs averaged to one system. These 10,000 runs are the sum of the 4,000 simulation performed for Figure 4.11 and 6,000 additional TRNSYS runs. A comparison of Figure 4.15 to Figure 4.11 on page 55 shows that the result of 10,000 simulations is slightly different from the result of 4,000 simulations, e.g. the first maximum of P_{SDHW} has a different shape in both figures, although the 4,000 simulations are included in the 10,000 simulations.

The cumulative frequency distribution of the power demand by both the SDHW and the conventional electric system during all 15 minute periods in August is shown in Figure 4.16 for 10,000 systems. It shows the maximum electric power demand ratio $\zeta = 0.78$, the energy ratio $\nu = 0.38$ (see Table 4.11) and the load factor ratio $\lambda = 0.49$. Figure 4.17, the cumulative frequency distribution for 15 minute periods of August between 1:00 PM and 4:00 PM yield, maximum electric power demand ratio $\zeta = 0.66$, the energy ratio $\nu = 0.09$ and the load factor ratio $\lambda = 0.14$. These numbers are also slightly different from the estimates obtained from the 4,000 runs (see page 57). Since the results for 10,000 runs and for 4,000 runs seem

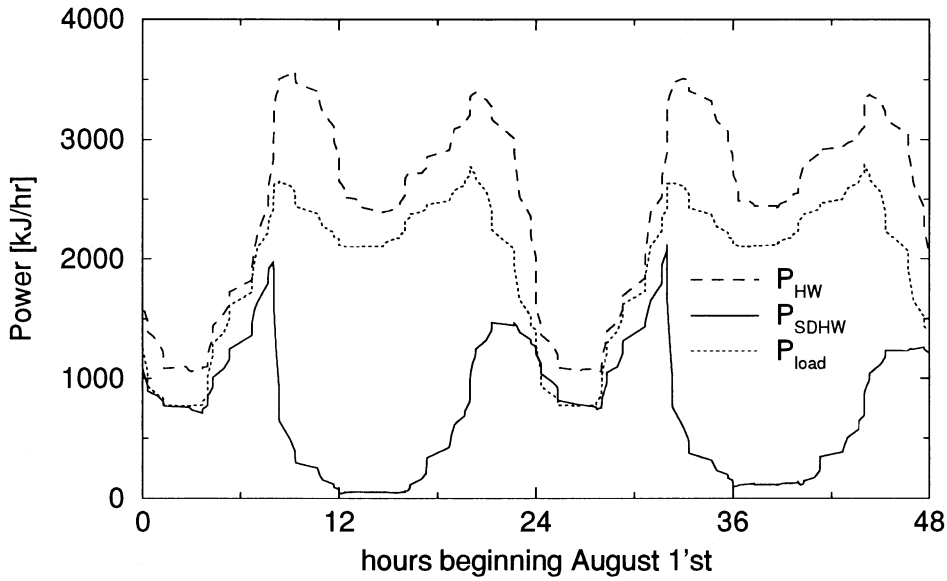

Figure 4.15: Electric power demand comparison between 10,000 conventional electric and SDHW systems in multiple TRNSYS runs series F normalized to one system. Plotted for the first two days of August.

to be different, the impact of the group size will be analyzed in more detail in the following paragraphs.

	maximum power demand fraction ζ	energy fraction ν
all hours	0.78	0.38
1:00 PM – 4:00 PM	0.66	0.09

Table 4.11: Maximum power demand and energy fractions for multiple TRNSYS simulation Series F run 10,000

In order to analyze the impact of the group size quantitatively ζ and ν are calculated for different group sizes. In series F, 10,000 simulations were performed and grouped for each 100 runs. This yields 100 groups of group size 100. The different results between the groups of size 100 are caused by the randomization of

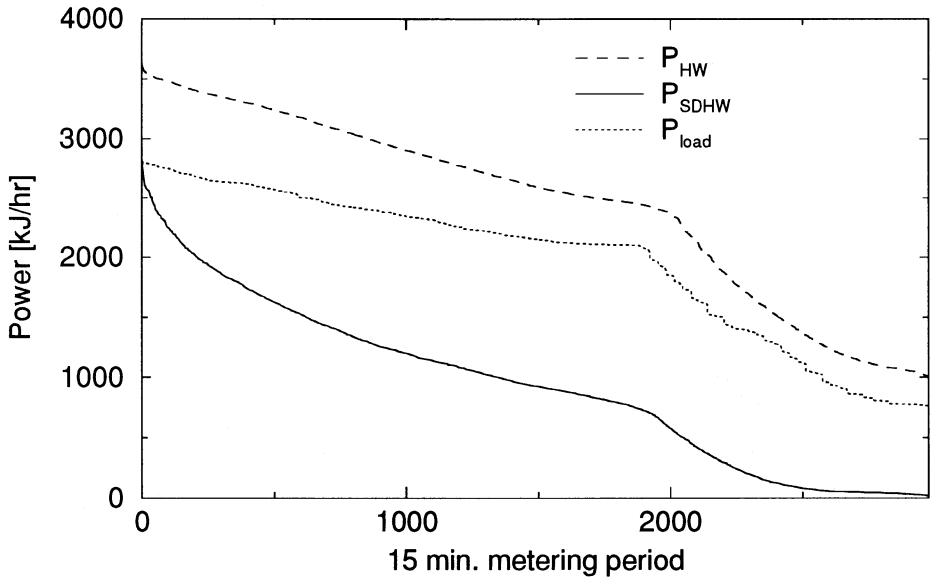

Figure 4.16: Cumulative frequency distribution of the power demand normalized to one system for 10,000 conventional electric and SDHW systems in multiple TRNSYS runs series F. Plotted are all 15 minute periods of August.

the system parameters and the hot water load profile. Each group will probably have a different load and thus a different impact on the total. Maximum electric power demand fractions and energy fractions for larger groups of sizes 400, 1,000, 2,000, 4,000 and 10,000 were obtained by computing the sum of 4, 10, 20, 40 and 100 randomly selected groups of size 100 using

$$P_{j,N_G^*}(t) = \frac{N_G}{N_G^*} \sum_{i=1}^{N_G/N_G^*} P_{r(i),N_G}(t) \tag{4.19}$$

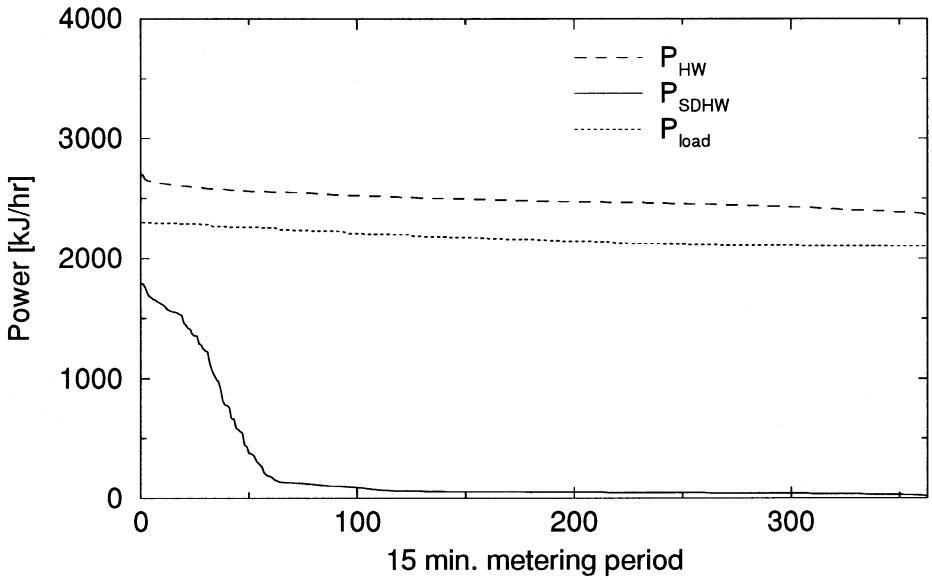

Figure 4.17: Cumulative frequency distribution of the power demand normalized to one system for 10,000 conventional electric and SDHW systems in multiple TRNSYS runs series F. Plotted are all 15 minute periods of August between 1:00 PM and 4:00 PM.

with N_G group size of the base groups, here $N_G = 100$

N_G^* "new" group size , here $N_G^* = 400$, 1,000, 2,000, 4,000 and 10,000

$r(i)$ random number between 1 and the number groups of size N_G. It is possible the a individual group may be selected more than once.

$P_{r,N_G}(t)$ electrical demand for group r of size N_G normalized to one system

$P_{j,N_G^*}(t)$ electrical demand for group j of size N_G^* normalized to one system

The electrical demand for both the SDHW and the conventional electric system were used to compute the maximum electric demand fraction and the maximum energy fraction. Figure 4.18 compares the maximum electric demand fractions ζ (marked with $\times$) and the energy fractions ν (marked with $\circ$) for different group sizes for August. In Figures 4.18 and 4.19 there are 100 data points for the group size 100 and 20 data points for the other group sizes. For the energy fractions and the group sizes 4,000 and 10,000 all 20 data points fall on top of each other. The full lines lines represent the results obtained for all consecutive 10,000 runs which are also presented in Table 4.11. Figure 4.19 compares ζ and ν of the hours from 1:00 PM to 4:00 PM for August. Table 4.12 and Table 4.13 give the means and standard deviations of the peak demand fractions and the energy fractions for the different group sizes. The mean values are very stable for both the maximum power demand ratios and the energy ratios whereas the standard deviation of ζ and ν decreases with increasing group size. The mean values of ζ and ν are not to be confused with the mean or normalized power or energy demands of many systems. The mean values of ζ and ν are used only to describe the distributions of ζ and ν which are obtained when the multiple TRNSYS runs are performed repeatedly with the same systems.

The fourth column of Table 4.12 shows the standard deviation of the demand fractions for all hours which is decreasing with increasing group size from the maximum of 0.057 for the group size 100 over 0.038 for the group size 400 to the minimum of 0.019 for the group size 10,000. The standard deviation of the energy fraction for all hours is shown in column 6 of Table 4.12. It decreases from the maximum of 0.008 for the group size 100 to the very small number of 0.003 for the

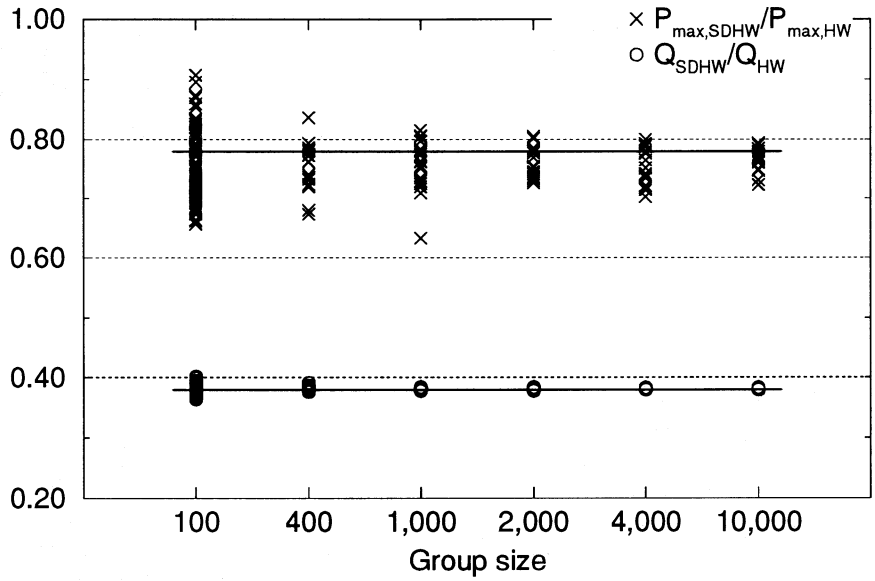

Figure 4.18: Comparison of maximum power ratios ζ and energy ratios ν for all hours of August for different group sizes.

group size 400. Going to larger groups, it decreases slightly to 0.001 for the group of size 10,000.

A similar decrease of the standard deviation of the energy and maximum power demand fractions for the hours from 1:00 PM to 4:00 PM can be seen. Table 4.13 shows the standard deviation of the maximum power fraction decreases from the maximum of 0.072 for the group size 100 over 0.055 for the groups of size 400 to the minimum value 0.023 for the group size 10,000. The standard deviation of the energy fractions for the hours from 1:00 PM to 4:00 PM (see also Table 4.13) decreases from the maximum 0.020 for the group size 100 over the small value of 0.005 for the group size 400 to the minimum of 0.001 for the groups of size 10,000.

It was shown that the spread of the energy fraction ν is small compared to the spread of the maximum power fractions ζ. To obtain a reliable estimate for

group-size N_G	sample-size	peak demand fraction $\bar{\zeta}$	s_ζ	energy fraction $\bar{\nu}$	s_ν
100	100	0.75	0.057	0.38	0.008
400	20	0.75	0.038	0.38	0.003
1,000	20	0.76	0.041	0.38	0.002
2,000	20	0.76	0.026	0.38	0.002
4,000	20	0.75	0.029	0.38	0.001
10,000	20	0.77	0.019	0.38	0.001

Table 4.12: Comparison of mean and standard deviation of maximum power ratios and energy ratios for all 15 minute periods of August and different group sizes computed for Figure 4.18

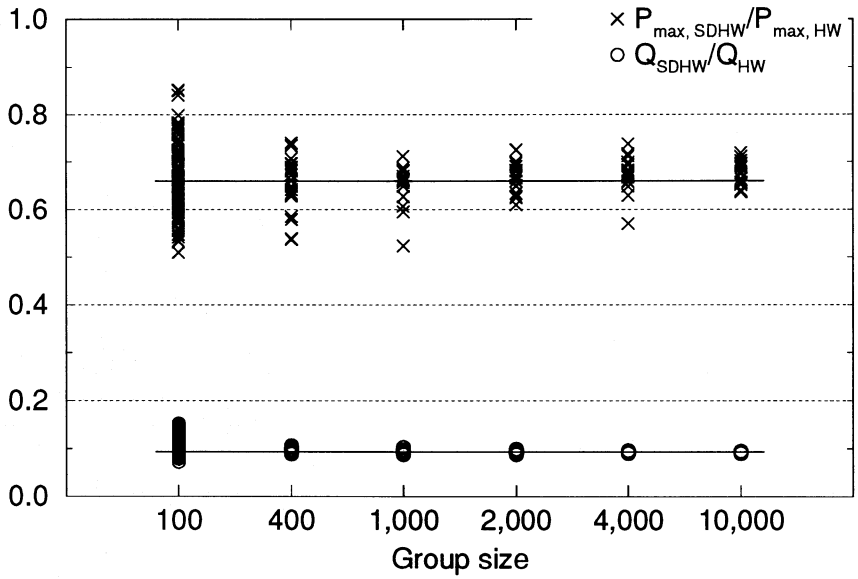

Figure 4.19: Comparison of maximum power ratios ζ and energy ratios ν for the hours from 1:00 PM to 4:00 PM in August for different group sizes.

group-size N_G	sample-size	peak demand fraction		energy fraction	
		$\bar{\zeta}$	s_ζ	$\bar{\nu}$	s_ν
100	100	0.67	0.072	0.11	0.020
400	20	0.65	0.055	0.10	0.005
1,000	20	0.66	0.040	0.09	0.004
2,000	20	0.66	0.029	0.09	0.003
4,000	20	0.67	0.037	0.09	0.002
10,000	20	0.68	0.023	0.09	0.002

Table 4.13: Comparison of mean and standard deviation of maximum power ratios and energy ratios for all 15 minute periods from 1:00 PM to 4:00 PM in August and different group sizes computed for Figure 4.19

the energy fraction η a small number of simulations is sufficient. The spread is already quite small for only 100 simulations. For the group size of 400 the standard deviation is less than 1%

The spread of the maximum power demand fractions ζ is larger. However, increasing the group size from 100 simulations per group to 400 decreases the spread considerably. The standard deviation at group size 400 is 4% and mean is 75% for all hours of August and 65% and 6% for the time period between 1:00 PM and 4:00 PM. Assuming that the data points are normally distributed, this means that 67% of the data point are between 71% $\pm$ 4%. This suggests that a few hundred simulations are sufficient to get a good estimate for the maximum power demand fraction. Nevertheless, the spread of the results is still slightly decreasing with an increasing number of simulations.

4.4.3 Control Strategies to Reduce the Peak Demand

It was shown in the preceding chapter that SDHW systems do have a lower electric peak demand than conventional electric systems. However, the energy reduction is much higher than the demand reduction. This results in a very poor load factor (0.13 in the peak hours) for the SDHW system. Since most utilities have their overall peak in August between 1:00 PM and 4:00 PM it would be useful if it was possible to reduce or eliminate the electric demand for water heating during this time period. The plot of the cumulative frequency distribution for the electric demand from 1:00 PM to 4:00 PM, e.g. Figure 4.14 on page 59, indicates that there is a high potential for peak reduction of the SDHW system by leveling out the profile and shifting the demand of some of the systems.

The two simulation series, Series H and Series I were performed using a SDHW and a conventional electric system very similar to the systems used for Series F. The only difference was that set point temperature T_{set} was varied with time. The system parameters are listed in Table 4.14

$V_{t,SDHW}$	$800l \pm 40\%$	$V_{t,HW}$	$240l \pm 40\%$
U_t	$9.5kJ/m^2hrK \pm 50\%$	P_{max}	$3kW = 10,800kJ/hr$
T_{set}	varied as a function of the time	$T_{db,t}$	$6°C \pm 50\%$
A_c	$7m^2 \pm 30\%$	β	$45 \pm 30\%$
$F_R(\tau\alpha)$	$0.65 \pm 20\%$	F_RU_L	$12kJ/m^2hrK \pm 20\%$
b_0	$0.1 \pm 20\%$	$T_{udb,c}$	$6°C \pm 20\%$

Table 4.14: System parameters for multiple TRNSYS runs series H and series I.

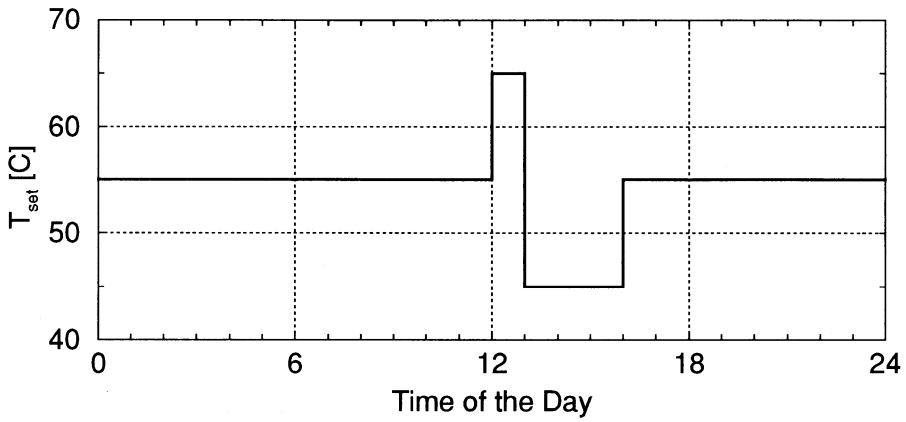

Figure 4.20: Set point temperature T_{set} as a function of the time of the day used for multiple TRNSYS runs series H

The hot water draw patterns and the randomization performed on the hot water load pattern are the same as in Series F. However, the hot water load defined as

$$P_{load} = \dot{m}_{load}(t) c_{p,load}(T_{load} - T_{mains}) \tag{4.20}$$

is different for Series F due to the change in the set point temperatures (further discussion can be found in Section 4.4.3.1 and Section 4.4.3.2).

4.4.3.1 Simulation Series H

One way to control the systems is to vary the set point temperature with time. For the simulations in this series H the set point temperature was varied as shown in Figure 4.20. During the night and the morning hours T_{set} is set to $55°C$, increased to $65°C$ at noon, decreased to $45°C$ at 1:00 PM, and increased to $55°C$ at 4:00 PM. The purpose of this time dependent temperature setting is to heat up the tank before the utility peak time and thus lower the electrical demand during the utility peak time from 1:00 PM to 4:00 PM.

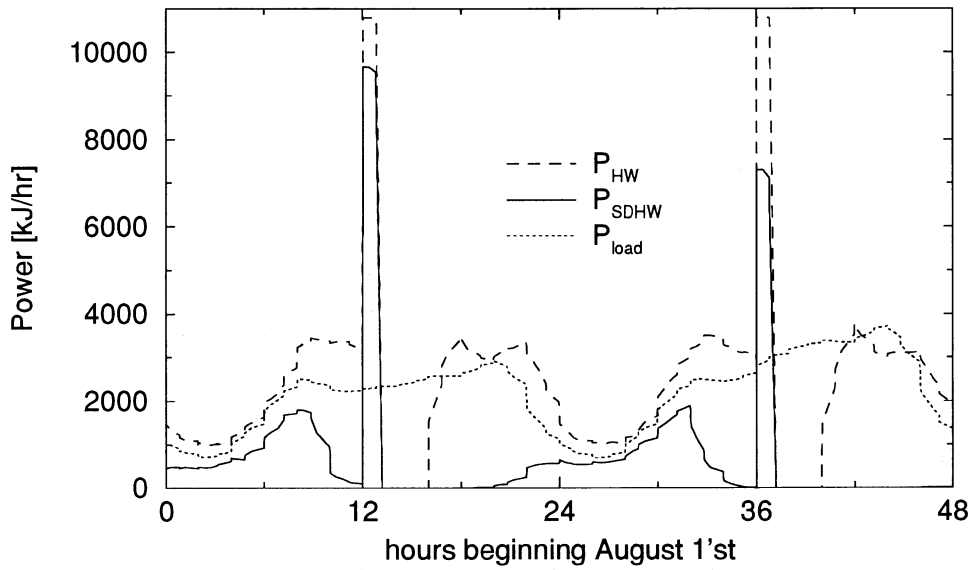

Figure 4.21: Electric power demand comparison between 4,000 conventional electric and SDHW systems normalized to one system in multiple TRNSYS runs series H. Plotted for the first two days of August.

Figure 4.21 shows the normalized electrical power demand for both SDHW and the conventional electric systems (with 4,000 simulations) with the control strategy described in the previous paragraph. Both P_{HW} and P_{SDHW} are zero from 1:00 PM to 4:00 PM, the time period with a lowered set point temperature T_{set}. However, P_{HW} goes up to $10,800kJ/hr$ at noon, the moment when the set point temperature is increased from $55°C$ to $65°C$, since all heating elements are turned on at exactly the same time. Therefore, the electric power demand is equal to the maximum power of the heating element which is $10,800kJ/hr$. The electric power demand of the SDHW system P_{SDHW} has a step function to $9,000kJ/hr$ on the first day and to $7,000kJ/hr$ on the second day. Both demands are less than

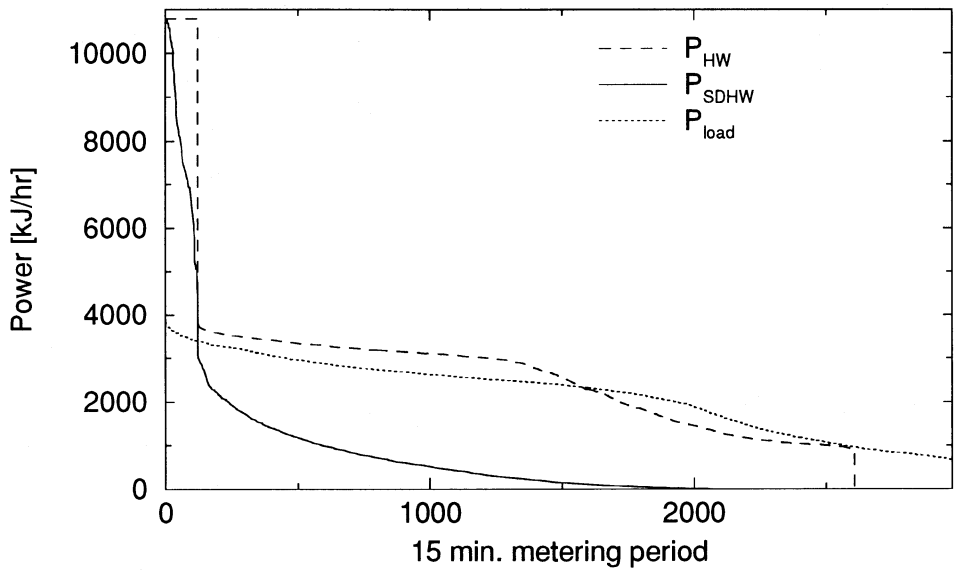

Figure 4.22: Cumulative frequency distribution of the power demand normalized to one system for 4,000 conventional electric and SDHW systems in multiple TRNSYS runs series H. Plotted are all 15 minute periods of August.

the maximum auxiliary power since some of the tanks were already at the high set point temperature due to heating by the solar collector.

Figure 4.22 gives the cumulative frequency distribution for all 15 minute periods in August. The cumulative frequency distribution for all 15 minute periods between 1:00 PM and 4:00 PM (not plotted here) shows that P_{HW} and P_{SDHW} are zero for all periods during this time of the day in August.

The monthly performance for August is summarized in Table 4.15. The total load is $Q_{load} = 1.62GJ$, electricity required by the conventional electric system is $Q_{HW} = 1.84GJ$, by the SDHW is $Q_{SDHW} = 0.56GJ$. The solar fraction is $F = 69\%$. However, the SDHW system has the same maximum electric power demand as the conventional electric system.

System	Q_{load}	$Q_{electric}$	Solar fraction
conventional electric	$1.62GJ$	$1.84GJ$	—
SDHW	$1.62GJ$	$0.56GJ$	65%

Table 4.15: Monthly electric energy consumption of the conventional electric and SDHW for multiple TRNSYS runs series H

4.4.3.2 Simulation Series I

The simulation of this series uses a time dependent setting of the set point temperatures as well. The temperatures are set according to Figure 4.23. $T_{set,t}$ the set point temperature for the tank is set to $55°C$ and increased to $65°C$ at 11:00 AM for one half of the systems (labeled $T_{set,tank,a}$) and at noon for the other half of the systems (labeled $T_{set,tank,b}$), decreased to $45°C$ at 1:00 PM and reset to $55°C$ at 4:00 PM. The set point temperature of the load is held constant at $55°C$ except from 1:00 PM to 4:00 PM where it is lowered to $45°C$. Setting the tank set point temperature to $65°C$ at 11:00 AM or at noon is randomly defined for each system but constant during the simulation of each single system.

Figure 4.24 shows the electric power demand for all 4,000 systems normalized to one system during the first two days of August. Both times at which the set point is increased can be identified easily. The power demand for the conventional system P_{HW} has a step function to $5,000kJ/hr$ at 11:00 AM when the first 50% of the system increase the tank set point temperature and a second step to over $10,000kJ/hr$ at noon when the second 50% of the system increases $T_{set,t}$.

Figures 4.25 gives the cumulative frequency distribution of the electric power demand for all 15 minute periods of August. The electricity required during the

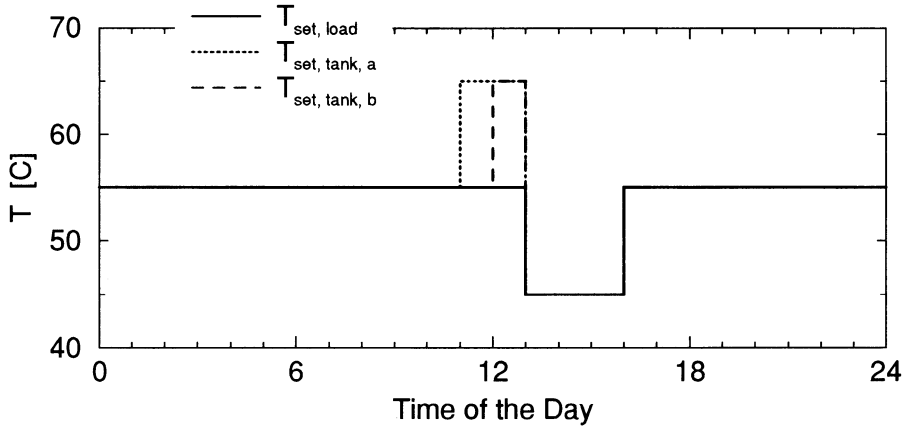

Figure 4.23: Set point temperature T_{set} as a function of the time of the day used for multiple TRNSYS runs series I

month by the conventional electric system is $Q_{HW} = 1.79GJ$, by the SDHW system is $Q_{SDHW} = 0.54GJ$ to supply to same load of $Q_{load} = 1.42GJ$. The solar fraction is $F = 0.70$. Figures 4.25 shows that the SDHW system reduces the energy demand but it does not reduce the peak electrical demand. The cumulative frequency distribution for the 15 minute periods from 1:00 PM to 4:00 PM (not displayed here) shows that the electrical demand during this time period is zero for both the conventional electric and the SDHW system.

4.4.3.3 Conclusions

Both control strategies investigated in this Section 4.4.3 eliminate the electrical demand between 1:00 PM and 4:00 PM for both the conventional electric and the SDHW system. However, the strategies create an very high peak power demand at 11:00 AM and and even higher demand at noon. The strategy used for series I is a improvement compared to series H, since the number of time periods with the extremely high power demand of over $10,000kJ/hr$ is reduced. However, the

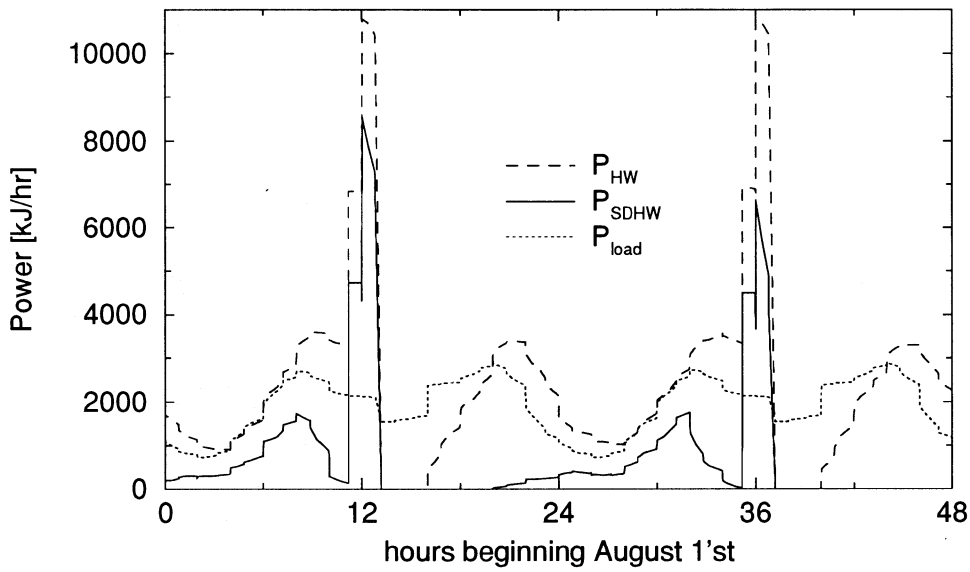

Figure 4.24: Electric power demand comparison between 4,000 conventional electric and SDHW systems normalized to one system in multiple TRNSYS runs series I. Plotted for the first two days of August.

maximum power demand is for both strategies equal to the maximum power of the auxiliary heater which is $10,800 kJ/hr$ for the SDHW system as well as for the conventional system. If either one of these control strategies is used the benefit of the SDHW system is only the energy reduction and no power demand reduction.

The control strategy needs improvement. It is suggested to i) lower the high set point temperature since $65°C$ may be unnecessarily to high and ii) spread the increase of the set point temperature over a larger time period, e.g. three or four hours.

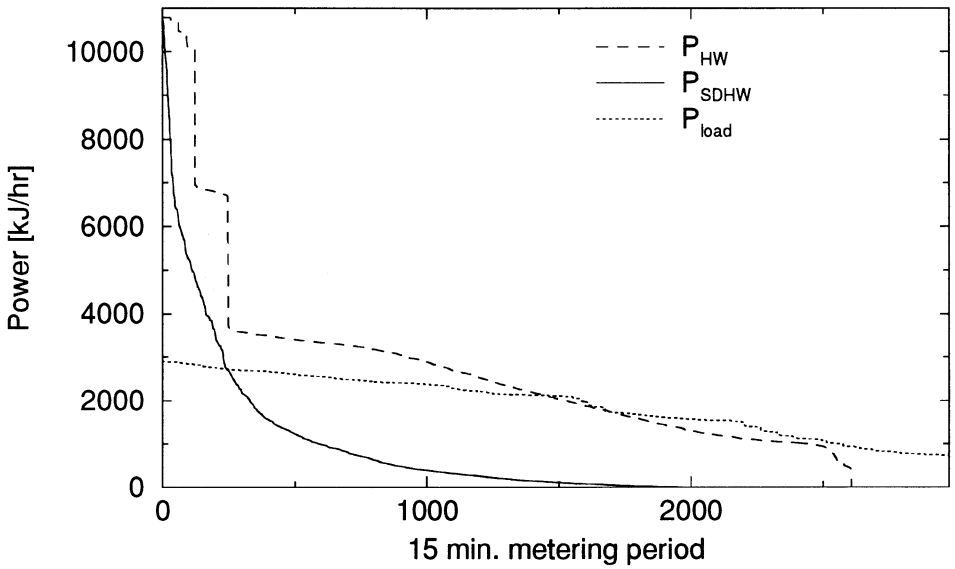

Figure 4.25: Cumulative frequency distribution of the power demand normalized to one system for 4,000 conventional electric and SDHW systems in multiple TRNSYS runs series I. Plotted are all 15 minute periods of August.

4.4.4 Impact of the Hot Water Load Pattern, Simulation Series K

The simulations in Series K were performed to investigate the impact of the hot water load profile on the results for the maximum demand fractions ζ and the energy fraction ν. The parameters for the simulated systems are the same for for the simulation Series F and are given in Table 4.16.

The hot water load profile used for Series K is the RAND profile and was adapted from [3, Figure 9.1.2]. It was randomized for each day of the simulation by shifting it in time up to 1 hour backward or forward and by scaling it by

a factor between 0.75 and 1.25. The monthly load $Q_{load} = 1.43GJ$ is slightly reduced compared to simulation series F ($Q_{load} = 1.78GJ$).

$V_{t,SDHW}$	$800l \pm 40\%$	$V_{t,HW}$	$240l \pm 40\%$
U_t	$9.5kJ/m^2hrK \pm 50\%$	P_{max}	$3kW = 10,800kJ/hr$
T_{set}	$55°C$	$T_{db,t}$	$6°C \pm 50\%$
A_c	$7m^2 \pm 30\%$	β	$45 \pm 30\%$
$F_R(\tau\alpha)$	$0.65 \pm 20\%$	$F_R U_L$	$12kJ/m^2hrK \pm 20\%$
b_0	$0.1 \pm 20\%$	$T_{udb,c}$	$6°C \pm 20\%$

Table 4.16: System parameters for multiple TRNSYS runs series K

4.4.4.1 Monthly Performance

The comparison of the monthly performance of the SDHW and the conventional electric system for August is given in Table 4.17. The total load for each of the systems is $Q_{load} = 1.43GJ$. The electrical energy required to meet the load is $Q_{HW} = 1.79GJ$ for the conventional electric system and $Q_{SDHW} = 0.62GJ$ for the SDHW system. The solar fraction is $F = 65\%$.

System	Q_{load}	$Q_{electric}$	Solar fraction
conventional electric	$1.43GJ$	$1.79GJ$	—
SDHW	$1.43GJ$	$0.62GJ$	65%

Table 4.17: Monthly electric energy consumption of the conventional electric and SDHW for multiple TRNSYS runs series K

4.4.4.2 Instantaneous Performance

Figure 4.26 shows the electrical power demand P_{HW} and P_{SDHW} for the first two days of August. It shows the RAND load profile has high peak at 9:00 AM with

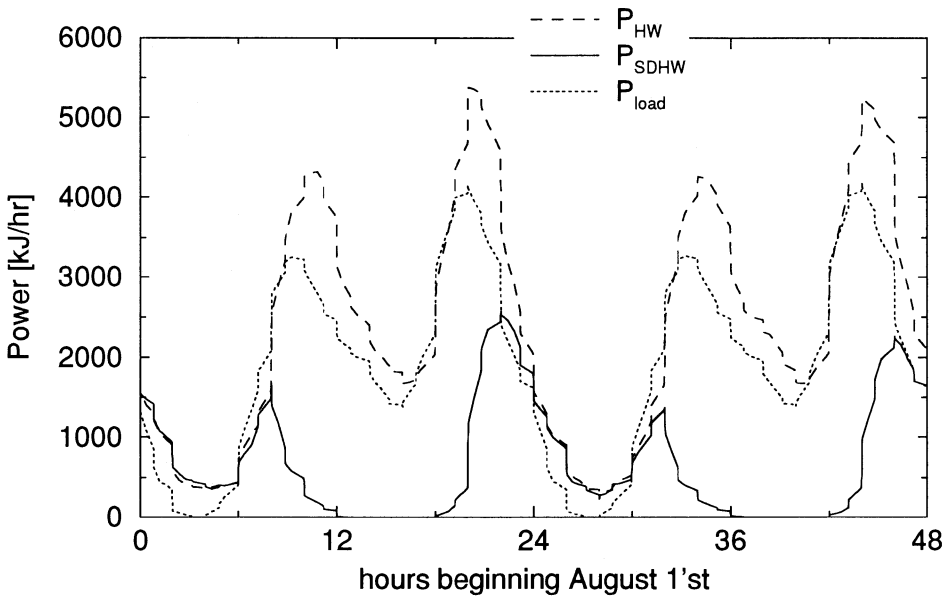

Figure 4.26: Electric power demand comparison between 4,000 conventional electric and SDHW systems normalized to one system in multiple TRNSYS runs series K. Plotted for the first two days of August.

over $3,000kJ/hr$ goes down to $1,500kJ/hr$ and has a second peak at 8:00 PM with $4,000kJ/hr$ (see also Appendix C, Figure C.6 on page 106).

Figure 4.28 and Figure 4.29 give the cumulative frequency distribution of the electric power demand P_{HW} and P_{SDHW} for all 15 minute periods and for the 15 minute periods between 1:00 PM and 4:00 PM in August. Table 4.18 gives the maximum power demand and energy fractions of series K and for comparison the result for series F. The maximum power demand fraction is $\zeta = 0.79$ for all hours and $\zeta = 0.86$ for the hours from 1:00 PM to 4:00 PM. The energy fraction is $\nu = 0.35$ for all hours and $\nu = 0.08$ for the hours from 1:00 PM to 4:00 PM. Comparing the results of this series K to the results of series F (Table 4.11, Figure 4.18 and Figure 4.19) shows that energy fractions are the same. The maximum power

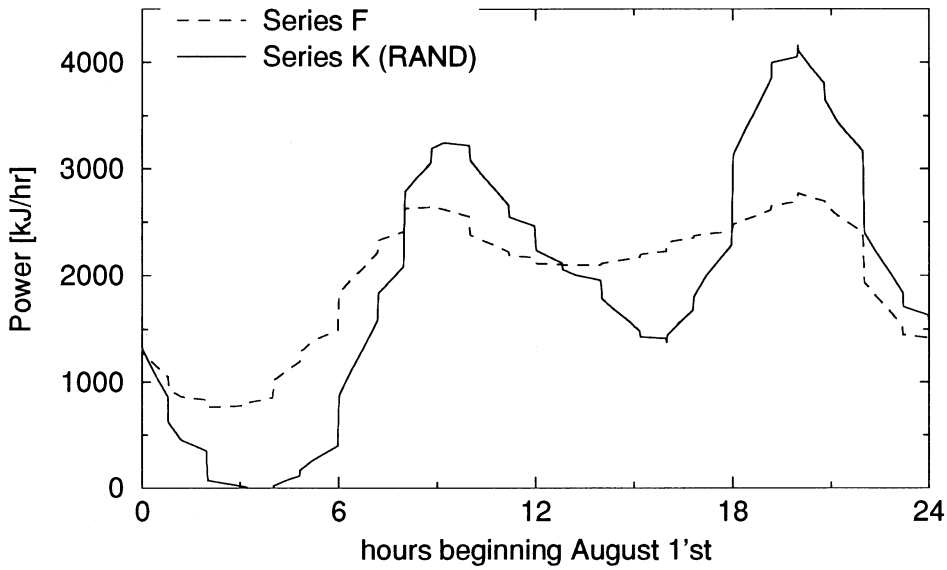

Figure 4.27: Comparison of the hot water load of series K to series F.

demand fraction for the hours from 1:00 PM to 4:00 PM are different (0.86 compared to 0.66) although the maximum power demand fractions for all hours are the same (0.35 compared to 0.38).

A comparison of the RAND hot water load profile used for series K with the average load profile used for series F is given in Figure 4.27. It can be seen that the load for series F is more flat than the load for series K. Both loads are the same for midnight but series K falls to almost zero while series F stays above $750kJ/hr$. The load of series F increases to its first peak of $2,650kJ/hr$ at 8:45 AM, decreases to $2,050kJ/hr$ at 1:00 PM, increases to the second peak of $2,750kJ/hr$ at 8:30 PM and falls to the low load at midnight. The RAND profile has the first peak of $3,250kJ/hr$, falls down to $1,370kJ/hr$, increases to its second peak of $4,150kJ/hr$ and falls to almost zero at 3:30 AM.

The instantaneous performance data was analyzed to count the number of days during which the power demand is above a certain limit. It was found that the power demand of the SDHW system P_{SDHW} between 1:00 PM and 4:00 PM is three days over $1,000kJ/hr$ and five days over $500kJ/hr$. The power demand off the conventional electric system P_{HW} is every day in August greater than $2,000kJ/hr$ from 1:00 PM to 4:00 PM. It was shown that the peak demand of the SDHW system occurs during days with low solar irradiation. Usually, the utility peak does not occur coincidentally. That being the case, the SDHW systems reduces the electric power demand during the peak period significantly from more than $2,000kJ/hr$ to less than $500kJ/hr$.

	Series K		Series F	
	power-fraction ζ	energy-fraction ν	power-fraction ζ	energy-fraction ν
all hours	0.79	0.35	0.78	0.38
1:00 PM – 4:00 PM	0.86	0.08	0.66	0.09

Table 4.18: Maximum power demand and energy fractions for multiple TRNSYS simulation Series K run 4,000

4.4.4.3 Conclusions

For the simulations of this series K the SDHW system reduces the maximum power demand by 21% during all hours of the day and by 14% during the hours from 1:00 PM to 4:00 PM. The energy use is reduced by 65% during all hours and by 92% during the hours from 1:00 PM to 4:00 PM.

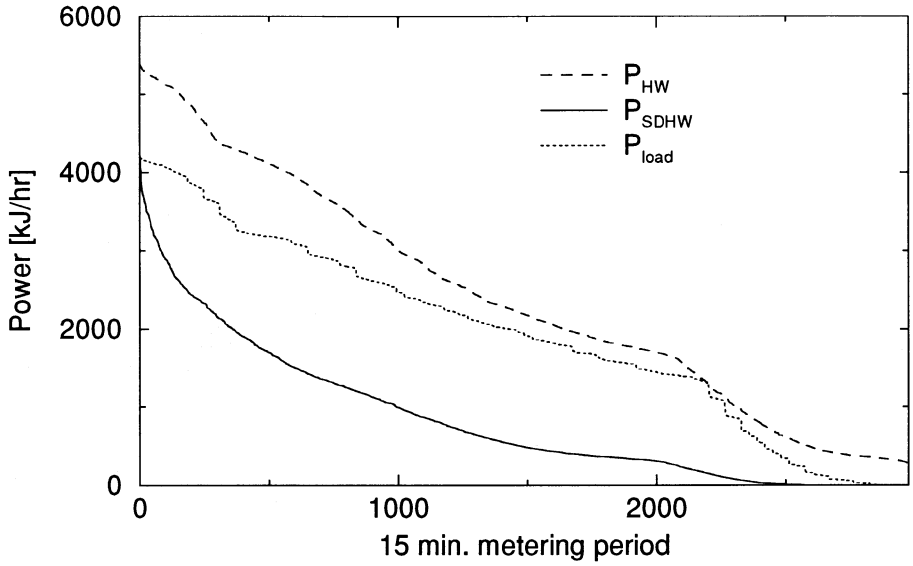

Figure 4.28: Cumulative frequency distribution of the power demand normalized to one system for 4,000 conventional electric and SDHW systems in multiple TRNSYS runs series K. Plotted are all 15 minute periods of August.

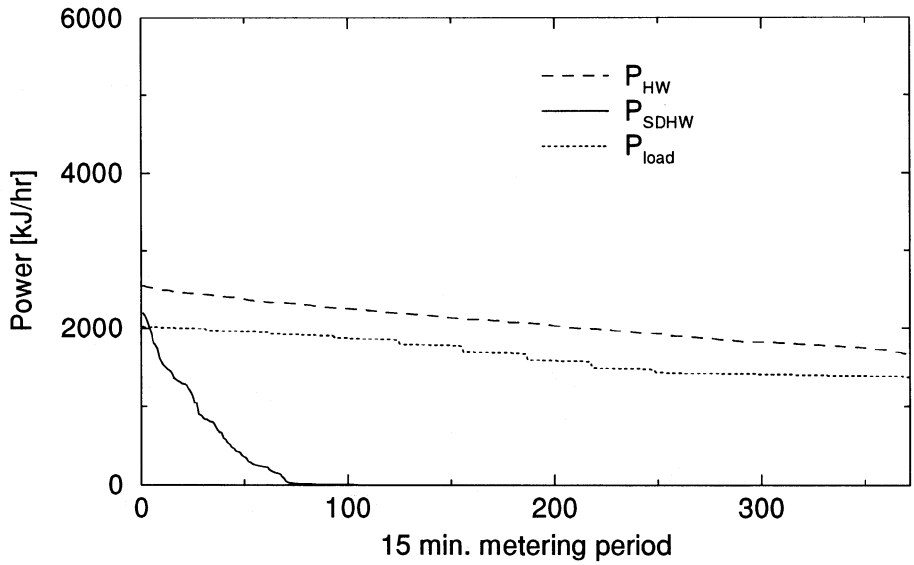

Figure 4.29: Cumulative frequency distribution of the power demand normalized to one system for 4,000 conventional electric and SDHW systems in multiple TRNSYS runs series K. Plotted are all 15 minute periods between 1:00 PM and 4:00 PM in August.

The energy demand fractions are the same for the series K and for series F†. The maximum power demand fractions for all hours of August are also the same for both series. However, the maximum power demand fraction for the hours from 1:00 PM to 4:00 PM for series K is greater than for series F.

It was shown that the peak electrical demand of the SDHW systems occurs for both series F and series K at only three days in August with low solar irradiation. The electrical demand of the conventional electric systems is the same every day. Since the utility peak load and the SDHW peak demand may not occur coincidentally the peak demand reduction by the SDHW systems is a much higher than indicated by the maximum power demand fraction. The electrical demand is reduced from over $2,000kJ/hr$ to less than $500kJ/hr$ which is a reduction by more than 75%. The maximum power demand fraction represent a "worst case" estimation.

4.4.5 Impact of the Collector Area, Simulation Series L

The TRNSYS runs in this section were perform to investigate the impact of the collector area and performance of SDHW system. Of special interest is the impact of the collector area on the maximum power demand.

In order to to compare the SDHW system with a conventional system simulations for both systems were performed with the system parameters that are given in Table 4.19.

The monthly performance of both the SDHW and the conventional electric system is given in Table 4.20. The total energy supplied to the load is $Q_{load} = 1.47GJ$.

†The only difference between the series F and the series K is the hot water load pattern.

$V_{t,SDHW}$	$800l \pm 40\%$	$V_{t,HW}$	$240l \pm 40\%$
U_t	$9.5kJ/m^2hrK \pm 50\%$	P_{max}	$3kW = 10,800kJ/hr$
$T_{set,t}$	$55°C$	$T_{db,t}$	$6°C \pm 50\%$
A_c	$3.5m^2 \pm 30\%$	β	$45 \pm 30\%$
$F_R(\tau\alpha)$	$0.65 \pm 20\%$	F_RU_L	$12kJ/m^2hrK \pm 20\%$
b_0	$0.1 \pm 20\%$	$T_{udb,c}$	$6°C \pm 20\%$

Table 4.19: System parameters for multiple TRNSYS runs series L

The electricity consumed by the conventional electric system is $Q_{HW} = 1.83GJ$ and the energy consumed by the SDHW system is $Q_{SDHW} = 0.96GJ$ which yields a solar fraction $F = 47\%$. The solar fraction for this series L is considerably smaller than the solar fractions for all other series (which are about 65%) since the collector area was cut in half for the simulation series L and the collector area, obviously, affects the solar fraction.

System	Q_{load}	$Q_{electric}$	Solar fraction
conventional electric	$1.47GJ$	$1.83GJ$	—
SDHW	$1.47GJ$	$0.96GJ$	47%

Table 4.20: Monthly electric energy consumption of the conventional electric and SDHW for multiple TRNSYS runs series L

Figure 4.30 shows the instantaneous electric power demand for the conventional electric and the SDHW system. The power demand of the conventional electric system P_{HW} follows the load P_{load}. The demand of the SDHW system P_{SDHW} follows the load during the night and the early morning. At about 8:00 AM P_{SDHW} decreases until it is almost down to zero at 12:30 PM. It stays at a very low level until 3:30PM then it increases until it reaches the same level as P_{load} at 9:30PM. Of course, this pattern is weather dependent and, therefore, different for each

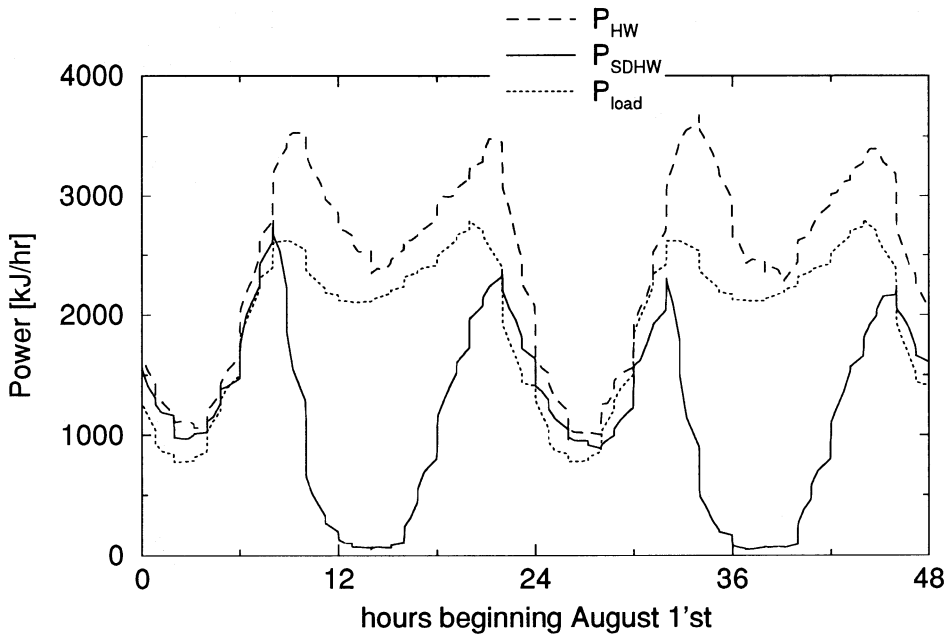

Figure 4.30: Electric power demand comparison between 4,000 conventional electric and SDHW systems normalized to one system in multiple TRNSYS runs series L. Plotted for the first two days of August.

day of the simulation. A comparison of the instantaneous demand of the systems simulated in series F (Figure 4.11) shows that the systems of series L perform worse since the collector area was cut to half from series F to series L.

The cumulative frequency distribution of the power demand for all 15 minute periods of August is displayed in Figure 4.31, the distribution for the 15 minute periods from 1:00 PM to 4:00 PM is shown in Figure 4.32. A comparison with Figure 4.13 on page 58 and Figure 4.14 on page 59 shows the impact of the smaller collector area of series L compared to series F. The maximum electric demand fractions and the energy fractions are given in Table 4.21 (compare to Table 4.11 on page 62). The energy fraction for all hours is 0.53 respectively 0.20 for the

	maximum power demand fraction ζ	energy fraction ν
all hours	0.85	0.53
1:00 PM – 4:00 PM	0.86	0.20

Table 4.21: Maximum power demand and energy fractions for multiple TRNSYS simulation Series L run 4,000

hours from 1:00 PM to 4:00 PM. The maximum electric power demand fraction is 0.85 for all day and 0.86 for the time from 1:00 PM to 4:00 PM.

4.4.5.1 Conclusions

Table 4.22 gives the maximum power demand and energy fractions for all 15 minute periods and from 1:00 PM to 4:00 PM in August for both a collector area of $7m^2$ and a collector area of $3.5m^2$. As expected, cutting the collector area in half yields an increase in the power and the energy fraction. For all hours of the day the power fraction ζ is increased by 8% from 0.78 to 0.85 and the energy fraction is increased by 39% from 0.38 to 0.53. For the time from 1:00 PM to 4:00 PM the power fraction is increase by 23% from 0.66 to 0.86 and the energy fraction by 122% from 0.09 to 0.20.

	collector area $A_c = 7m^2$		collector area $A_c = 3.5m^2$	
	power-fraction ζ	energy-fraction ν	power-fraction ζ	energy-fraction ν
all hours	0.78	0.38	0.85	0.53
1:00 PM – 4:00 PM	0.66	0.09	0.86	0.20

Table 4.22: Comparing maximum power demand fractions and energy fractions for different collector areas

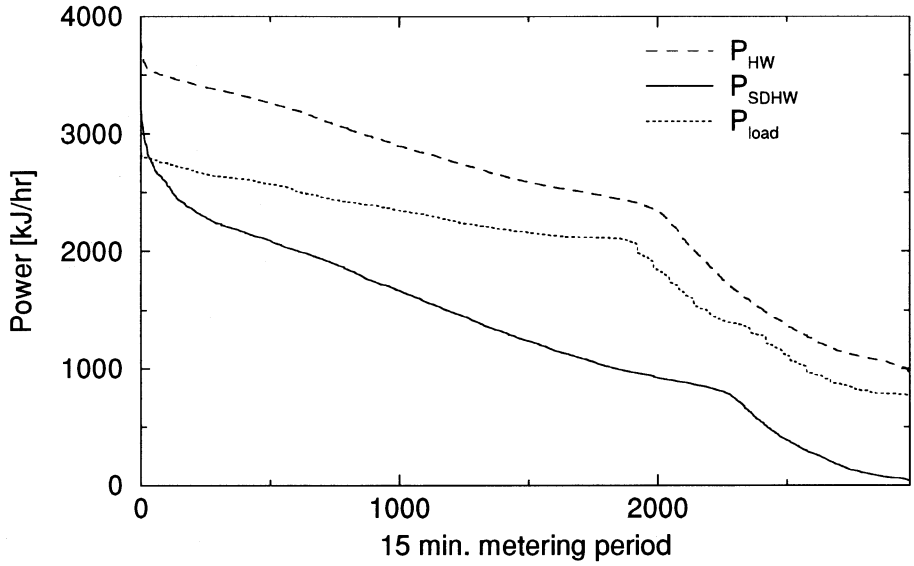

Figure 4.31: Cumulative frequency distribution of the power demand normalized to one system for 4,000 conventional electric and SDHW systems in multiple TRNSYS runs series L. Plotted are all 15 minute periods of August.

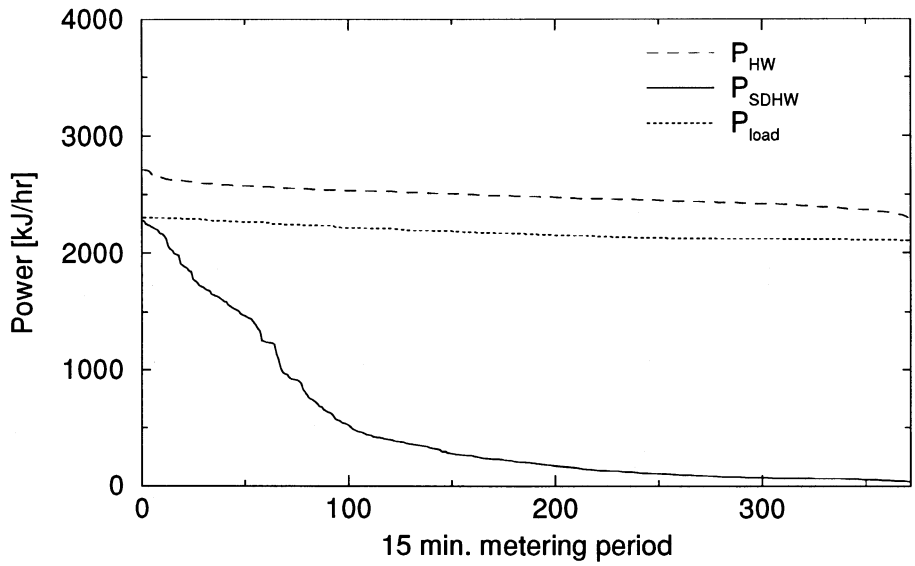

Figure 4.32: Cumulative frequency distribution of the power demand normalized to one system for 4,000 conventional electric and SDHW systems in multiple TRNSYS runs series L. Plotted are all 15 minute periods of the month August between 1:00 PM and 4:00 PM.

Chapter 5

Conclusions and Recommendations

5.1 Conclusions

The TRNSYS simulation of an individual, base case (average) system shows that the use of a SDHW system in place of a conventional electric water heating system yields a decrease of the energy consumption and that the peak electricity demand is the same for both systems. However, it was shown that the result of the simulation of the instantaneous performance of a single system can not be extrapolated to a large number of installations. Therefore, multiple simulation have to be performed to estimate the performance of many systems. A brief summary of the multiple simulation performed in this thesis is given in Table 5.1.

Multiple TRNSYS simulations of a variety of conventional electric water heating systems with different hot water load profiles show that the instantaneous

electrical power demand of all systems can be estimated from the average hot water load profile and a constant loss term. The constant loss term can be obtained by simulating the average system supplying the average load. The multiple simulations shows as well a considerably lower peak power demand than single simulation of the average system.

Multiple TRNSYS simulation have also been performed for a variety of SDHW systems. They show a significantly lower peak power demand than the single simulation of the base case (average) SDHW system.

A comparison of the SDHW system with the conventional electric system in multiple TRNSYS runs shows that the peak electrical demand by the SDHW system is lower than the demand by the conventional electric. Most electric utilities have their peak load between 1:00 PM and 4:00 PM in August. The electrical peak demand during this time period is lower for the SDHW system than for the conventional electric. It is possible to cancel the electricity demand for both the SDHW and the conventional electric system by using a control strategy that preheats the tank before 1:00 PM and lowers the set point temperature between 1:00 PM and 4:00 PM.

It was shown that the peak power demand for that SDHW system occurs during three days in August. These three days are days with low incident irradiation. Therefore, the utility peak and the peak of the SDHW system do not occur coincidentally. That being the case, the demand during utility peak load is reduced by the SDHW systems by more than 75%. The maximum power demand fraction is a worst case analysis of the demand reduction by the SDHW system. It gives the

demand reduction if both the SDHW peak demand and the utility peak load were to occur coincidentally.

Multiple simulations with a different average water load pattern shows that the energy fraction is independent of the shape of the hot water load and that the maximum power demand fraction is dependent on the hot water load pattern. However, this maximum power demand fraction is a worst case analysis. The demand reduction by the SDHW system during utility peak time is not affected by the shape of the hot water load.

A reduction of the collector area yields a increase in both energy and maximum power demand. Furthermore, the demand reduction during utility peak time is reduced.

The accuracy of the results of the multiple simulations improves with increasing number of simulations. The spread of the results for the energy fractions is already very small for a group size of 100. For the group size of 400 the standard deviation is less than 1%. The standard deviation of the results for the maximum power demand fraction is 4% for all hours and 6% for the hours from 1:00 PM to 4:00 PM for the group size 400, which allows a good estimate of the maximum power demand fraction with a group size of 400.

The different series of multiple TRNSYS runs yield different energy and maximum power fractions. However, they all have in common that the SDHW system consumes less energy and has a lower peak power demand than the conventional electric system.

Simulation of either SDHW or conventional electric systems			
A	conventional electric systems, analyze on/off pattern, maximum power demand, estimate electrical demand from load		
B	conventional electric systems, different load pattern to compare results with A		
D	SDHW systems, same load pattern as A, on/off pattern, maximum power demand		

Comparing SDHW with conventional electric systems					
		all hours		1:00PM – 4:00PM	
		ζ	ν	ζ	ν
F	analyze demand and energy reduction by SDHW systems, analyze impact of group size on results, compute number of SDHW peak electric demand days	0.78	0.38	0.66	0.09
H	same as F but control strategy i to reduce demand from 1:00 PM to 4:00 PM	1.00	0.35	no demand	
I	same as F but control strategy ii to reduce demand from 1:00 PM to 4:00 PM	1.00	0.30	no demand	
K	same as F but different hot water load pattern	0.79	0.35	0.86	0.08
L	same as F but half the collector area	0.85	0.53	0.86	0.20

Table 5.1: Summary of multiple TRNSYS runs

5.2 Recommendations

The system parameters and hot water loads were chosen to constitute a reasonable range. However, in order to estimate the impact of a real, existing technology on a real, existing utility, very specific data about this technology and the electric load for the utility and the hot water load profiles has to be acquired.

More research has to be done to estimate the instantaneous power demand of the SDHW system. It should be possible to predict the power of the SDHW systems like it is possible to predict the power demand of the conventional system which was shown in this research. The author suggests that a correlation can be found involving monthly performance data of the average system, weather data, and the average hot water load pattern to estimate the instantaneous performance of many systems.

It is suggested to develop a better control strategy to reduce the electrical demand during the utility peak period from 1:00 PM to 4:00 PM without creating a new high peak earlier in the day. A possibility would be to lower the preheat set point temperature or to spread the timer settings over a larger time period.

Appendix A

Xlisp–Stat Programs

A.1 Randomize-load.lsp

The following program is used to generate the randomized load profiles for the multiple TRNSYS runs. It reads the basic load profile from an input disk file and writes the randomized load profile to an output disk file. Xlisp–Stat is an interpreter language, therefore, the easiest way to change some parameters is to edit the beginning of the source code. To run it, use a Unix command to run Xlisp–Stat, pipe the program text to the standard input and pipe the output to a file or ignore it, e.g. `xlispstat <randomize-load.lsp >&! /dev/null`.

```
;;
;; randomize-load
;;
;; define min, max shift and scale
;; note: unit of shift is no of time steps
;;
(def min-shift -2)
(def max-shift 2)
```

```
(def min-scale .75)
(def max-scale 1.25)
;;
;; list of file names of the basic profiles
;; note: Unix is case sensitive
;; load has to be supplied in equally spaced
;; time intervals
;;
(def file-names
     (list "CL_K_CL_CL.WLOAD" "CL_L_CL_CL.WLOAD"
           "CL_M_CL_CL.WLOAD" "CL_P_CL_CL.WLOAD"
           "CL_Q_CL_CL.WLOAD" "CL_R_CL_CL.WLOAD"
           "CL_S_CL_CL.WLOAD" "CL_T_CL_CL.WLOAD"
           "CL_U_CL_CL.WLOAD" "CL_WA_CL_CL.WLOAD"
           "CL_WB_CL_CL.WLOAD" "CL_WC_CL_CL.WLOAD"
           "CL_WD_CL_CL.WLOAD" "CL_WE_CL_CL.WLOAD"
           "CL_WF_CL_CL.WLOAD" "CL_WG_CL_CL.WLOAD"
           "CL_WH_CL_CL.WLOAD" "CL_WI_CL_CL.WLOAD" ))
;;
;; define the path to the basic loads
;;
(def path "/usr/users/grater/trnsys/randomruns/g/loads/")
;;
;; and the name of the output file, use full path name
;; if desired
;;
(def out-file "RLOAD.DATA")
;;
;; define column of data and time in the file
;;
(def column-data 1)
(def column-time 0)
;;
;; define the desired length of the output
(def output-length (* 31 2))
;;
;;;;;;;;;;;;;;;;;;;;;;;;;;;;;;;;;;;;;;;;;;;;;;;;;;;;;;;;;;;;;
;;
;; end of user defined parameters
;;
;; do not edit beyond this line!!!!!!!!!!!!!!!!!!!!!!!!!
;; (except you know what you are doing)
;;
```

```
;;;;;;;;;;;;;;;;;;;;;;;;;;;;;;;;;;;;;;;;;;;;;;;;;;;;;;;;;;;;;;;;;;;;;;;;
;;
;; lets read the basic load profiles from disk, assign
;; it to the variables data and time, and junk the last value
;;
(dotimes (i (length file-names))
         (setf (select file-names i)
               (format nil "~a~a"
                       path (select file-names i))))
(def tmp (read-data-columns
          (select
           file-names (random (length file-names)))))
(def data (select (select
                   tmp column-data)
                  (iseq (- (length (car tmp)) 1))))
(def time (select
           (select tmp column-time)
           (iseq (- (length (car tmp)) 1))))
(def last-step (last (select tmp column-time)))
;;
;; define a function to do the desired randomization
;;
(defun random-it (data)
  ;;
  ;; get shift and scale within the user supplied limits
  ;;
  (let* ( (shift (+
                  (random ( + 1 (- max-shift min-shift)))
                  min-shift))
          (scale (+ min-scale (* (- max-scale min-scale)
                                 (/ (random 999999) 999998))))
          (l-data (length data)))
    ;;
    ;; scale it
    ;;
    (setf data (* data scale))
    ;;
    ;; shift it
    ;;
    (when (/= shift 0)
          (setf data (if (> shift 0)
                         (append (select data
                                         (iseq (- l-data shift 1)
```

```
                                                (- l-data 1 1)))
                                    (select data
                                       (iseq 0 (- l-data 1 shift))))
                           (append (select data
                                           (iseq
                                            (- shift)
                                            (- l-data 2 )))
                                   (select data
                                           (iseq 0 (- (- shift) 1)))
                                   (list
                                    (select data (- shift))))))) data))
;;
;; open the output file, kill the old one
;; write the new randomized data to the file
;; repeat it the desired number of times
;;
(with-open-file (f out-file :direction
                    :output)
                (dotimes (i output-length)
                         (def new-data (random-it data))
                         (dotimes (i (length new-data))
                                  (format f "~a ~%"
                                     (select new-data i)))))
;; thats it, we have the new load profile and are done
```

A.2 Getrandom

This, very short Xlisp–Stat program creates the file `random.data` containing 500 uniformly distributed random numbers between 0 and 1.

```
(with-open-file (f "random.data" :direction :output)
  (dotimes (i 500)
           (format f "~a~%" (/ (random 999999) 999998))))
```

Appendix B

C-shell script files

B.1 Gt

Gt was written to generate a TRNSYS deck from four files which contain four different parts of the TRNSYS deck.

```
#!/bin/csh
set trn = ~/trnsys/
if ( -e $1 ) then
  set base = $1
else
  set base = $trn"bases/"$1
endif
if ( -e $2 ) then
  set load = $2
else
  set load = $trn"loads/"$2
endif
if ( -e $3 ) then
  set var = $3
else
  set var = $trn"vars/"$3
```

```
endif
if ( -e $4 ) then
  set finvar = $4
else
  set finvar = $trn"finvars/"$4
endif

set tailload = $load:t
set tailvar = $var:t
set tailfinvar = $finvar:t
set tailbase = $base:t
set name = $tailbase:r"_"$tailload:r"_"$tailvar:r"_"$tailfinvar:r
set dck = $trn"inout/"$name".DCK"
set out = $trn"inout/"$name".OUT"
set rt = runlastgt

source $finvar
echo ---------------------- `date` ---------------------
echo Generating: $dck
echo Basefile: $base
echo Water Use Load Profile: $load
echo Varaible Definition: $var
echo Filenames and special Variables Definition: $finvar
if ( $#prn != $#unom ) then
   echo Number of names is not the same as number of lus!
   echo generation aborted
   exit
endif

rm -f $dck

cat /usr/users/grater/trnsys/gendck.autowarning > $dck

set i = 1
while ( $i <= $#prn )
   echo assign $name.$prn[$i] $unom[$i] >> $dck
   @ i = ($i + 1)
end
echo "*defining the logical unit numbers" >> $dck
echo Equations $#prn  >> $dck
set i = 1
while ( $i <= $#prn )
   echo Uout$i = $unom[$i] >> $dck
```

```
   @ i = ($i + 1)
end

echo "*defining the variables that are not in .vardef" >> $dck
echo Equations $#vars  >> $dck
set i = 1
while ( $i <= $#vars )
   echo $vars[$i] = $varvals[$i] >> $dck
   @ i = ($i + 1)
end

echo "*including the file .vardef" >> $dck
cat $var >> $dck

echo Simulation Start Stop Step >> $dck
echo Limits 50 30 >> $dck
echo Tolerances 0.0001 0.0001  >> $dck

echo "*including the file .load" >> $dck
cat $load >> $dck
echo "*including the file .base" >> $dck
cat $base >> $dck

echo end >> $dck

rm -f $rt
echo \#\!/bin/csh  >$rt
echo #command files to run the last generateed trnsys dck >>$rt
echo if \( \$\#argv == 1 \) then >>$rt
echo    set nice = \$1 >>$rt
echo else >>$rt
echo    set nice = 1 >>$rt
echo endif >>$rt
echo cd $trn"inout" >>$rt
echo rm -f $out  >>$rt
echo nice -\$nice trnsys \< $dck \>\& $out  >>$rt

chmod u+x $rt
```

B.2 Fmruns

Fmruns is a Unix command sequence that was used to run multiple TRNSYS simulations.

```
#!/bin/csh -x
# unset the environment variable DISPLAY, so that XLISP-STAT
# does not attempt to connect to the X-window system.
unsetenv DISPLAY
/bin/cp dummy.august old.august
set ii  = 0
# total number of runs is 4000
while ($ii < 41)
  set i = 1
# save the results every 100 TRNSYS runs
  /bin/cp old.august F$ii.august
  while ($i < 101)
    xlispstat < cmruns.lsp >&! /dev/null
    gt SB.BASE RRR.load R9.var SB.finvar
    randomdck < cmruns.ranfilenames
    /bin/nice -5 trnsys < SB_RRR_R9_SB.MODDCK >! trnsys.out
    /bin/nice -5 add2files < cmruns.add2files
    /bin/mv new.august old.august
    @ i = $i + 1
  end
@ ii = $ii + 1
end
exit
```

Appendix C

Hot Water Load Profiles

The following load profiles were used in the simulations. But not all profiles were used in all simulations. For the multiple runs with the randomized load profile they were randomize by shifting them in time and scaling up or down.

The profiles labeled A – U are imaginary load profiles. Some of this profiles represent "limiting cases".

The profile labeled WA – WI, shown in are adapted from data from the Wisconsin Center for Demand Side Research. The original data was electricity consumption for water heating. This data was converted to water consumption in l/hr.

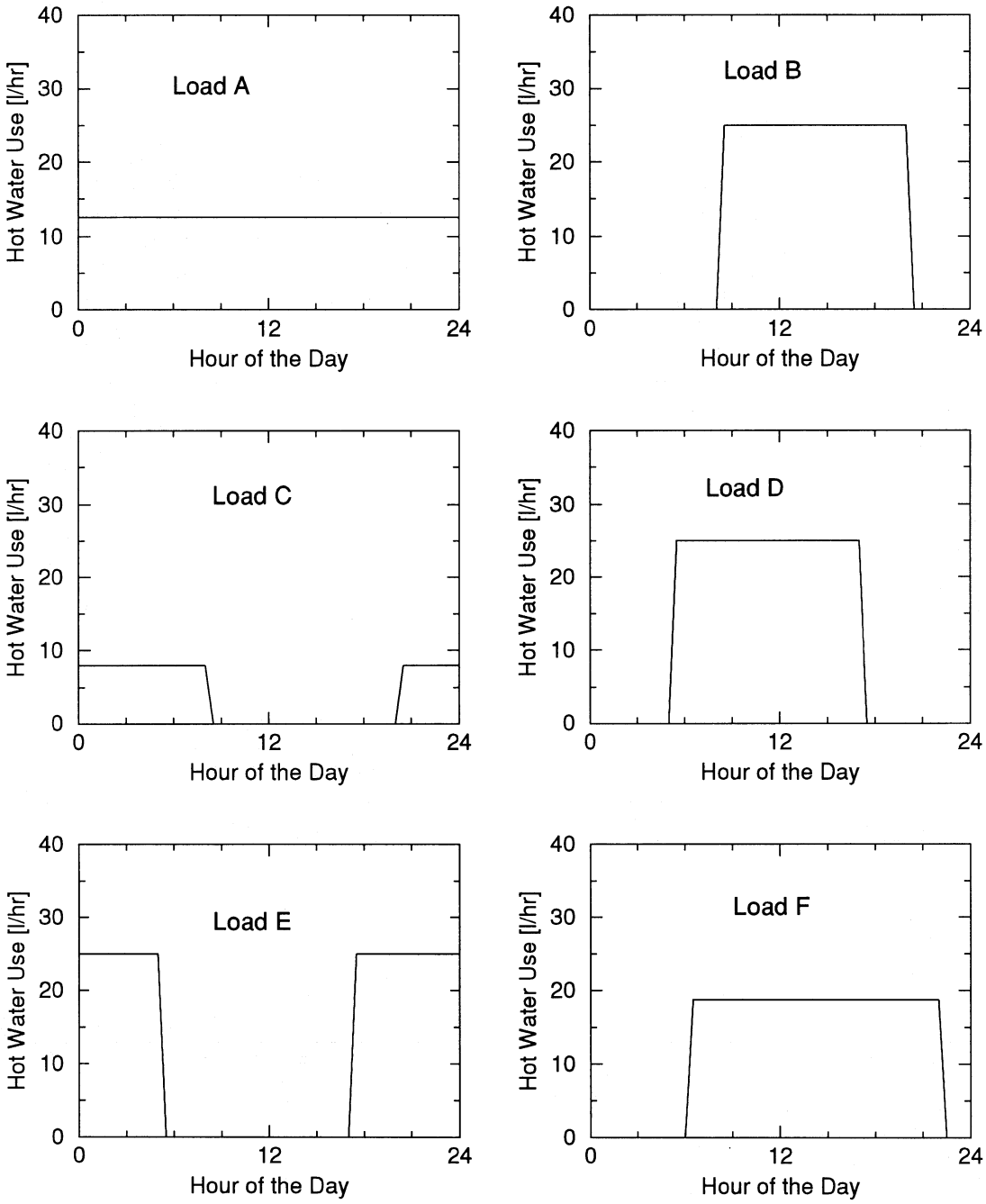

Figure C.1: Hot Water Load Profile A through F

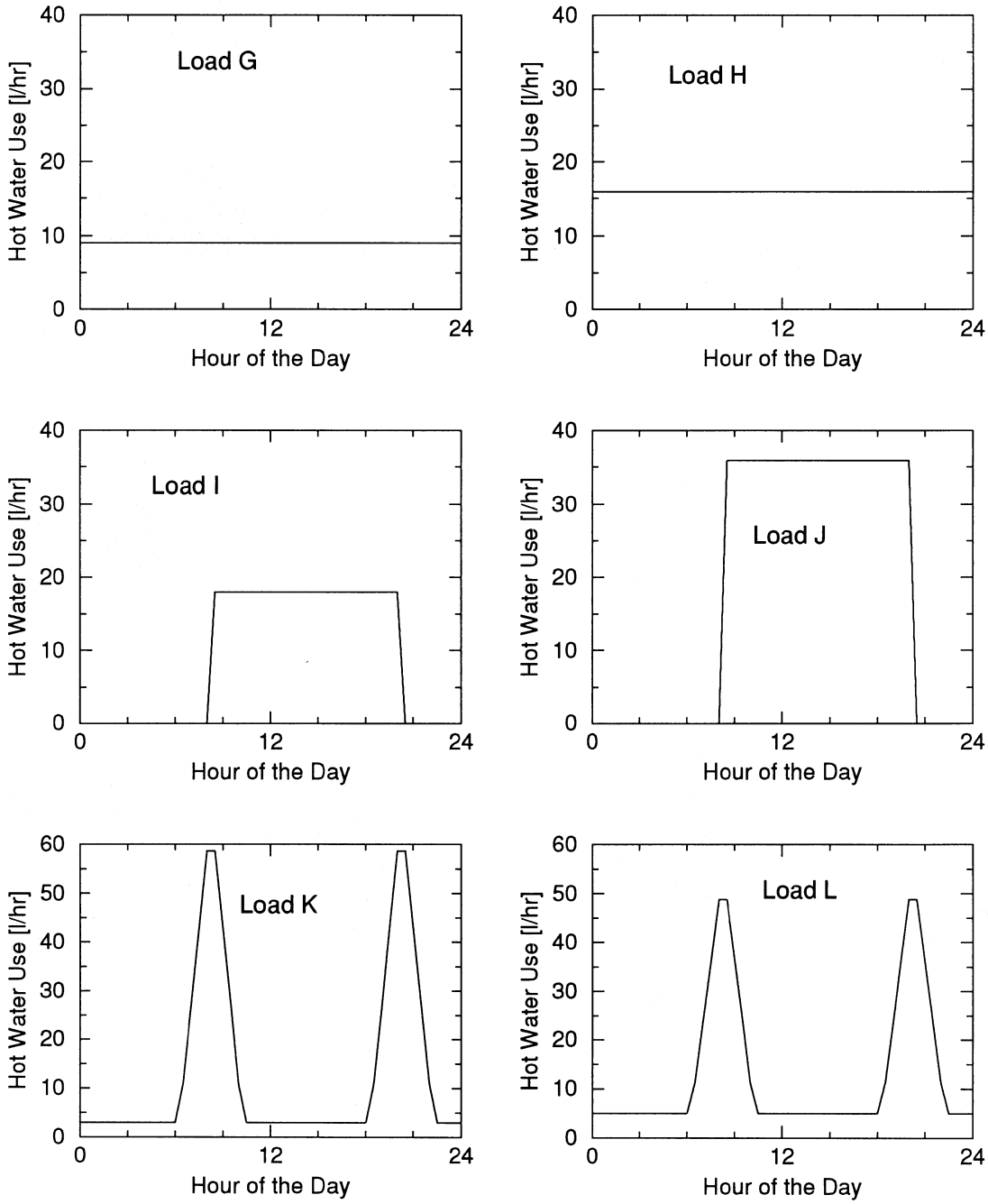

Figure C.2: Hot Water Load Profile G through L

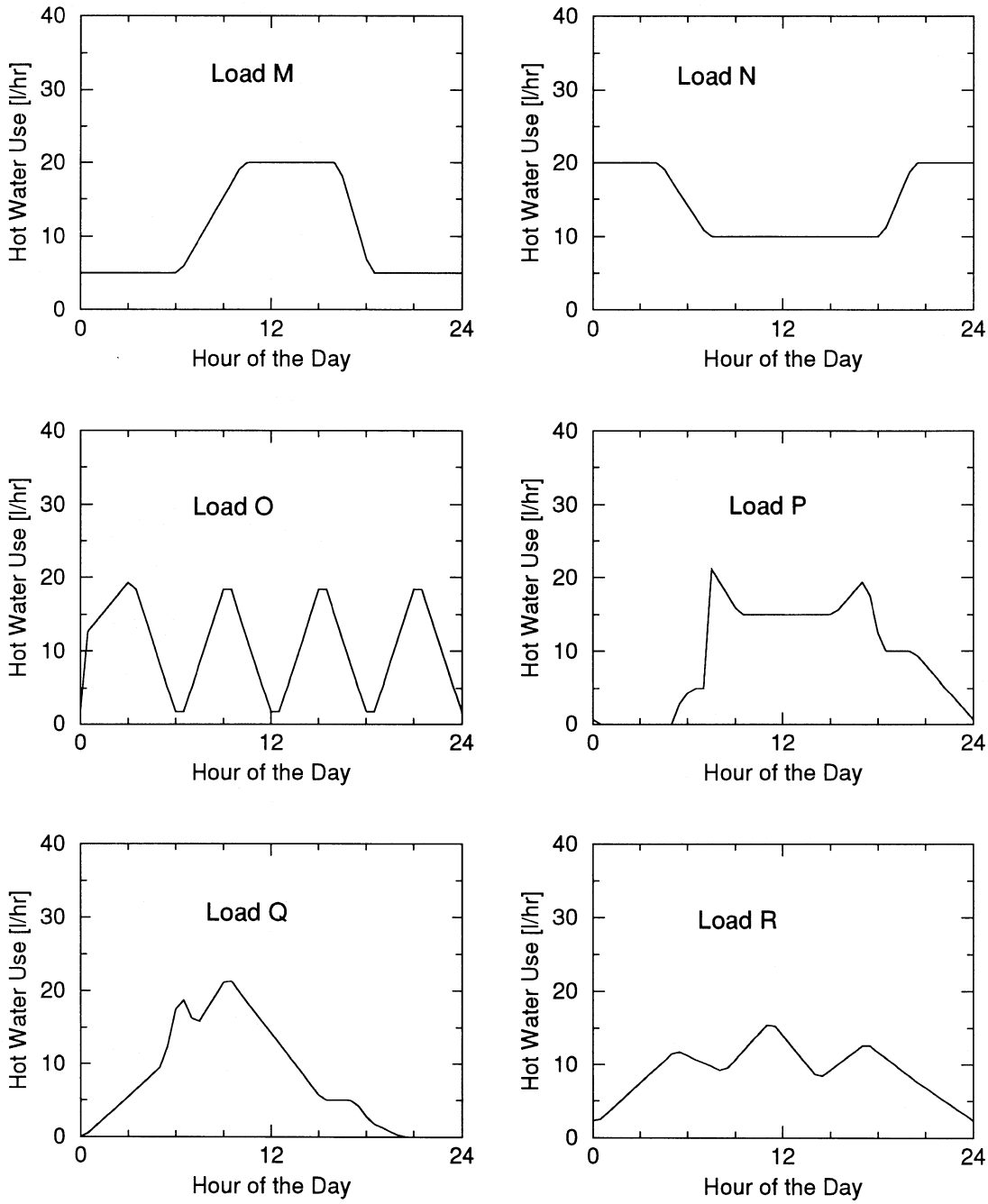

Figure C.3: Hot Water Load Profile M through R

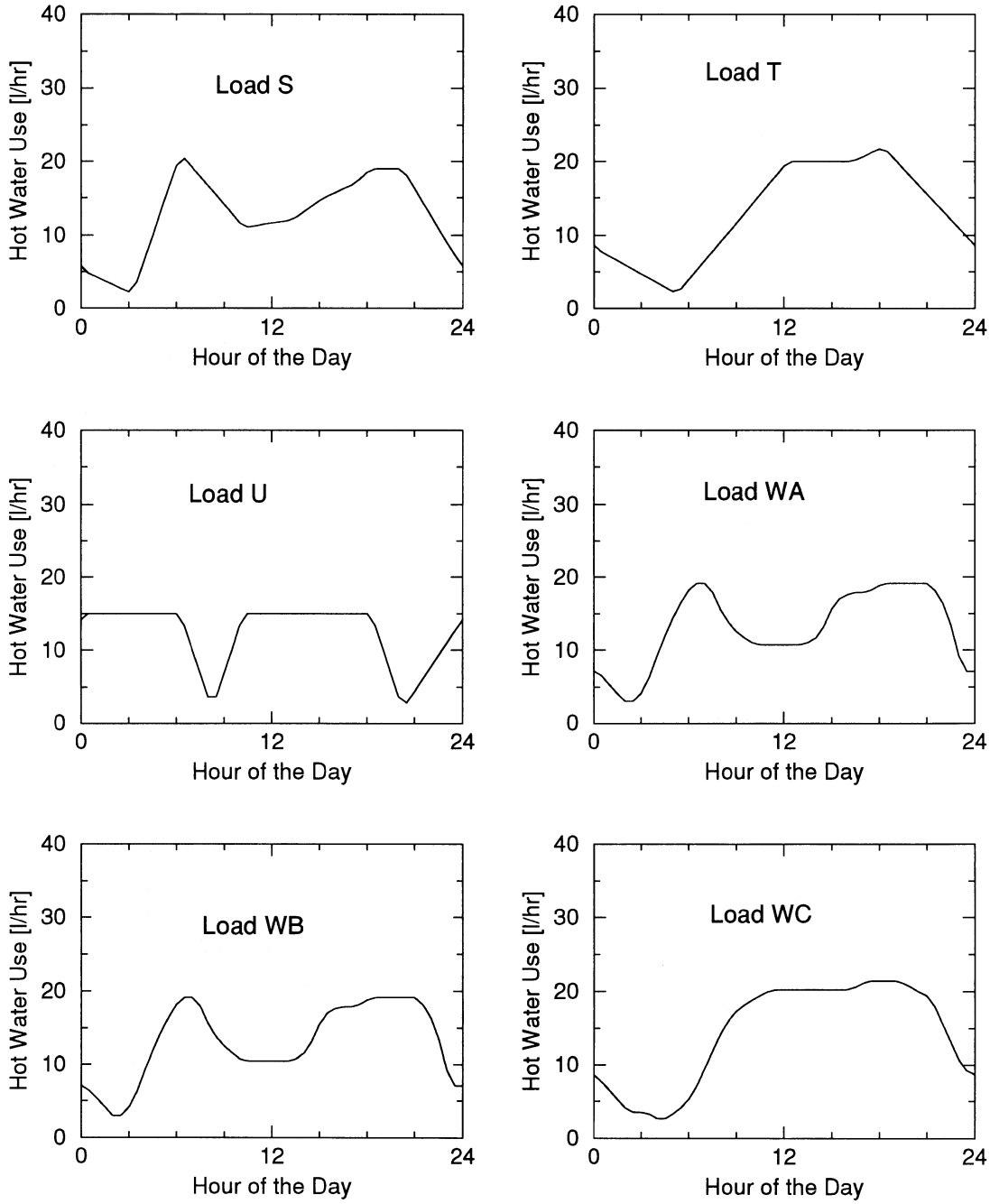

Figure C.4: Hot Water Load Profile T through U and WA throug WC

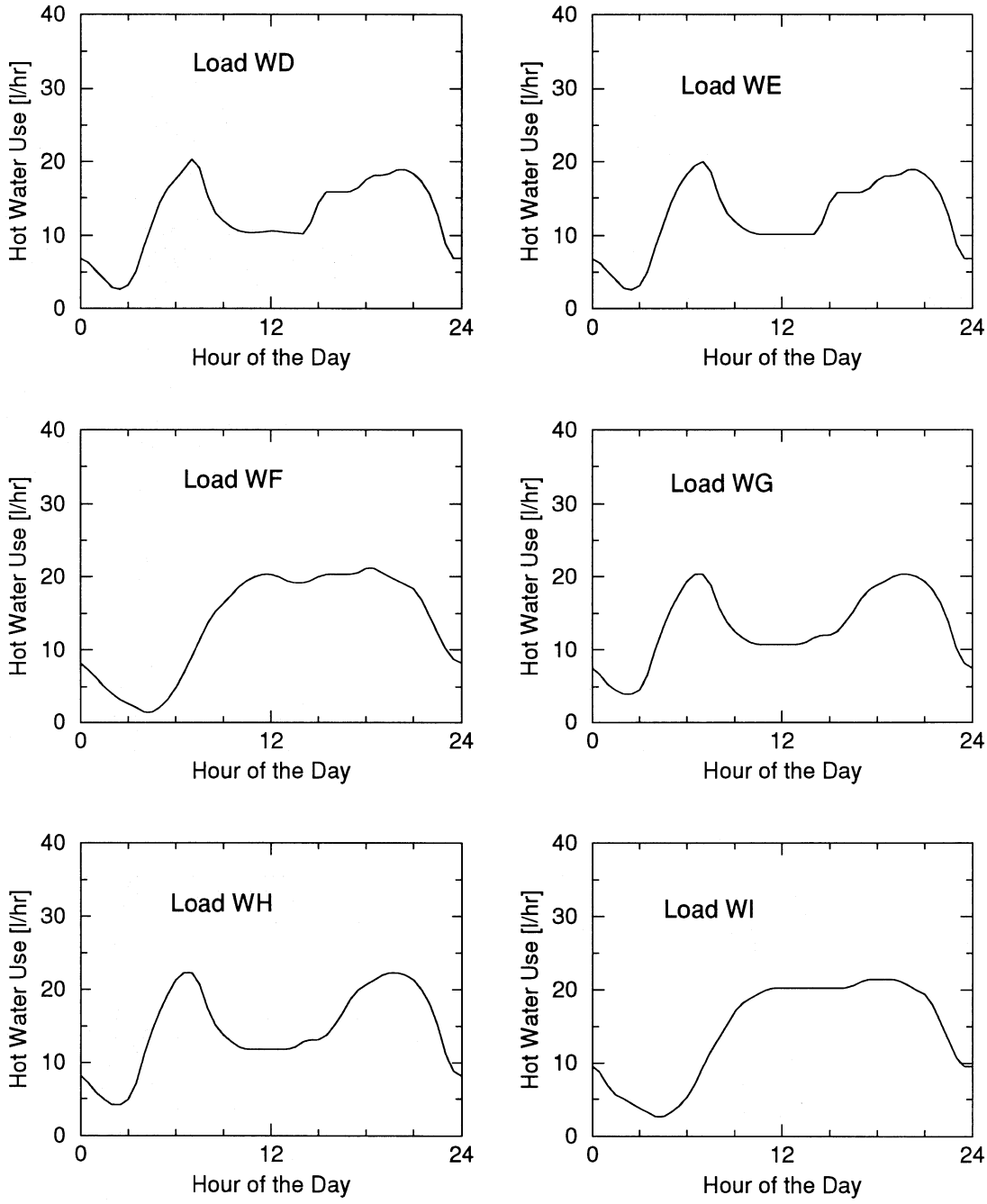

Figure C.5: Hot Water Load Profile WD through WI

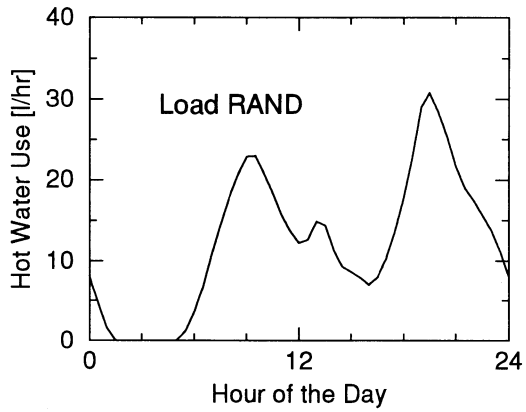

Figure C.6: Hot Water Load Profile RAND

Appendix D

TRNSYS Decks

D.1 Deck Used for Simulation of the Single System

```
assign sin.year 14
assign sin.month 30
assign sin.august 32
*defining the logical unit numbers
Equations 3
Uout1 = 14
Uout2 = 30
Uout3 = 32
*defining the variables that are not in .vardef
Equations 3
CityNo = 127
Lat = 43.13
Shift = 0
*including the file .vardef
Equations 1
SC      = 4871
*star, stop and step of simulation
```

```
Equations 5
Prefa   = 14
*Start   = (4*31 + 2*30 + 28 - Prefa) * 24
*Stop    = Start + ( 32 + Prefa ) * 24
Start   = 1.0
Stop    = 8760
Day     = (Start-1.0)/24.0+1.
step    = 1/4
*Collector Parameters
Equations 11
AreaPan = 7
GdotTest= 227
CPCOLL  = 4.189
RhoColl = 1000
Gtest   = GdotTest*RhoColl/AreaPan/1000
Slope   = 45
Gamma   = 0
Rhog    = 0.2
FrTAn   = 0.65
FrUl    = 12
b0      = .1
*DHW System Parameters
Equations 6
Npanel  = 1
Area    = AreaPan * Npanel
Nser    = 1
*Number of panels in series
Vcoll   = 23
*Collector flow rate
MFColl  = Vcoll * RhoColl / 1000
Qpar    = 0
*Solar Storage Tank
Equations 11
RhoTnk  = 1000
VolSol  = 0.8
HTsol   = .9
cpTnk   = 4.189
HT      = -1*HTsol
UAsol   = 9.5
Qaumax  = 3 * 3600
NNodes  = 6
LocHe   = 3
LocTh   = 2
```

```
Ti      = 22
*        Controller
Equations 6
UDB     = 6
LDB     = 1
Tenv    = 20.
Tset    = 55.
Tdbtnk  = 6.
Tmains  = 17.0
Simulation Start Stop Step
Limits 50 30
Tolerances 0.0001 0.0001
*including the file .load
Unit 14 Type 14 randomized load
Parameters 1490
..... 1490 parameters deleted .....
*including the file .base
Unit 54 Type 54 Weather Generator
Parameters 7
*Iunits Ounits Lu City# Model Hrc Rand
1 1 21 Cityno 1 2 1

Unit 16 Type 16 Radiation Processor
Parameters 7
* Radmode Trackmode Tiltmode Day Lat Sc Shft
1 1 1 Day Lat Sc Shift
Inputs 6
* I Td1 Td2 Rhog Betai Gamma
54,7 54,19 54,20 Rhog Slope Gamma
0.0 0.0 0.0 Rhog Slope Gamma

Unit 1 Type 1 Solar Collector
Parameters 12
* Mode Ns A Cpc Effmode Gtest A B C Eff Cpf Omode Bo
1 Nser Area Cpcoll 1 Gtest FrTAn Frul -1 Cpcoll 1 b0
Inputs 10
*Tin Mc Mf Ta It I Id Rhog Theta Slope
3,1 3,2 3,2 54,4 16,6 16,4 16,5 Rhog 16,9 Slope
22.0 Mfcoll Mfcoll 22.0 0.0 0.0 0.0 Rhog 0.0 Slope

Unit 3 Type 3 Pump
Parameters 1
Mfcoll
```

```
Inputs 3
4,1 Mfcoll 2,1
22.0 Mfcoll 0.0

Unit 2 Type 2 Pump Controller
Parameters 3
3 Udb Ldb
Inputs 3
1,1 4,1 2,1
22.0 22.0 0.0

equations 6
tn1 = tset
tn2 = tset
tn3 = tset
tn4 = tn3  - 3
tn5 = tn4  - 3
tn6 = tn5  - 3

Unit 4 Type 4 Main Storage Tank
Parameters 13
2 Volsol Cptnk Rhotnk UaSol Ht Qaumax LocHe
LocTh Tset Tdbtnk 0 Tset
Inputs 5
1,1  1,2  Tmains 14,1 Tenv
22.0 0.0  Tmains 0.0  Tenv
Derivatives NNodes
Tn1 Tn2 Tn3 Tn4 Tn5 Tn6

Unit 5 Type 4 Main Storage Tank
Parameters 13
2 Volsol Cptnk Rhotnk UaSol Ht Qaumax LocHe
LocTh Tset Tdbtnk 0 Tset
Inputs 5
0,0    0,0  Tmains 14,1 Tenv
Tmains 0.0  Tmains 0.0  Tenv
Derivatives NNodes
Tn1 Tn2 Tn3 Tn4 Tn5 Tn6

Equations 3
Qreq = [14,1] * Cptnk * ([4,3] - tmains)
MtLd = Max ( ( GT ( Tset , [4,3] ) * ( Tset-[4,3] ) ) , 7.5) - 7.5
Qload = (Tset - Tmains) * Cptnk * [14,1]
```

```
Unit 24 Type 24 Integrator Yearly
Inputs 5
4,8  Qreq  4,5  Qload    MtLd
0.0  0.0   0.0  0.0     0.0
*Qaux Qreq Qenv Qload Meetload

equations 1
SolF = ( [24,3] + [24,4] - [24,1] ) / ( [24,3] + [24,4] + 1 )

Unit 25 Type 25 Printer Yearly
Parameters 4
Step Stop Stop uout1
inputs 6
24,1 24,2 24,3 24,4 24,5 SolF
Qaux Qreq Qenv Qload Meetload SolF
Equations 2
augst = 24 * ( 31 * 4 + 2 * 30 + 28 )
augend = augst + 24 * 31
Unit 31 Type 25 Printer each Timestep for August only
Parameters 4
step augst augend uout3
Inputs 4
5,8    4,8    Qload    4,3
Qauxwo Qauxw  Qload   Tout

Unit 23 Type 24 Integrator Monthly
Parameters 1
-1
Inputs 5
4,8  Qreq  4,5  Qload   MtLd
0.0  0.0   0.0   0.0   0.0
*Qaux Qreq Qenv Qload Meetload
equations 1
SolFm = ( [23,3] + [23,4] - [23,1] ) / ( [23,3] + [23,4] + 1 )
Unit 30 Type 25 Printer Monthly
Parameters 4
-1 Start Stop uout2
inputs 6
23,1 23,2 23,3 23,4 23,5 SolFm
Qaux Qreq Qenv Qload Meetload SolFm
end
```

D.2 Deck Used for Multiple Runs Series I

```
assign SBI_DR_RC_SBC.august 30
assign SBI_DR_RC_SBC.month 32

*defining the logical unit numbers
Equations 2
Uout1 = 30
Uout2 = 32
*
*defining the variables that are not in .vardef
Equations 3
CityNo = 127
Lat = 43.13
Shift = 0
*including the file .vardef
*setting up the parameters for city and location,
*solar constant, shift
Equations 1
SC      = 4871
*start, stop and step of simulation
Equations 5
Prefa   = 14
Start   = (4*31 + 2*30 + 28 - Prefa) * 24
Stop    = Start + ( 32 + Prefa ) * 24
*Start   = 1.0
*Stop    = 8760
Day     = (Start-1.0)/24.0+1.
step    = 1/4
*Collector Parameters
Equations 11
AreaPan = 7 * |r|+00.70+01.30
GdotTest= 227 * |r|+00.90+01.10
CPCOLL  = 4.189
RhoColl = 1000
Gtest   = GdotTest*RhoColl/AreaPan/1000
Slope   = 45 * |r|+00.70+01.30
Gamma   = 0
Rhog    = 0.2
FrTAn   = 0.65 * |r|+00.80+01.20
FrUl    = 12 * |r|+00.80+01.20
```

```
b0      = .1 * |r|+00.80+01.20
*DHW System Parameters
Equations 6
Npanel  = 1
Area    = AreaPan * Npanel
Nser    = 1
*Number of panels in series
Vcoll   = 23 * |r|+00.80+01.20
*Collector flow rate
MFColl  = Vcoll * RhoColl / 1000
Qpar    = 0
*Solar Storage Tank
Equations 11
RhoTnk  = 1000
VolSol  = 0.8 * |r|+00.60+01.40
HTsol   = .9 * |r|+00.60+01.40
cpTnk   = 4.189
HT      = -1*HTsol
UAsol   = 9.5 * |r|+00.50+01.50
Qaumax  = 3 * 3600
NNodes  = 6
LocHe   = 3
LocTh   = 2
Ti      = 22
*        Controller
Equations 5
UDB     = 6 * |r|+00.80+01.20
LDB     = 1
Tenv    = 20.
Tdbtnk  = 6. * |r|+00.50+01.50
Tmains  = 17.0
Simulation Start Stop Step
Limits 50 30
Tolerances 0.0001 0.0001
*including the file .load
unit 14 type 9
parameters 6
1 0.5  1 1 0 -1
*including the file .base
Unit 54 Type 54 Weather Generator
Parameters 7
*Iunits Ounits Lu City# Model Hrc Rand
1 1 21 Cityno 1 2 1
```

```
*
Unit 16 Type 16 Radiation Processor
Parameters 7
* Radmode Trackmode Tiltmode Day Lat Sc Shft
1 1 1 Day Lat Sc Shift
Inputs 6
* I Td1 Td2 Rhog Betai Gamma
54,7 54,19 54,20 Rhog Slope Gamma
0.0 0.0 0.0 Rhog Slope Gamma
*
Unit 1 Type 1 Solar Collector
Parameters 12
* Mode Ns A Cpc Effmode Gtest A B C Eff Cpf Omode Bo
1 Nser Area Cpcoll 1 Gtest FrTAn Frul -1 Cpcoll 1 b0
Inputs 10
*Tin Mc Mf Ta It I Id Rhog Theta Slope
3,1 3,2 3,2 54,4 16,6 16,4 16,5 Rhog 16,9 Slope
22.0 Mfcoll Mfcoll 22.0 0.0 0.0 0.0 Rhog 0.0 Slope
*
Unit 3 Type 3 Pump
Parameters 1
Mfcoll
Inputs 3
4,1 Mfcoll 2,1
22.0 Mfcoll 0.0
*
Unit 2 Type 2 Pump Controller
Parameters 3
3 Udb Ldb
Inputs 3
1,1 4,1 2,1
22.0 22.0 0.0
*
equations 6
tn1 = 55
tn2 = tn1
tn3 = tn2  - 3
tn4 = tn3  - 3
tn5 = tn4  - 3
tn6 = tn5  - 3
*
Unit 15 Type 14 Tset load forcing function
Parameters 12
```

```
0 55     13 55   13 45   16 45    16 55   24 55
*
Equations 2
U16b = |r|+00.00+01.00
U16a = 11 + gt ( U16b  , 0.5)
*
Unit 17 Type 14 Tset load forcing function
Parameters 16
0 55     u16a 55    u16a 65     13 65    13 45
16 45    16 55    24 55
*
Equations 2
TsetLo = [15,1]
TsetTa = [17,1]
*
* simulation mixing valve, using equation statement
Equations 4
tmpW = [14,1] * (TsetLo-Tmains) / ([4,3] - Tmains)
ToLoW = GT ( [4,3], TsetLo) *tmpW + GT(TsetLo, [4,3])*[14,1]
tmpW0 = [14,1] * (TsetLo-Tmains) / ([5,3] - Tmains)
ToLoW0 = GT([5,3], TsetLo)*tmpW0 + GT(TsetLo, [5,3])*[14,1]
*
Equations 1
tdummy = 55
*
Unit 4 Type 4 Main Storage Tank
Parameters 13
2 Volsol Cptnk Rhotnk UaSol Ht Qaumax LocHe
LocTh Tdummy Tdbtnk 0 Tdummy
Inputs 7
1,1  1,2  Tmains ToLoW Tenv 0,0 TsetTa
22.0 0.0  Tmains 0.0  Tenv 1 55
Derivatives NNodes
Tn1 Tn2 Tn3 Tn4 Tn5 Tn6
*
Unit 5 Type 4 Main Storage Tank
Parameters 13
2 Volsol Cptnk Rhotnk UaSol Ht Qaumax LocHe
LocTh Tdummy Tdbtnk 0 Tdummy
Inputs 7
0,0    0,0  Tmains ToLoW0 Tenv 0,0 TsetTa
Tmains 0.0  Tmains 0.0  Tenv 1 55
Derivatives NNodes
```

```
Tn1 Tn2 Tn3 Tn4 Tn5 Tn6
Equations 3
Qload = (TsetLo - Tmains) * Cptnk * [14,1]
augst = 24 * ( 31 * 4 + 2 * 30 + 28 )
augend = augst + 24 * 31
Unit 31 Type 25 Printer each Timestep for August only
Parameters 4
step augst augend uout1
Inputs 5
5,8    4,8    14,1  Qload   16,4
Qauxwo Qauxw  Qwater  Qload radiation
*
Unit 23 Type 24 Integrator Monthly
Parameters 1
-1
Inputs 5
5,8    4,8    14,1  Qload    4,9
0      0       0     0       0
*Qauxwo Qauxw  Qwater  Qload Qfcol
*
equations 1
SolFm = [23,5] / ( [23,5] + [23,2] + 1 )
*
Unit 30 Type 25 Printer Monthly
Parameters 4
-1 Start Stop uout2
inputs 6
23,1 23,2 23,3 23,4 23,5 SolFm
Qaux Qreq Qenv Qload Meetload SolFm
end
```

Appendix E

FORTRAN77 Programs

E.1 Randomdck

```
************************************************************************
*     modifies a ascii input file                                      *
*     all occurrences of                                               *
*     |r|-ll.ll+hh.hh are replaced by an uniformly distributed         *
*     random numbers between ll.ll and hh.hh                           *
*     requires the random numbers between 0 and 1 supplied             *
*     in a file                                                        *
************************************************************************
      program randomdck
c     declare all variables
      implicit none
      real rdummy, low, high, ran, randat
      integer inno, outno, ranno, idummy, i, i1, maxcol, maxpos,
     +     pos, lm, lbound
      character*100 inname, outname, ranname
      character*75 indata, outdata, str, cdummy
      character mark*3
c     set parameters
c     inno:    logical unit number of the input file
c     outno:  logical unit number of the output file
c     ranno:  logical unit number of the random number file
```

```
c     mark:   string that defines the beginning of the limits
c     maxcol: maximum number of columns of the input file
c     maxpos: last possible column in which mark may occur
c     lbound: length of the limit string
      parameter (inno=10, outno=12, ranno=13, mark = '|r|',
     +     maxcol=75, maxpos=60, lbound=6 )
      lm = len(mark)
c     read the random number file name from standard input
      read(*,'(A)') ranname
      open (unit=ranno, file=ranname, status='old')
c     read input and output file names from standard input
 5    read(*,'(A)') inname
      read(*,'(A)') outname
      open (unit=inno, file=inname, status='old')
      open (unit=outno, file=outname, status='unknown')

c     get one line from the input file
 10   read (inno,'(A)', end = 200) indata
      outdata = indata
c     search for mark
      do 50, pos = 1, maxpos
         if ( indata(pos:pos+lm-1) .eq. mark) then
c           mark found --> read the lower and upper limit and
c           replace mark and limits by the radomnumber
            str = indata(pos+lm:pos+lm+lbound-1)
            read (str,*) low
            str = indata(pos+lm+lbound-1:pos+lm+lbound*2-1)
            read (str,*) high
            read (ranno,*) randat
            ran = randat * (high-low) + low
            write (outdata(pos-1:),*) ran
            goto 70
         endif
 50   continue
c     write one "new" line to the output file
 70   write (outno,'(A)') outdata
      goto 10
 200  continue
c     end of this input file, close the files
      close (inno)
      close (outno)
c     it there more work to do?
      read(*,'(A)',end=300) cdummy
```

```
c     yes, start from the beginning
      goto 5
c     no, we are done, close the random number file and exit
 300  continue
      close (ranno)
 1000 end
```

Bibliography

[1] Becker, B.R., Stogsdill, K.E.: *Development of a hot water use data base*, ASHRAE Transactions, Vol. 96, Part 2, 1990

[2] Becker, B.R., Thrasher, W.H., DeWerth, D.W.: *Comparison of collected and compiled existing data on service hot water use patterns in residential and commercial establishments*, ASHRAE Transactions, Vol. 97, Part 2, 1991

[3] Beckman, W.A., Duffie, J.A.: *Solar engineering of thermal processes*, John Wiley & Sons, Inc., New York, Chichest, Brisbane, Toronto, Singapore, 1991

[4] Box, G.E.P., Hunter, W.G., Hunter, J.S.: *Statistics for Experimenters*, John Wiley & Sons, Inc., New York, Chichester, Toronto, Singapore, 1978

[5] Burch, J.D.: *personal communication*

[6] Carpenter, A. et.al.: *The Potential for Utility Peak Load Reduction Through the Use of Solar Domestic Hot Water Systems*, 1991 SESCI conference, Toronto, Ontario, June 1991

[7] Klein, S.A., et.al., TRNSYS: *A Transient Simulation Program,* University of Wisconsin—Madison, Engineering Experiment Station Report 38-12, Version 13.1, September 1990

[8] Nyhoff, L., Leestma, S.: *FORTRAN77 for Engineers and Scientists*, Macmilan Publishing Company, New York, 1985

[9] Perlman, M., Mills, B.E.: *Development of residential hot water use patterns*, ASHRAE Report 430

[10] Starkweather, S.: *An exogenous analysis of solar domestic hot water heating as a DSM technology*, not published, prepared for the Solar Energy Laboratory at the University of Wisconsin—Madison, 1992

[11] Steven, R.S.: *Residential Solar DSM Programs at Florida Power and Light*, Solar Today, page 23–25, September/October 1991

[12] Tierney, L.: *Lisp-Stat : an object-oriented environment for statistical computing and dynamic graphics*, John Wiley & Sons, Inc., New York, 1990